Dissertation

zur Erlangung des Doktorgrades der Fakultät für Chemie und

Pharmazie der Ludwig-Maximilian-Universität München

Improved nonviral gene vectors: Efficient and non-toxic

polyplexes with enhanced endosomolytic activity

vorgelegt von

Sabine Boeckle

aus Nürnberg

2005

Table of Contents

1 Introduction

1.1 Gene therapy

Gene therapy, as first proposed 1972 by Friedman and Roblin (1), aims at the delivery of nucleic acids (DNA or RNA) into target cells in order to cure patients suffering from different diseases. The transferred nucleic acids are mostly used to turn on or restore a gene function ('gain of function'). A relatively new field in gene therapy applies nucleic acids to suppress specific gene functions ('loss of function') by turning off genes with antisense oligonucleotides or double-stranded small interfering RNA (siRNA).

Although gene therapy has not yet been established as standard treatment, it was already applied in various clinical studies, e.g. in the field of cancer therapy (most clinical trials), monogenic diseases (Hemophilia A and B, cystic fibrosis, severe combined immunodeficiency syndrome (SCID)), infectious diseases, vascular diseases, or DNA vaccination (2). Gene therapy may hold the potential to revolutionize modern molecular medicine, provided that appropriate nucleic acid delivery systems ('*vector systems*') are available.

1.2 Viral and nonviral vectors

Current vectors can be divided into two major groups, namely viral vectors derived from natural viruses and nonviral, synthetically manufactured vectors.

1.2.1 Viral vectors

Since it is the nature of viruses to deliver their genes into host cells, they present good candidates for the development of effective gene delivery. Natural evolution, however, optimized them for infecting and replicating their genome in host cells, but not necessarily for survival of the transduced cells or maintenance of the expressed genes. Nevertheless, replication-defective viruses, where viral genes were partly replaced by therapeutic genes, were historically the first generation of 'viral vectors' applied in gene therapy.

Retroviral vectors and adenoviral vectors have been most commonly used in clinical trials (2). Other viruses that were used to develop viral vectors include adeno-associated virus (AAV), herpes virus, pox virus, and more recently lentivirus. Viruses in general are highly efficient regarding cellular uptake and intracellular delivery of therapeutic genes to the nucleus. Therefore, few viral particles are sufficient for the transduction of cells.

Gene transfer activity of viral vectors also strongly depends on the type of virus used for transduction. Murine retroviral vectors, for example, are very useful for *ex vivo* gene transfer because of their high efficiency to integrate into the host cell genome. In particular, they have been optimized for gene transfer into hematopoietic stem cells. The gene therapy of human SCID-X1 can be regarded as the first success story in gene therapy (3). All ten children treated in this trial were cured of the immunodeficiency symptoms. The therapy, however, was associated with the incidence of leukemia in two of the treated children, and subsequent chemotherapy was required. Insertional oncogenesis by the retroviral vector was identified as the reason for this severe side effect, highlighting a serious risk of such stably but randomly integrating viral vector systems that may cause fatal long term changes in gene expression in addition to the desired therapeutic effect.

Adenoviral vectors do not bear the risk of insertional oncogenesis, since these vectors do not integrate into the host genome. Moreover, adenoviral vectors can efficiently transfer genes into both dividing and non-dividing cells. However, natural immunity against adenovirus (the virus causes human respiratory diseases) and acute inflammatory and immune responses limit clinical application to few areas such as localized cancer gene therapy. Systemic administration of a large amount of adenovirus (e.g. into the liver) may cause serious side effects including thrombocytopenia, intravascular coagulation and multiple organ system failure that even caused the death of one patient (4;5). Recent approaches to improve viral vector safety included strategies to reduce the number of remaining adenoviral genes, from 'first generation' adenoviruses, where only one early gene segment was removed, to so-called high-capacity 'gutless' adenoviruses, where all viral genes have been replaced (6). Unfortunately, even high-capacity 'gutless' adenoviruses triggered inflammatory and immune responses (6;7).

Such host responses are obviously independent of the type of virus and of viral gene expression but they are rather attributed to the viral infection process and to viral proteins in the vector particle. Inflammatory and immune host responses to viruses therefore exclude repeated *in vivo* administration of viral vectors in general.

1.2.2 Nonviral vectors

Nonviral vectors are more flexible in terms of type and size of the delivered nucleic acids (8). A broad range of nucleic acids from small double-stranded RNA for interfering with gene expression up to large artificial chromosomes can be used for transfection. Both the nucleic acids and the carrier molecules can be produced at large scale with rather low cost. Their synthetic design allows high flexibility of the formulation that can be easily modified by diverse chemical reactions and physical interactions. The great advantage of nonviral vectors is their low immunogenicity, since synthetic vectors present far less or no immunogenic proteins or peptides in comparison to viral vectors. Nonviral vectors are usually based on chemically defined lipids or polycations and can be generated protein-free or using non-immunogenic human or humanized proteins and peptides only.

An obvious weakness of nonviral vectors is their low efficiency in intracellular nucleic acid delivery which currently is partly compensated by administration of large amounts of the vectors. Direct injection of mg quantities of 'naked' DNA is usually well tolerated but still only yields very low levels of transfection. Nevertheless, application of naked DNA led to protein expression that was sufficient for triggering immune responses and was used for human DNA vaccination trials (9). To enhance the delivery of naked DNA, a series of strategies have been applied that used physical forces, such as electric pulses, mechanical forces, or hydrodynamic pressure. Electroporation, for example, enhanced transgene expression by two or three orders of magnitude and was sufficient to stimulate strong immune responses in DNA vaccine applications (10).

Since degradation of naked DNA by serum nucleases limits systemic administration, different complex-based gene transfer vectors have been developed in order to enhance the stability of the delivered nucleic acids. In these vectors, the nucleic acids are condensed with cationic lipids or polycations to generate complexes called

'lipoplexes' or 'polyplexes', respectively. The cationic agents bind to DNA or RNA due to electrostatic interactions and form particles of nanometer range. Such compaction protects the nucleic acids from enzymatic degradation. Cationic lipids usually consist of a cationic headgroup for electrostatic binding to the nucleic acid and a lipophilic tail, which enables the generation of a nucleic acid/lipid complex (for review see (11)). Polycationic carriers are naturally occurring proteins like histones or protamines, chemically synthesized polyaminoacids, e.g. polylysine and polyarginine, or other polycationic polymers (for review see (12) and (13)). More recently, polyethylenimine (PEI) has been described as an useful carrier for the condensation of DNA, and it has become one of the most efficient reagents for gene delivery into cells (for review see (14)).

1.2.3 Gene delivery with PEI polyplexes

Jean-Paul Behr and colleagues were the first to report the successful use of PEI for the delivery of DNA and oligonucleotides (15). PEI polymers can be synthesized with a linear or a branched topology (Fig. 1) and are available in a wide range of molecular weights (16).

Linear PEI

$H_3C-CH_2-NH-[CH_2-CH_2-NH]_n-CH_2-CH_2-NH_3$
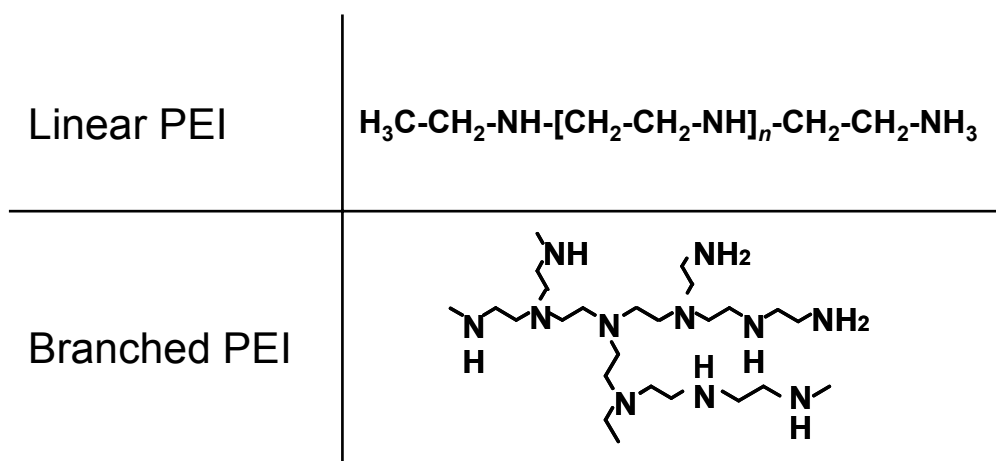
Branched PEI

Fig. 1 Structure of linear and branched PEI

PEI is the organic macromolecule with the highest density of protonable amine functions and is therefore ideal to condense nucleic acids into particles of nanometer range (17). The amino groups allow easy chemical modification, and different biologically active moieties such as cell targeting ligands or compounds promoting intracellular delivery have been coupled to PEI (18). Since these compounds mimic

viral delivery functions, such complex vector systems carrying multiple functional domains have been termed 'artificial viruses' (18).

The condensation process of DNA with the polycation PEI has been studied extensively. The particle size of DNA/PEI complexes depends on the molar ratio of PEI nitrogen to DNA phosphate (N/P ratio) and on the present salt concentration. Small individual particles are formed at low salt concentration ($<$ 50 mM NaCl) and/or N/P ratios above 5, whereas formation of large aggregated particles is observed in the presence of salt ($>$ 50 mM NaCl) at lower N/P ratios (19;20). The net positive surface charge and an excess of free PEI during complex formation can prevent aggregation by repulsion of positive charges, whereas an increase in salt concentration reduces the hydration layer around the particles and promotes particle aggregation.

1.2.4 Barriers to gene transfer with PEI polyplexes

For successful gene delivery, gene vectors have to overcome a number of extracellular and intracellular barriers until the carried nucleic acids reach their final destination, the nucleus. The *in vivo* delivery of viral vectors is strongly hampered by extracellular barriers. For example, systemic targeting of viral vectors towards the desired tissue is difficult to realize due to host immune responses that trigger viral clearance. Viral vectors, however, are very efficient in overcoming intracellular barriers such as internalization into the host cell and delivery of the therapeutic gene towards the nucleus. In contrast, poor intracellular delivery of the carried nucleic acid remains the major barrier to effective gene transfer with nonviral vectors. The following section gives an overview of barriers to nonviral vectors in general and gives examples of how these barriers can be overcome using PEI polyplexes.

1.2.4.1 *Extracellular barriers*

As explained above, many nonviral vectors are generated using positively charged lipids or polycations resulting in particles with a net positive surface charge. Although positively charged vectors like PEI polyplexes expose high gene transfer activity in *vitro* (for example see (19;20)), systemic administration of such particles is rather restricted. After tail vein injection of different positively charged lipo- and polyplexes

into mice, complexes were rapidly cleared from the circulation and mainly accumulated in the lung. Gene expression levels found in the lung were several log units higher than in any other organ (for example see (21)). In addition, gene transfer at effective DNA doses was associated with acute toxicity. *Ex vivo* experiments revealed that positively charged polyplexes induced aggregation of erythrocytes. It was proposed that both unspecific lung expression and toxicity were attributed to the aggregation of initially small polyplexes with blood components and their subsequent entrapment in the lung capillary bed (22). Obviously, the positive surface charge of complexes mediates unspecific interactions with non-target cells and blood-components resulting in the observed systemic side effects. These adverse effects can be overcome by 'shielding' of the positive surface charge of the vectors with hydrophilic polymers like polyethylene glycol (PEG). PEGylation of PEI polyplexes prevented erythrocyte aggregation, enhanced systemic circulation time and reduced toxicity of polyplexes (21;23). Shielding with PEG, however, also reduces the overall transfection efficiency because of reduced interaction with cell membranes of all cells including the target cells.

In order to direct the shielded particles towards the desired tissue and to promote specific uptake into target cells, different targeting ligands have been incorporated into the vectors. These ligands recognize specific cellular receptors present on the plasma membrane of the target cells. Ligands that have been used to promote targeted delivery of vectors include small chemical compounds (24), carbohydrates (25), peptide ligands (26), growth factors and proteins (27-29), or antibodies (30;31). More details of applied targeting ligands are summarized in (32) and (33). For example, systemic targeting of PEI polyplexes towards tumors was demonstrated using the transferrin receptor (21;29;34) or the epidermal growth factor (EGF) receptor (28) as targets. Targeting efficiencies, however, remain to be improved, because transfection efficiencies of shielded and targeted nonviral vectors are rather poor both *in vitro* and *in vivo*. This low transfection efficiencies are mainly attributed to different intracellular barriers within the transfection process.

1.2.4.2 Intracellular barriers

After cellular association of nonviral vectors to the target cells, particles are internalized by receptor-mediated endocytosis, macropinocytosis, phagocytosis or related processes (35-37). For successful transgene expression, several intracellular barriers then have to be overcome. Fig. 2 illustrates cellular uptake of artificial virus-like PEI polyplexes carrying multiple functional domains to overcome these barriers.
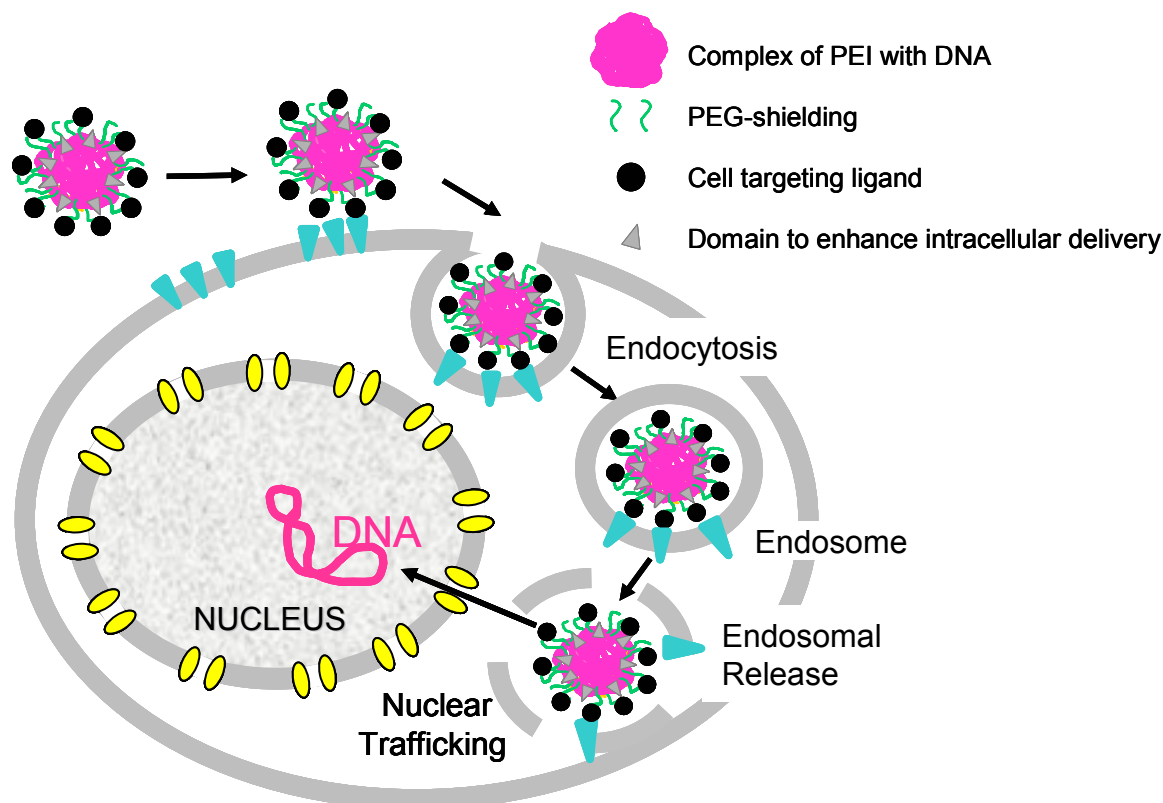
Fig. 2 Cellular uptake of artificial virus-like PEI polyplexes. PEG-shielded and receptor-targeted PEI polyplexes are mainly internalized into cells by receptor-mediated endocytosis after association of polyplex-ligands to receptors present on the plasma membrane. Internalized particles are captured in intracellular vesicles such as endosomes. For effective gene delivery, polyplexes need to escape from endosomes by endosomal release, and the released particles and/or the carried nucleic acid need to traffic towards the nucleus, enter the nucleus and expose the DNA to the cell's transcription machinery. Different functional domains incorporated into the polyplexes may help to overcome these intracellular barriers.

Internalized gene transfer complexes are mostly found in intracellular vesicles such as endosomes. Entrapment in endosomes is thought to be associated with degradation of the complexes upon endosomal acidification. Therefore, subsequent release of particles into the cytoplasm represents a major bottleneck to gene delivery (38;39). PEI polyplexes can promote endosomal escape to some degree because of the 'proton sponge' effect (16). PEI polyplexes and free PEI have considerable

buffering capacity, because PEI is only partially protonated at physiological pH (40). Upon intracellular delivery of the DNA particle, the natural acidification within the endosome triggers protonation of complex-bound and free PEI, inducing chloride ion influx, osmotic swelling and destabilization of the vesicle which finally leads to release of the polyplexes into the cytoplasm (41). However, this proton sponge effect is apparently not sufficient to release the majority of PEI particles from the vesicles. In particular, endosomal escape represents a major hurdle to efficient gene transfer with small PEI polyplexes at low concentrations (19).

Since viruses have developed mechanisms to induce efficient endosomal escape, inactivated viruses, for example adenovirus, have been combined with PEI polyplexes to promote better endosomal release (42). A major drawback in using viruses, however, is their immunogenicity as well as their capacity to trigger inflammatory responses. To overcome these obstacles, a novel strategy to improve intracellular delivery of nonviral vectors was to incorporate membrane active peptides into the vector system. Such peptides were derived from viral proteins (25), toxins (43;44) or were synthetically designed (43;45); for review see (46). Among these membrane active peptides, the bee venom peptide melittin displayed particular strong membrane destabilizing activity, and this peptide successfully enhanced gene transfer with lipoplexes (47) and PEI polyplexes (48;49).

After endosomal release DNA complexes or free DNA have to traffic through the cytoplasm towards the nucleus, enter the nucleus and expose the DNA to the cell's transcription machinery. This process is not clearly elucidated yet. Passive diffusion of DNA within the cytoplasm is restricted (50) especially for larger plasmids, and free DNA can be degraded by nucleases within the cytoplasm. Therefore, the delivery of DNA towards the nucleus is supposed to depend mainly on the transport of intact complexes by microtubule or actin filaments (51). Nuclear import of DNA or DNA complexes is another big hurdle, which is currently only easily overcome in rapidly dividing cells. For example, transfection of non-dividing cells with PEI polyplexes was several log units less effective compared to transfection of mitotic cells where the nuclear envelope was broken down (52). Either before or after nuclear import dissociation of the complex has to occur in order to allow transcription of the DNA. Dissociation of the DNA from PEI in the cytosol or within the nucleus could be due to

interaction with an excess of anionic macromolecules such as RNA (53) and/or exchange reactions with positively charged histone proteins.

Despite these barriers, some nonviral vectors such as PEI polyplexes have reached high transfection efficiencies *in vitro* and also *in vivo*. For example, PEI polyplexes carrying a DNA vector for TNF-α expression demonstrated encouraging therapeutic effects in various tumor models (54). Notably, tail vein administration of such TNF-α polyplexes into tumor bearing mice led to tumor-specific TNF-α expression, tumor necrosis and remarkable tumor regression. Therefore, PEI polyplexes are promising candidates for the development of improved vector systems.

1.2.5 Key issues for improved PEI polyplexes

For improved gene delivery with PEI polyplexes two major issues are *i)* to improve the toxicity profile of the applied vectors and *ii)* to enhance endosomal escape, one of the major barriers limiting gene transfer efficiency.

1.2.5.1 Improving the toxicity profile of PEI polyplexes

The low efficiency of PEI polyplexes is currently partly compensated by administration of high amounts of these nonviral vectors. However, even PEG-shielded polyplexes are not inert, and polyplex components can mediate toxic side effects. In addition, it was observed previously that in standard PEI polyplexes generated at charge ratios above N/P 5 up to 80 % of PEI is unbound (55;56) and that cellular toxicity of polyplexes directly correlates with increased N/P ratios (57;58). Toxic effects of PEI observed at the cellular level range from changes in the gene expression pattern of e.g. endothelial cells (57) to the induction of apoptosis, for example in spleen lymphocytes (59). These results suggest that toxicity is at least partially attributed to free PEI and that purification of polyplexes to remove such contaminating polycations would be desirable. A stable formulation of clearly defined composition is also indispensable to fulfill general requirements of a potential therapeutic gene delivery system. Recently, a method based on ultrafiltration was used in order to remove free PEI (55). However, the removal of free PEI using this method was incomplete (56).

Therefore, the first aim of this thesis was to develop an easy and effective method which allows complete removal of free PEI from polyplexes. Based on this method, a further aim was to study transfection properties of such purified polyplexes *in vitro* and to evaluate their toxicity profiles in comparison to non-purified polyplexes. Moreover, the aim was to clarify the role of free PEI in gene delivery with PEI polyplexes at the cellular level.

1.2.5.2 Enhancing endosomal escape of PEI polyplexes

As mentioned above, one major barrier limiting the transfection efficiencies of current polyplexes is poor endosomal release. The membrane active peptide melittin is one example of a pore-forming peptide that has been used to enhance the delivery of lipoplexes (47) and polyplexes (48). Melittin is the major toxic component of the honey bee venom and consists of 26 amino acids. Its structure can be divided into three domains (Fig. 3): an α-helical, hydrophobic domain (residue 1 to 13), an α-helical amphipathic region (residue 14 to 20) and a non-helical positively charged C-terminal region (residue 21 to 26).
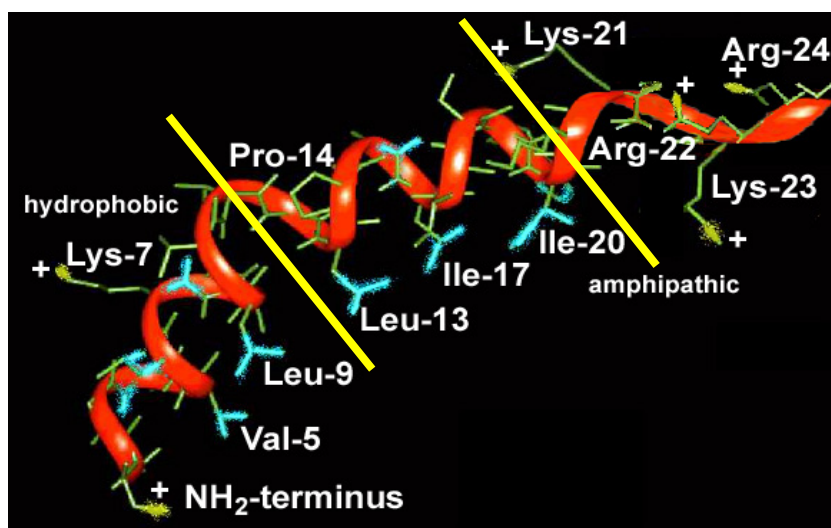
Fig. 3 Structure of melittin. Melittin contains a hydrophobic (residue 1 to 13) and an amphipathic (residue 14 to 20) α-helical region, which are connected by the helix breaker proline at position 14. The cationic C-terminal region (residue 21 to 26) is non-helical.

Because of its positive charges, melittin has been used as DNA condensing agent (47;60). Gene transfer efficiency of melittin/DNA complexes, however, was low and concomitant high toxicity was observed most likely because such complexes were unstable, and free melittin exposed pronounced cellular toxic effects in the

transfected cells. To achieve efficient and stable gene transfer formulations endosomal release agents like melittin have to be stably incorporated into the complexes. Therefore, melittin was covalently bound to the lipophilic residue dioleoyl-phosphatidylethanolamine. The hybrid molecule dioleoyl-melittin enabled efficient binding to DNA and high levels of reporter gene expression in different mammalian cells (47). Melittin was also used in PEI polyplexes. Melittin covalently attached to PEI significantly increased reporter gene expression in a broad range of cell lines, and even slowly dividing primary cells were susceptible to transfection (48). Another melittin-PEI conjugate with low molecular weight PEI was used to successfully enhance the delivery of RNA polyplexes (49). In these melittin-PEI conjugates, the polycation was covalently bound to the N-terminus of melittin.

These results indicate that melittin has the capacity to improve endosomal escape of nonviral vectors such as PEI polyplexes. The cationic character of melittin is of advantage for the use in polycation-based gene delivery systems, since covalent attachment of a positive peptide to a polycation will not lead to aggregation effects due to charge interactions between the peptide and the polycation. Incorporation of melittin into DNA polyplexes can even further stabilize the complex with DNA. In addition, synthetic all-(*D*)-melittin has hemolytic and antibacterial activities comparable to the L-enantiomer (61;62) which offers the opportunity to use non-immunogenic all-(*D*)-melittin for the generation of non-immunogenic polyplexes. Therefore, melittin was of special interest in the current thesis for the development of optimized PEI polyplexes with improved endosomal release capacity.

For the optimal incorporation of melittin into PEI polyplexes, the site of linkage to PEI was considered to be important, since it might affect the process of melittin-induced membrane pore formation triggering endosome destabilization. According to literature, melittin first inserts its N-terminus into the lipid bilayer (Fig. 4). In contrast, the cationic C-terminus does not insert but serves as a membrane anchor by interaction with the negatively charged lipid headgroups (63-66).
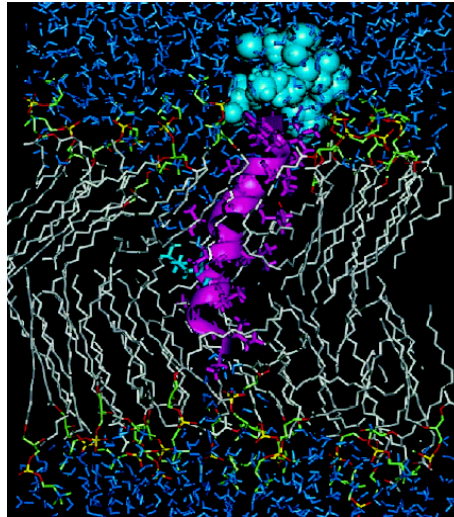
Fig. 4 Model of melittin inserted into a lipid bilayer. The cationic C-terminus of melittin (blue) anchors the peptide at the negatively charged lipid headgroups. The hydrophobic and amphipathic α-helical regions of melittin (purple) are inserted into the lipophilic core of the bilayer. Adapted from Bachar et al. (65).

With an increase in membrane-bound melittin, the peptide induces transmembrane pores according to the carpet or toroidal model (Fig. 5) (67). This results in lysis of bilayer membranes, e.g. lysis of erythrocytes. Sequence requirements for lytic melittin analogs include a free positively charged N-terminus (68;69) and a positively charged C-terminus (69;70).
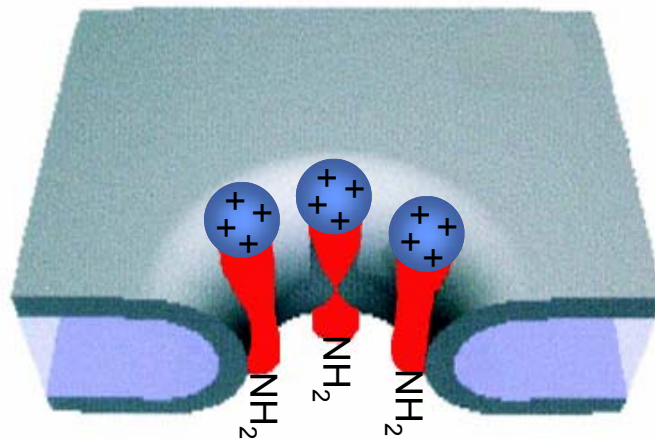
Fig. 5 Schematics of the toroidal model. The dark layers represent the headgroup regions of bilayers. Melittin monomers are represented by the red cylinders with the cationic C-terminal region shown in blue. The toroidal pore is formed by the lipid monolayer and melittin peptides which are in contact with the lipid headgroups. Adapted from Yang et al. (67).

Although the exact mechanism of pore formation remains to be elucidated, covalent attachment of the polycation PEI to the N-terminus of melittin is expected to prevent

membrane insertion and pore formation, whereas conjugation via the C-terminus is thought to enhance membrane anchoring and insertion of melittin.

To determine the optimal site of melittin-linkage to PEI, the strategy applied in this thesis was to synthesize two different melittin-PEI conjugates with PEI covalently attached to either the C-terminus or the N-terminus of non-immunogenic all-*(D)*-melittin. Polyplexes generated with these conjugates should be compared regarding their gene transfer efficiency, their membrane destabilizing activity and their capacity to induce endosomal release. The conjugate which shows the highest potency of membrane destabilization should then be further optimized for lytic activity at pH 5 to produce conjugates that are highly active inside acidic vesicles such as endosomes.

To obtain melittin-PEI conjugates with high lytic activity at pH 5, sequence modifications with glutamic acid residues or histidine residues were introduced at the C-terminus or the N-terminus of melittin. At physiological pH such melittin analogs do not fulfill the charge requirements of active melittin analogs. At acidic pH, however, glutamic acid and histidine are fully protonated which should restore all sequence requirements resulting in active pore-forming peptides and peptide conjugates.

Finally, the aim was to incorporate the most active melittin PEI conjugates into surface-shielded and receptor-targeted PEI polyplexes. These polyplexes should be purified from unbound, potentially toxic PEI or melittin-PEI conjugates. Such a polyplex formulation would represent an example for the development of an artificial virus-like vector: it carries different functional domains which enable stabilization, shielding against unspecific interactions, cell targeting, and efficient intracellular delivery.

2   Materials and Methods

2.1   Chemicals and reagents

Branched PEI (B-PEI) with an average molecular weight of 25 kDa was obtained from Sigma-Aldrich (Taufkirchen, Germany). Linear PEI (L-PEI) with an average molecular weight of 22 kDa is available from Euromedex (Exgen 500, Euromedex, Souffelweyersheim, France). PEI was used at a 1 mg/ml stock solution neutralized with HCl.

Succinimidyl 3-(2-pyridyldithio) propionate (SPDP) was purchased from Fluka (Buchs, Switzerland).

Cysteine-modified melittin peptides and melittin analogs were obtained from Genzentrum (group of G.J. Arnold, Munich, Germany), or IRIS Biotech (Marktredwitz, Germany). Peptides were synthesized with a purity of > 95 % and were used as acetate salts after lyophilization in 4 % acetic acid.

Melittin with a cysteine residue at the N-terminus of melittin (N-mel) had the following sequence:

N-mel: CIGA VLKV LTTG LPAL ISWI KRKR QQ

Glycine-1 of native melittin was replaced by cysteine.

The sequence of melittin with cysteine at the C-terminus of melittin (C-mel) was:

C-mel: GIGA VLKV LTTG LPAL ISWI KRKR QQC

Cysteine was added to the sequence of native melittin at position 27.

N-mel was synthesized both in all-(*L*) and in all-(*D*)-configuration. C-mel was synthesized using (*D*)-amino acids.

C-mel-analogs (CMA) with acidic modified sequences were synthesized using (*L*)-amino acids and had the following structures:

CMA-1:   EE GIGA VLKV LTTG LPAL ISWI KRKR QQC

CMA-2:   GIGA VLKV LTTG LPAL ISWI HHHH EEC

CMA-3:   GIGA VLKV LTTG LPAL ISWI KRKR EEC

CMA-4:   EE GIGA VLKV LTTG LPAL ISWI HHHH QQC

Egg phosphatidylcholine (egg PC) was purchased from Lipoid (Ludwigshafen, Germany). Calcein, trinitrobenzenesulfonic acid (TNBS) and all other chemicals were purchased from Sigma-Aldrich (Taufkirchen, Germany).

PEG-PEI22 (molar ratio of 20 kDa PEG to 22 kDa L-PEI was 2/1) and PEG-PEI25 conjugates (molar ratio of 20 kDa PEG to 25 kDa B-PEI was 1/1) were synthesized and purified as previously described in Kursa et al. (71). EGF-PEG-PEI25 conjugate linked with a heterobifunctional 3.4 kDa PEG derivative was synthesized as described in (28).

Plasmid pCMVLuc (Photinus pyralis luciferase under control of the CMV enhancer/promoter) described in Plank et al. (25) was produced endotoxin-free by Elim Biopharmaceuticals (San Francisco, CA, USA) or Aldevron (Fargo, ND, USA). Plasmid pEGFP-N1 (encoding Enhanced Green Fluorescent Protein (EGFP) under the control of the CMV promoter) was purchased from Clontech Laboratories, Inc. (Palo Alto, CA, USA).

2.2   Quantitative analysis of B-PEI and L-PEI

2.2.1 TNBS assay

The concentration of L-PEI and B-PEI was measured by trinitrobenzenesulfonic acid (TNBS) assay (72). Standard PEI solutions and test solutions containing B-PEI or L-PEI were serially diluted in 0.1 M sodium tetraborate to a final volume of 100 µl using a 96 well plate, resulting in PEI concentrations of 10 to 40 µg/ml or 100 to 400 µg/ml for B-PEI or L-PEI, respectively. To each well 2.5 µl of TNBS (75 nmol) diluted in water was added. TNBS reacts with primary amino groups of PEI to form colored trinitrophenylated derivatives. After 10 min at room temperature (RT), absorption was measured at 405 nm using a microplate plate reader (Spectrafluor Plus, Tecan Austria GmbH, Grödig, Austria).

2.2.2 Copper complex assay

L-PEI was also quantified by a copper complex assay at 285 nm following the procedure published by Ungaro et al. (73). Equal amounts (100 µl) of Copper-(II)-sulfate dissolved 0.1 M sodium acetate (0.23 mg/ml), pH 5.4 were mixed with standard L-PEI samples or test solutions of L-PEI containing 10 to 60 µg/ml L-PEI diluted in water. The resulting Cu(II)/PEI-complexes were quantified by measuring the absorbance at 285 nm using a Cary 3 Bio spectrophotometer (Varian, Mulgrave, Australia). For the quantification of L-PEI in the presence of DNA, the concentration of L-PEI is calculated by the equation:

$$C_{L\text{-}PEI} = (ABS_{TOT} - ABS_{DNA}) / \varepsilon_{L\text{-}PEI/Cu(II)} * b$$

ABS_{TOT}: absorbance at 285 nm of L-PEI/Cu(II) in the presence of DNA

ABS_{DNA}: absorbance at 285 nm of the L-PEI polyplex

$\varepsilon_{L\text{-}PEI/Cu\,(II)}$: molar absorptivity of L-PEI/Cu(II) at 285 nm ($\varepsilon_{L\text{-}PEI/Cu(II)} = 6.31 \times 10^{5}$)

b: fixed optical path length (cm)

Since the L-PEI content is measured at 285 nm (as L-PEI/Cu(II) complex), the absorption of DNA (ABS_{DNA}) present in the solution is substantial and must be subtracted from the total absorption (ABS_{TOT}).

2.3 Covalent labeling of DNA and PEI

Plasmid pCMVLuc was covalently labeled with the fluorophore Cy3 using the Label IT kit (MIRUS, Madison, WI, USA) according to the manufacturer's instructions. Cy3 content was measured by absorption at 552 nm and DNA was quantified by measuring the absorbance at 260 nm. On average one Cy3 molecule was bound per 50 bp.

PEI was covalently labeled with Cy5 by suspending one vial of FluoroLink™ Cy5 monofunctional dye (Amersham Biosciences, Freiburg, Germany) in 1 ml of L- or B-PEI solution (1 mg/ml PEI) in HEPES-buffered saline (HBS, 150 mM NaCl, 20 mM HEPES, pH 7.1). After 2 h at RT unreacted dye was removed by size exclusion chromatography using a Sephadex G25 superfine column (Pharmacia Biotech, Uppsala, Sweden) equilibrated in HBS. Cy5 content was measured by absorption at

663 nm; PEI content was measured by TNBS assay (2.2.1). The molar ratios of PEI/Cy5 were 1/2 and 2/1 for L-PEI and B-PEI, respectively.

2.4 Conjugate synthesis

2.4.1 Synthesis of 3-(2-pyridyldithio)-propionate-modified B-PEI

B-PEI (1.25 μmol) in 2 ml buffer (0.35 M NaCl, 20 mM HEPES, pH 8) was mixed with 3-(2-pyridyldithio)propionic acid N-hydroxy-succinimide ester (SPDP, 25 μmol) dissolved in 200 μl dimethyl sulfoxide (DMSO). After 2 h at RT B-PEI with pyridyldithio-propionate-linkers (B-PEI-PDP) was purified by gel filtration using an Äkta Basic HPLC System (Amersham Biosciences, Freiburg, Germany) equipped with a Sephadex G-25 superfine HR 10/30 column (Pharmacia Biotech, Uppsala, Sweden) equilibrated in 250 mM NaCl, 20 mM HEPES, pH 7.4; the flow rate was 0.5 ml/min. The void fractions containing PEI were pooled, aliquots were snap frozen in liquid nitrogen and stored at -80°C. PEI content was measured by TNBS assay (2.2.1). The degree of modification with dithiopyridine linker was determined spectrophotometrically at 343 nm by release of pyridine-2-thion (molar absorptivity = 8080 M^{-1} cm^{-1}) after reduction of an aliquot with excess dithiothreitol (DTT, 100 mM). For the synthesis of mel-PEI and CMA-PEI conjugates, two different PEI-PDP batches were used with a molar ratio of PEI/PDP of approximately 1/15 and 1/10, respectively.

2.4.2 Synthesis of C-mel-PEI and N-mel-PEI conjugates

The cysteine-modified C-mel or N-mel peptides (2.5 μmol) were dissolved in 500 μl of 0.5 M NaCl, 20 mM HEPES, pH 7.1 and mixed with 450 μl PEI-PDP (90 nmol PEI, 1.35 μmol PDP) diluted in the same buffer under argon. The molar excess (1.8-fold) of peptide to PDP present in PEI-PDP was used to enhance reaction with the dithiopyridine linker. After 4 h at RT released thiopyridone was measured at 343 nm to determine the extent of the reaction. Melittin-PEI conjugates were purified on a Macroprep High S cation-exchange column (Bio-Scale MT 2, BioRad, Munich, Germany) by gradient elution with 10 % to 60 % of buffer A (Buffer A: 5 M NaCl, 20 mM HEPES, pH 7.1; buffer B: 20 mM HEPES pH 7.1) at a flow rate of 0.5 ml/min.

Conjugates were eluted between 2 and 3 M NaCl as monitored at 230 nm and 280 nm. Main fractions were pooled, concentrated and desalted (final salt concentration 75 to 150 mM) on Centricon Plus-20 centrifugal filter units (10 kDa cut off, Millipore, Bedford MA, USA). Conjugates were sterile filtered and aliquots were snap frozen in liquid nitrogen and stored at -80°C. B-PEI content of the melittin-PEI conjugates was determined by TNBS assay (2.2.1). Melittin also reacts with TNBS but molar absorptivity of trinitrophenylated melittin derivatives is approximately 10-fold lower than the colored product with PEI and, therefore, quantification of B-PEI is not significantly affected by the presence of melittin. The concentration of melittin in the conjugates was measured by absorption at 280 nm (molar absorptivity of melittin = 5570 M^{-1} cm^{-1}). C-mel-PEI and N-mel-PEI conjugates were obtained with a mean recovery of 55 % based on analysis of PEI (50 nmol of PEI and 840 nmol of melittin). The molar ratio of PEI to melittin was 1/16.

2.4.3 Synthesis of CMA-PEI conjugates

PEI conjugates of melittin analogs (CMA-PEI conjugates) were prepared similarly as described for C- and N-mel-PEI conjugates (2.4.2). In brief, the dissolved peptides were mixed with PEI-PDP (molar ratio of PEI/PDP was 1/10) at a 1.7- (CMA-1), 2.5- (CMA-2), 2.2- (CMA-3) and 2.2-fold (CMA-4) molar excess of peptide to PDP. Since the melittin analogs CMA-3 and CMA-4 had limited solubility at pH 7, the pH of the reaction mixture was adjusted to pH 5 and pH 4 for synthesis of CMA-3-PEI and CMA-4-PEI, respectively. Conjugates were purified by cation-exchange chromatography as described above and then concentrated using a 10 ml stirred ultrafiltration cell (Millipore, Bedford MA, USA) equipped with an ultrafiltration membrane of regenerated cellulose (10 kDa cut off, Millipore, Bedford MA, USA). Before use, the membrane was conditioned with PEI by filtration of PEI (2 mg) in 10 ml water to reduce unspecific binding of the conjugates to the membrane. The conjugates were then concentrated and desalted to a final salt concentration of 30 to 60 mM NaCl, 20mM HEPES, pH 7.1. Conjugates were sterile filtered and aliquots were snap frozen and stored at -80°C. PEI concentration of the conjugates was measured by TNBS assay (2.2.1), and the peptide concentration was calculated based on the molar absorptivity of melittin at 280 nm. In the case of incomplete

reaction of the peptides with the PDP linkers, the amount of conjugated peptide was determined at 343 nm by release of pyridine-2-thion from residual PDP linkers after reduction with DTT. Conjugates were obtained with recoveries based on analysis of PEI of 40 % (CMA-1-PEI, 80 nmol PEI, 380 nmol CMA-1), 7 % (CMA-2-PEI, 10 nmol PEI, 80 nmol CMA-2), 15 % (CMA-3-PEI, 35 nmol PEI, 225 nmol CMA-3) and 11 % (CMA-4-PEI, 20 nmol PEI, 150 nmol CMA-4); the molar ratios of PEI to CMA-peptide were 1/5-8.

An improved purification procedure was developed for the synthesis of CMA-2-PEI and CMA-3-PEI conjugates. The new protocol is based on size exclusion chromatography and leads to higher yields of purified conjugates. Superdex 75 prep grade (60 ml) in water (Amersham Biosciences, Freiburg, Germany) was conditioned by drop wise application of 10 ml B-PEI (10 mg) to reduce unspecific binding of the conjugates. The conditioned gel material was filled into a HR 10/30 column (Pharmacia Biotech, Uppsala, Sweden) and equilibrated in 0.5 M NaCl, 20 mM sodium acetate, pH 5 at a flow rate of 0.5 ml/min. Conjugates were applied to the column and the void fractions containing PEI were dialyzed against 50 mM NaCl 20 mM HEPES, pH 7.4 using a 5 ml QuixSep dialyzer (Roth, Karlsruhe, Germany) equipped with a 14 kDa cut off membrane. After dialysis, conjugates were sterile filtered and aliquots were snap frozen in liquid nitrogen and stored at -80°C. CMA-2-PEI and CMA-3-PEI conjugates were obtained with a recovery of 53 % (CMA-2-PEI, 100 nmol PEI, 900 nmol CMA-2) and 30 % (CMA-3-PEI, 60 nmol PEI, 540 nmol CMA-3) based on analysis of PEI.

2.5   Polyplex formation

Plasmid DNA encoding luciferase or EGFP was condensed with PEI or peptide-PEI conjugates at an N/P ratio of 6. DNA/PEI polyplexes were prepared at a final DNA concentration of 20, 100 or 200 µg/ml as described in (74). Briefly, indicated amounts of plasmid DNA and PEI or peptide-PEI conjugates were each diluted in HEPES-buffered glucose (HBG, 5% (w/w) glucose, 20 mM HEPES, pH 7.1) and rapidly mixed by pipetting up and down 5 to 8 times.

EGF-receptor-targeted polyplexes were prepared by first diluting and mixing EGF-PEG-PEI and PEG-PEI conjugates with free PEI or peptide-PEI conjugates at indicated ratios in HBG. The used ratios (% w/w) were all based on the PEI content of the different components. The PEI conjugate buffer solution was then mixed with plasmid DNA diluted in HBG at an N/P ratio of 6 and a final DNA concentration of 20 or 100 µg/ml.

Targeted and non-targeted polyplexes were allowed to stand for at least 20 min at RT before use.

2.6 Measurement of particle size and zeta potential

Particle size of transfection complexes was measured by laser-light scattering using a Malvern Zetasizer 3000HS (Malvern Instruments, Worcestershire, UK). Polyplexes were generated in HBG at DNA concentrations of 100 or 200 µg/ml and subsequently diluted to 10 µg/ml prior to measurement. Targeted polyplexes were prepared and analyzed in HBS at a DNA concentration of 20 µg/ml. For estimation of the surface charge, transfection complexes were diluted in 10 mM NaCl to give a final DNA concentration of 2 µg/ml and the zeta potential was measured as previously described (75). The average conductivity observed for all formulations was approximately 1 mS.

2.7 Purification of polyplexes by size exclusion chromatography

Size exclusion chromatography (SEC) was performed using a BioLogic HR System equipped with a Bio-Scale MT 2 column (7 x 52mm, 2.3 ml column volume; Bio-Rad Munich, Germany) packed with Sephacryl S-200 HR (molecular weight exclusion limit 250 kDa for globular proteins; Pharmacia Biotech, Uppsala, Sweden). After equilibration in HBG, the column was conditioned by a single application of 200 µg L- or B-PEI to reduce unspecific adsorption of polyplexes. Volumes up to 2 ml containing up to 200 µg/ml DNA/PEI polyplexes were loaded onto the column. SEC was performed at a flow rate of 0.5 ml/min and fractions of 0.3 ml were collected. The elution of DNA polyplexes was monitored at 254 nm. Fractions containing the major amounts of DNA were pooled and the DNA was quantified by measuring the absorbance at 260 nm. DNA concentration was calculated by 1 OD_{260} = 45 µg/ml or

40 µg/ml for DNA bound to L-PEI or B-PEI, respectively. These values have been calculated by comparing standard PEI polyplexes with free plasmid DNA (1 OD_{260} = 50 µg/ml). L-PEI content of the fractions was quantified by copper complex assay (2.2.2) and B-PEI content was analyzed by TNBS assay (2.2.1). The TNBS assay is not significantly affected by the presence of DNA. From the concentrations of PEI and DNA determined in the purified polyplexes, their final N/P ratios were calculated. N/P ratios of purified complexes were also verified by DNA mobility shift assay using agarose gel electrophoresis (76).

2.8   Cell culture

Cell culture media, antibiotics and fetal calf serum (FCS) were purchased from Invitrogen GmbH (Karlsruhe, Germany). All cultured cells were grown at 37° C in 5 % CO_2 humidified atmosphere. CT 26 murine colon carcinoma cells (ATCC CRL-2638), B16-F10 murine melanoma cells (kindly provided by I.J. Fidler, Texas Medical Center, Houston, TX, USA) and HeLa human cervical carcinoma cells (ATCC CCL-2) were cultured in DMEM supplemented with 10 % FCS. A-10 rat aortic smooth muscle cells (DSZM, ACC 132) were grown in DMEM supplemented with 20 % FCS. Neuro2A murine neuroblastoma cells (ATCC CCl-131) and Renca-EGFR mouse renal carcinoma cells stably transfected with pLTR-EGFR and pSV2neo (kindly provided by Winfried Wels, Georg-Speyer-Haus, Frankfurt am Main, Germany) were cultured in RPMI-1640 with Glutamax I medium supplemented with 10 % FCS and 0.5 mg/ml geneticin (for Renca-EGFR only). HUH-7 hepatocellular carcinoma cells (JCRB 0403; Tokyo, Japan) were grown in DMEM high glucose/F12 (1/1) supplemented with 10 % FCS. Primary endothelial cells (PEC) were isolated from explants of porcine aortic vessels and cultured in M 199 medium supplemented with 10 % FCS, 4 mM glutamine, 100 U/ml penicillin, 100 µg/ml streptomycin and 2.5 mg/ml amphotericine B as described in (77).

2.9   Luciferase reporter gene expression

Cells were plated in 96 well plates (TPP, Trasadingen, Switzerland) at a density of 10^4 cells (PEC and Neuro2A cells) or 5 x 10^3 cells (all other cell lines) per well 24 h prior to transfection. Transfection complexes with indicated amounts of DNA

(pCMVLuc) were added to the cells in 100 µl fresh culture medium containing 100 U/ml penicillin and 100 µg/ml streptomycin. Culture medium (100 µl) was added 4 h after transfection. When using targeted polyplexes for transfection, medium was replaced after 4 h by 200 µl fresh culture medium. Gene expression was measured after 24 h. Detection of luciferase activity was carried out as described recently (48). Transfection efficiency was expressed as relative light units (RLU) per seeded cells (mean +/- SD of triplicates). Two ng of recombinant luciferase (Promega, Mannheim, Germany) correspond to 10^7 light units.

2.10 EGFP reporter gene expression

HeLa cells were seeded in 24 well plates (TPP, Trasadingen, Switzerland) at a density of 3×10^4 cells per well 24 h prior to transfection. Transfection complexes with indicated amounts of DNA (pEGFP-N1) were added to the cells in 500 µl fresh culture medium containing 100 U/ml penicillin and 100 µg/ml streptomycin. Culture medium (500 µl) was added 4 h after transfection. Cells were harvested 24 h after transfection by treatment with trypsin/EDTA solution (Invitrogen GmbH, Karlsruhe, Germany) and kept on ice until analysis. The DNA stain propidium iodide (PI) was added to the cell suspension at 1 µg/ml to discriminate between viable and dead cells. PI only penetrates the nucleus after cell membrane integrity is lost. The percentage of dead cells and transfected cells was quantified using a Cyan™ MLE flow cytometer (DakoCytomation, Copenhagen, Denmark). PI fluorescence was excited by a UV line at 351-364 nm and emission was detected using a 665±20 nm bandpass filter. Dead cells were excluded by gating PI-positive cells by forward scatter versus PI fluorescence. EGFP fluorescence was excited at 488 nm and emission was detected using a 530±40 nm bandpass filter and a 613±20 nm bandpass filter to analyze EGFP positive cells by diagonal gating (19). To exclude doublets, cells were appropriately gated by forward scatter versus pulse width, and 2×10^4 gated events per sample were collected. Experiments were performed in triplicates.

2.11 Metabolic activity of transfected cells

Cells were plated in white, clear bottom 96 well plates (Nalge Nunc International, Naperville, IL, USA) at a density of 5 x 10^3 cells per well 24 h prior to transfection. Transfection of cells was carried out as described above (2.9). Metabolic activity was assayed 24 h after transfection using the CellTiter-Glo Luminescent Cell Viability Assay (Promega, Mannheim, Germany) according to the manufacturer's instructions. The assay is based on the quantitative measurement of the cellular ATP content. Metabolic activity was calculated as percentage of non-transfected control cells (corresponding to 100 % metabolic activity).

2.12 Flow cytometric analysis of cellular polyplex association

Cells were seeded in 12 well plates (TPP, Trasadingen, Switzerland) at a density of 10^5 cells per well 24 h prior to transfection. PEI polyplexes containing Cy3-labeled DNA (10 %) and Cy5-labeled PEI (2 % or 10 % for L-PEI or B-PEI, respectively) were added to the cells at a concentration of 3 µg/ml DNA per well in 1 ml fresh culture medium. Cells were harvested after 4 h incubation at 37° C by treatment with trypsin/EDTA solution (Invitrogen GmbH, Karlsruhe, Germany) and kept on ice until cell association of polyplexes was assayed using a Cyan MLE flow cytometer (DakoCytomation, Copenhagen, Denmark). The fluorophores Cy3 and Cy5 were excited at 488 nm and 635 nm, respectively, and emission was detected at 575±25 nm and 665±20 nm, respectively. Data acquisition was performed in linear mode and data were analyzed in logarithmic mode. To discriminate between viable and dead cells, cells were appropriately gated by forward versus sideward scatter; to exclude doublets cells were gated by forward scatter versus pulse width, and 2 x 10^4 gated events per sample were collected. Experiments were performed at least in triplicates.

2.13 Laser scanning microscopy

Cells were seeded in Lab-Tek 8 Chambered Coverglasses (Nalge Nunc International, Naperville, IL, USA) at a density of 2 x 10^4 cells per chamber 24 h prior to transfection. Cells were transfected with Cy3-labeled DNA complexes (4 % Cy3-DNA) at a concentration of 2 µg/ml DNA per chamber in 200 µl fresh culture medium

supplemented with 20 mM HEPES, pH 7.4. For co-localization analysis, free PEI containing 75 % Cy5-labeled PEI was added simultaneously or 4 h post-transfection.

Live cell imaging was performed 8 h after transfection using a confocal laser scanning microscope (LSM 510 Meta, Carl Zeiss, Jena, Germany) equipped with an argon and two helium/neon lasers delivering light at 488, 543 and 633 nm, respectively. Light was collected through a 63 x 1.4 NA oil immersion objective (Zeiss). Cy3 fluorescence was excited with the 543 nm line; emission was collected using a 560 nm long-pass filter. Excitation of Cy5 fluorescence was achieved by using the 633 nm line, with the resulting fluorescent wavelengths observed using a 650 nm long-pass filter. No signal overspill between the individual fluorescence channels was observed. An optical section thickness of 0.6 µm was chosen. Transmitted light images (excitation at 488 nm) were collected using differential interference contrast (DIC). Digital image recording and image analysis were performed with the LSM 5 software, version 3.0 (Zeiss).

2.14 Transmission light and epifluorescence microscopy

Cells were seeded in 48 well plates at a density of 3×10^4 cells per well 24 h prior to transfection. Cells were transfected with DNA complexes encoding for EGFP at a concentration of 2 µg/ml or 4 µg/ml DNA per well in 500 µl fresh culture medium. Transmission light microscopy of living cells was performed 2 h after transfection using an Axiovert 200 microscope (Carl Zeiss, Jena, Germany) equipped with a Sony DSC-S75 digital camera (Sony Corporation, Tokyo, Japan). Light was collected through a 32 x 0.25 NA objective (Zeiss), and images were captured using phase contrast.

Live cell imaging of EGFP expressing cells was performed 24 h after transfection using an Axiovert 200 fluorescence microscope (Carl Zeiss, Jena, Germany) equipped with a Zeiss Axiocam camera. Light was collected through a 10 x 0.25 NA or 20 x 0.4 NA objective (Zeiss). EGFP fluorescence was excited using a 470±20 nm bandpass filter, and emission was collected using a 540±25 nm bandpass filter. For the labeling of dead cells, PI was added to the culture medium at a concentration of 1 µg/ml, and PI fluorescence was excited using a 560±30 nm bandpass filter;

emission was collected through a 615 nm long-pass filter. Digital image recording and image analysis were performed with the Axiovision 3.1 software (Zeiss).

2.15 Video fluorescence microscopy

Collagen-coated cover slips were fixed with mounting medium to the bottom of a Petri dish containing a hole, thereby forming a round cavity with a glass bottom of defined optical thickness and a diameter of approximately 1 cm. HeLa cells were seeded into this cavity at a density of 5×10^3 cells. After 24 h the cell membrane was labeled by incubation of cells with 2.6 nmol of the lipophilic dye 1,1'-dioctadecyl-3,3,3',3'-tetramethylindodicarbocyanine (DiD) (Molecular Probes, Leiden, The Netherlands) diluted in 1 μl of DMSO and 200 μl culture medium for 10 to 60 min at 37°C. To generate labeled polyplexes, plasmid DNA was first stained with the dimeric cyanine nucleic acid stain TOTO-1 (Molecular Probes) by mixing pCMVLuc (0.25 mg) diluted in 100 μl water with TOTO-1 (1.26 nmol) dissolved in 1.26 μl of DMSO. This results in an approximate ratio of 300 DNA base pairs to one TOTO-1 dye molecule. Such labeled DNA was then used to prepare C-mel-PEI polyplexes as described above (2.5). Polyplexes were added to the DiD-labeled cells at a DNA concentration of 4 μg/ml in 30 μl of fresh culture medium and cells were immediately viewed by video fluorescence microscopy using the spinning disk confocal laser scanning microscope system UltraView Live Cell Imager (PerkinElmer, Boston, MA, USA). A Krypton-Argon ion laser delivered light at 488 and 568 nm to the confocal scanning head. Emission was selected by a 500 nm long-pass and a 600±20 nm bandpass emission filter. Light was collected through a 100 x 1.4 NA oil immersion objective and images were captured by a cooled digital CCD camera (Hamamatsu Photonics K.K., Hamamatsu City, Japan) and acquired using the ImagingSuite Acquisition and Processing Software (PerkinElmer). Time-lapse confocal images of cells after the addition of C-mel-PEI polyplexes were collected at 34 s intervals for 20 min. An optical thickness of 1 μm was chosen. DiD fluorescence was excited with the 568 nm line, and emission was collected using a 600±20 nm bandpass filter. Excitation of TOTO-1 fluorescence was achieved by using the 488 nm line, with the resulting fluorescent wavelengths observed using a 500 nm long-pass filter. Images were

processed into AVI movies by using the Volocity 3-D/4-D Visualization software (Improvision, Lexington, KY, USA).

2.16 Erythrocyte leakage assay

Human erythrocytes were isolated from fresh citrate treated blood and washed in phosphate-buffered saline (PBS) by four centrifugation cycles, each at 800 g for 10 min at 4° C. The erythrocyte pellet was diluted 10-fold in 150 mM NaCl. Peptides and peptide conjugates were serially diluted in 90 µl buffer (HBS, pH 7.1 or 150 mM NaCl, 15mM citric acid, pH 5) using a V-bottom 96 well plate, resulting in peptide concentrations of 0.25 – 16 µM. For 100 % lysis, control wells contained buffer with 1 % Triton-X-100. Erythrocyte suspension (10 µl, containing approximately 10^9 erythrocytes) was added to each well and the plates were incubated at 37 °C for 30 min under constant shaking. After centrifugation at 300 g for 10 min, 50 µl supernatant was analyzed for hemoglobin release at 450 nm using a microplate plate reader (Spectrafluor Plus, Tecan Austria GmbH, Grödig, Austria). Experiments were performed in duplicates.

2.17 Liposome leakage assay

Phosphatidylcholine (PC) liposomes loaded with calcein at a self-quenching concentration were prepared using the film-method. Egg PC (12.5 µmol) was dissolved in chloroform in a round bottom flask. Solvent evaporation resulted in the formation of a thin film on the wall of the glass vessel. The lipid film was dried under high vacuum and then hydrated with 5 ml solution of 100 mM calcein (dissolved by the addition of 375 mM NaOH) and 50 mM NaCl. Hydration and formation of liposomes were facilitated by rotating the flask for 4 h at 40°C. The liposomes were subsequently extruded through a 200 nm polycarbonate filter using a hand extruder (LiposoFast-Basic, Avestin, Ottawa, Canada) heated to 40°C. Non-entrapped material was removed from liposomes by gel filtration on a Sephadex G 25 column in 200 mM NaCl, 20 mM HEPES, pH 7.4. Purified liposomes were diluted 100-fold in 150 mM NaCl, 30 mM citrate, pH 5. For leakage assays, peptide conjugates were serially diluted in 150 mM NaCl, 30 mM citric acid, pH 5, resulting in peptide concentrations of 0.125 – 4 µM. Liposome suspension (100 µl) was added to 100 µl

of diluted peptide conjugates in black 96 well plates. For 100 % lysis, liposomes were added to control wells containing 1 % Triton-X-100 in buffer. After 30 min incubation at RT, plates were assayed for calcein fluorescence at 530 nm (excitation at 485 nm) on a microplate reader (Spectrafluor Plus, Tecan Austria GmbH, Grödig, Austria). Experiments were performed in duplicates.

2.18 Cell lysis assay

HeLa cells were plated in 96 well plates (TPP, Trasadingen, Switzerland) at a density of 5 x 10^3 cells per well, 24 h prior to analysis. Culture medium was removed and 100 µl of melittin-PEI conjugates serially diluted in serum free DMEM with 30 mM citrate, pH 5 were added to the cells at peptide concentrations of 0.125 – 16 µM. After 30 min incubation at 37°C metabolic activity of viable, non-lysed cells was assayed using the CellTiter-Glo Luminescent Cell Viability Assay (Promega, Mannheim, Germany) according to the manufacturer's instructions. Control cells incubated with DMEM pH 5 correspond to 100 % metabolic activity. Experiments were performed in duplicates.

3   Results

3.1   Purification of PEI polyplexes

3.1.1   Purification of PEI polyplexes by size exclusion chromatography

PEI polyplexes were prepared in HEPES-buffered glucose (HBG) resulting in the formation of 100-150 nm particles (see also (19;20)). Size exclusion chromatography (SEC) on a Sephacryl S-200 matrix pre-conditioned with PEI was used to purify PEI polyplexes after polyplex formation. SEC allowed complete removal of free PEI from polyplexes (Fig. 6). Column conditioning with PEI reduced unspecific binding of polyplexes and improved polyplex recovery. Up to 80 % recovery rates for both plasmid DNA and PEI were obtained (mean recovery of 53 % or 63 % for DNA and 68 % or 72 % for PEI after SEC of L-PEI and B-PEI polyplexes, respectively).
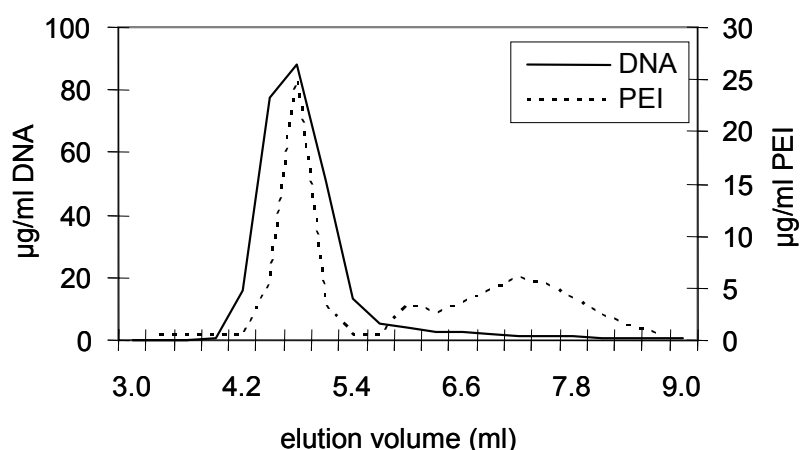
Fig. 6. Purification of PEI polyplexes by SEC. Typical elution profile of DNA and L-PEI after purification of 650µl DNA/L-PEI polyplex N/P 6 in HBG containing 200µg/ml DNA

The biophysical properties of L-PEI and B-PEI polyplexes before and after SEC were analyzed (Table 1). For both PEI polyplexes, size and surface charge were not significantly changed after the removal of free PEI by SEC. SEC of polyplexes with different N/P ratios ranging from 6 to 12 resulted in purified polyplexes with a similar final N/P ratio of approximately 2.5, suggesting that at this N/P ratio all DNA phosphate residues are saturated with positively charged PEI nitrogens.

Polyplex	SEC	Size (nm)	Zeta potential (mV)	N/P ratio
L-PEI N/P 6	-	150 +/- 35	20.8 +/- 3.2	6
	+	140 +/- 31	23.8 +/- 3.6	2.5
B-PEI N/P 6	-	130 +/- 27	27.6 +/- 5.6	6
	+	124 +/- 10	21.6 +/- 2.6	2.8
B-PEI N/P 12	-	116 +/- 26	41.7 +/- 7.2	12
	+	103 +/- 25	23.0 +/- 7.5	2.3

Table 1. Biophysical properties of polyplexes before and after SEC purification

Purification was also tested with polyplexes generated at a low N/P ratio of 3 or in a salt containing buffer (75 mM NaCl, 2.5 % glucose). Polyplex recovery, however, was as low as 10 % (data not shown). This is most likely attributed to the increased initial particle size (> 300 nm and > 1 µm, respectively) and subsequent loss of the material on the column. Aggregated polyplexes probably could not pass in between the gel beads and therefore got stuck on the column.

3.1.2 Reporter gene expression and toxicity of purified polyplexes

Reporter gene expression (luciferase activity) and cellular toxicity were evaluated in three different tumor cell lines (CT 26, B16-F10 and HeLa cells) after the application of different polyplex preparations (Fig. 7). For transfection experiments, all polyplexes were generated at an N/P ratio of 6. Polyplex preparations included non-purified polyplexes, SEC-purified polyplexes and purified polyplexes supplemented with free PEI equivalent to the amount of free PEI present in non-purified polyplexes (purified plus free PEI).
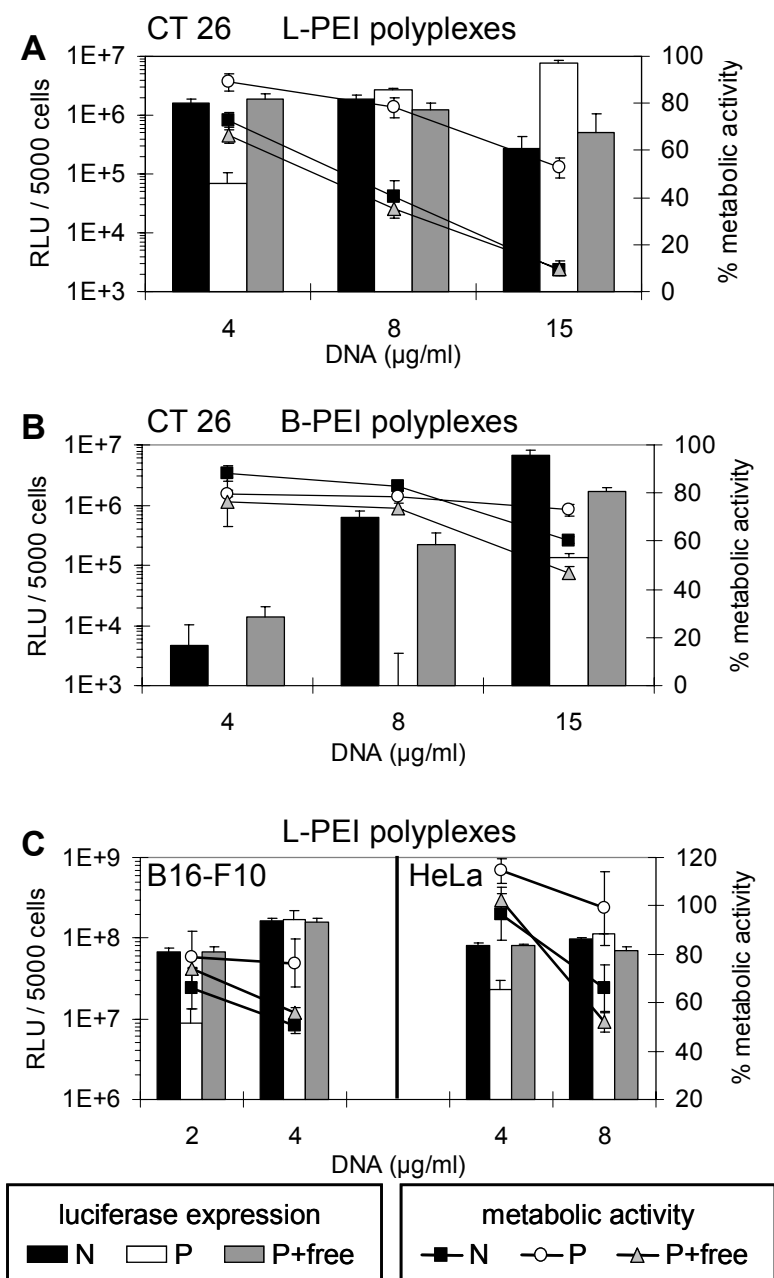
Fig. 7. Reporter gene expression and metabolic activity in different tumor cell lines. CT 26 cells were transfected with L-PEI (A) and B-PEI polyplexes (B) with increasing concentrations of DNA. (C) B16-F10 cells (left) and HeLa cells (right) were transfected with L-PEI polyplexes. Luciferase activity is displayed in bars (RLU, left y-axis), metabolic activity is displayed as lines in % of untransfected control cells (right y-axis). 'N': non-purified polyplexes; 'P': purified polyplexes; P + free: purified polyplexes plus free PEI added. Mean values + SD of triplicates are shown.

At low DNA concentrations, purified L-PEI polyplexes (Fig. 7A and C) were up to 20-fold less efficient in transfection compared to polyplexes containing free PEI (with or without SEC). At high DNA concentrations [≥ 8 µg/ml (Fig. 7A CT 26, Fig. 7C HeLa) and ≥ 4 µg/ml (Fig. 7C, B16-F10)], however, purified L-PEI polyplexes showed equivalent or even higher transfection efficiency than polyplexes with free PEI. The

enhanced transfection efficiency may be attributed to a low toxicity of purified particles, resulting in the survival of more transfected cells in the absence of excess PEI.

In order to evaluate toxicity of purified polyplexes, metabolic activity of cells was determined 24 h after transfection by measuring intracellular ATP levels. L-PEI polyplexes containing free PEI exerted high toxicity at high DNA doses [≥ 8 μg/ml (Fig. 7A CT 26, Fig. 7C HeLa) and ≥ 4 μg/ml (Fig. 7C, B16-F10)]; metabolic activity determined 24 h after transfection was reduced to as low as 10 % of the untransfected control cells (Fig. 7A). Using purified L-PEI polyplexes, however, metabolic activity was maintained at 50 - 90 % compared to control cells (Fig. 7A and Fig. 7C). This indicated that at high DNA doses the calculated enhanced transfection efficiency of purified polyplexes was mainly due to the lower toxicity of these particles in comparison to non-purified complexes. Therefore, to better estimate gene expression of surviving cells, luciferase activity was calculated as RLU related to metabolic activity (Fig. 8). Notably, at high DNA doses (15 μg/ml) normalized gene expression of purified, low toxic polyplexes was still five-fold higher than that of non-purified polyplexes which displayed pronounced toxicity (viability 10%, Fig. 7A right).
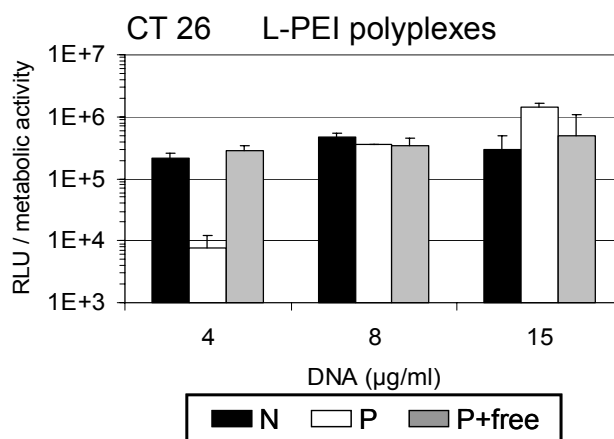
Fig. 8 Normalized gene expression. Luciferase activity data from Fig. 7A (transfection of CT 26 cells with L-PEI polyplexes) were normalized to the metabolic activity. 'N': non-purified polyplexes; 'P': purified polyplexes; P + free: purified polyplexes plus free PEI added. Mean values + SD of triplicates are shown.

In line with the results obtained with L-PEI particles, purified B-PEI polyplexes showed reduced transfection efficiency in CT 26 cells in comparison to polyplexes containing free PEI (Fig. 7B). Furthermore, Fig. 7B shows that the difference in

transfection efficiency is becoming smaller with rising DNA concentrations. Similar results were obtained with B16-F10 and HeLa cells (data not shown). At DNA concentrations below 15 µg/ml metabolic activity after transfection with all B-PEI polyplexes was only slightly reduced compared to untransfected control cells (Fig. 7B). At the highest DNA dose tested (15 µg/ml DNA) purified B-PEI polyplexes were the least toxic resulting in 10 - 20 % higher metabolic activity compared to polyplexes with free PEI.
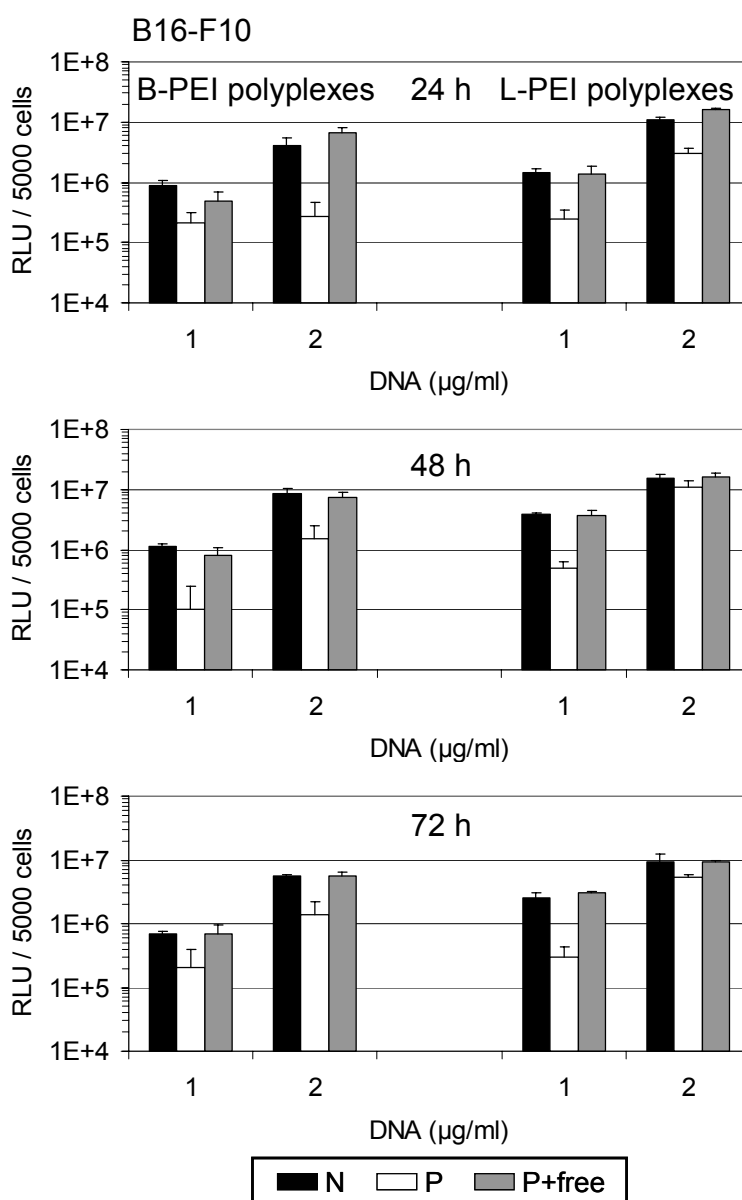
Fig. 9 Long term reporter gene expression. B16-F10 cells were transfected with B-PEI (left) and L-PEI (right) polyplexes. Luciferase activity was analyzed 24 h, 48 h and 72 h after transfection. 'N': non-purified polyplexes; 'P': purified polyplexes; P + free: purified polyplexes plus free PEI added. Mean values + SD of triplicates are shown.

Long term gene expression using low doses of DNA was analyzed 48 h and 72 h after transfection of B16-F10 cells with purified polyplexes or polyplexes containing free PEI, and gene expression levels were compared to the levels measured after 24 h (Fig. 9). The applied low DNA doses were overall non-toxic and transfection with all polyplexes resulted in stable levels of gene expression over 72 h. Luciferase activity after transfection with purified polyplexes was reduced compared to polyplexes with free PEI over the whole expression time monitored.
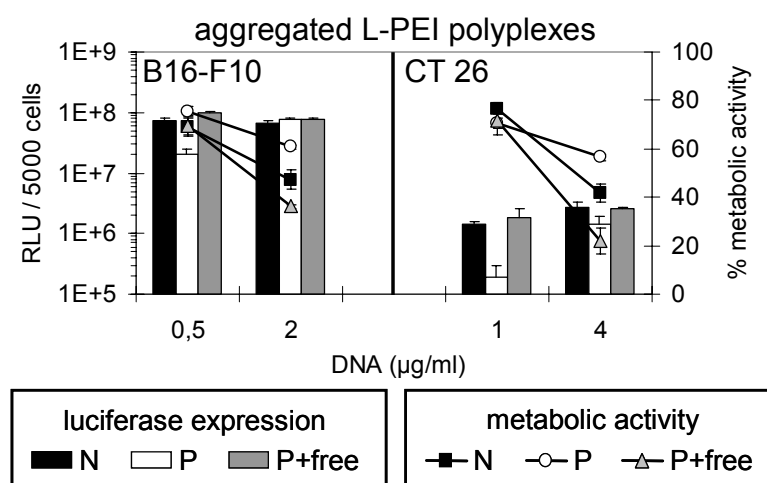

Fig. 10 Reporter gene expression and metabolic activity after transfection with aggregated polyplexes. B16-F10 cells (left) and CT 26 cells (right) were transfected with aggregated L-PEI polyplexes (size > 1µm) with increasing concentrations of DNA. Polyplex aggregates were obtained by adding salt to polyplexes generated in HBG. Luciferase activity is displayed in bars (RLU, left y-axis), metabolic activity is displayed as lines in % of untransfected control cells (right y-axis). 'N': non-purified polyplexes; 'P': purified polyplexes; P + free: purified polyplexes plus free PEI added. Mean values + SD of triplicates are shown.

Aggregated polyplexes (≥ 1 µm) are known to mediate high gene transfer efficiency *in vitro* (19;20). Therefore, aggregated L-PEI polyplexes were generated by adding HEPES-buffered saline (HBS, 150 mM NaCl) to polyplexes prepared in HBG (final DNA concentration 20 µg/ml, final buffer concentration 75 mM NaCl). HBS was added 30 min prior to transfection to either non-purified or purified L-PEI polyplexes with or without free PEI. Particle size of all aggregated L-PEI polyplexes was larger than 1 µm. Gene transfer with non-purified aggregated polyplexes was up to 10-fold higher than with the respective purified polyplexes. Metabolic activity with aggregated polyplexes containing free PEI was 20 – 70 % compared to control cells, whereas the metabolic activity was 60 – 70 % with purified polyplexes (Fig. 10). The influence of

free PEI on both gene transfer and toxicity was less pronounced with aggregated polyplexes than observed with the small polyplexes generated in HBG.

3.1.3 Enhanced cellular association of purified PEI polyplexes

Since purified polyplexes displayed lower transfection efficiency at low DNA concentrations, it was further investigated whether this was due to altered cellular association. This was studied by flow cytometry using Cy3-labeled plasmid and Cy5-labeled PEI for complex formation (Table 2).

L-PEI-polyplex	Cy3 signal (DNA)	Cy5 signal (PEI)
control	2.26 +/- 0.07	2.17 +/- 0.19
non-purified	10.89 +/- 0.47	79.50 +/- 8.22
purified	15.22 +/- 1.46	38.26 +/- 2.94
purified + free PEI-Cy5	10.15 +/- 0.72	56.51 +/- 6.10
purified + free PEI	10.39 +/- 1.46	29.82 +/- 1.51
B-PEI-polyplex	Cy3 signal (DNA)	Cy5 signal (PEI)
control	2.60 +/- 0.05	2.48 +/- 0.09
non-purified	19.04 +/- 1.79	213.26 +/- 14.45
purified	38.69 +/- 0.76	217.83 +/- 12.85
purified + free PEI-Cy5	16.37 +/- 0.89	186.76 +/- 10.35
purified + free PEI	16.17 +/- 0.89	94.24 +/- 3.87

Table 2. Cellular association of double-labeled L-PEI and B-PEI polyplexes determined by flow cytometry. Median channel values +/- SD of at least triplicates are shown.

For both L-PEI and B-PEI polyplexes, cellular association of DNA (Cy3 signal) was increased with purified polyplexes, and DNA association was reduced upon addition of free PEI (purified plus free PEI or free Cy5-PEI). The absence of free PEI in purified polyplexes led to significantly reduced total PEI association (Cy5 signal) after incubation with L-PEI polyplexes, whereas total PEI association was not altered in the corresponding experiment with B-PEI polyplexes. For both L-PEI and B-PEI polyplexes, the addition of unlabeled PEI to purified polyplexes reduced cellular PEI

association. Control experiments confirmed that fluorescence intensities of Cy5-PEI and Cy3-DNA before and after polyplex formation were similar (no fluorescence quenching upon DNA compaction), and there was no signal overspill between the two fluorescence channels for Cy3 and Cy5 (data not shown).

Despite enhanced cellular association, gene transfer efficiency of purified polyplexes was reduced compared to non-purified complexes. These results implicated that not cellular association but reduced internalization and/or intracellular delivery were the major obstacles to efficient gene delivery with purified polyplexes.

3.1.4 Delayed administration of free PEI enhances gene expression

To determine whether simultaneous application of free PEI with the polyplexes was required for the observed transfection effects, a time course experiment was performed. L-PEI was added to CT 26 cells at equivalent amounts that had been removed by SEC, either simultaneously with purified L-PEI polyplexes or at 1 h or 4 h after transfection without replacing the transfection medium. Luciferase expression was determined 24 h after transfection (Fig. 11).

In line with previous transfection experiments (3.1.2), simultaneous addition of free PEI restored the transfection efficiency of purified polyplexes to the level of non-purified polyplexes. Surprisingly, the addition of free PEI to purified polyplexes at 1 h or 4 h after transfection increased reporter gene expression up to 100-fold compared to non-purified polyplexes; this effect was most pronounced at low DNA doses. Similar results were obtained in B16-F10 cells (Fig. 11B) and with B-PEI polyplexes in both CT 26 (Fig. 11C) and B16-F10 cells (Fig. 11D). Metabolic activity of all transfected cells was > 80 %.
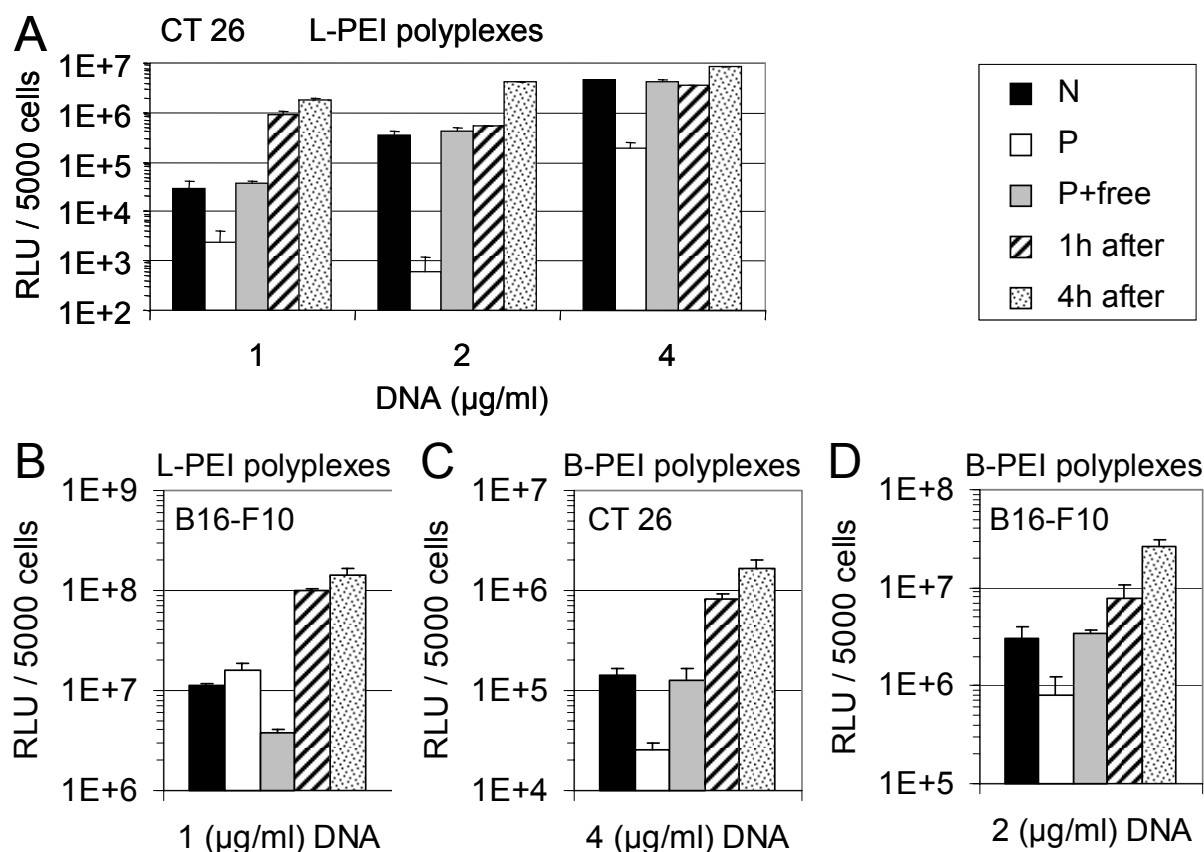
Fig. 11. *Reporter gene expression in CT 26 and B16-F10 cells with free L-PEI or B-PEI added at different time points. CT 26 cells (A) or B16-F10 cells (B) were transfected with the indicated concentrations of L-PEI polyplexes (both purified and non-purified) and free L-PEI was added to the cells at different time points after transfection without replacing the transfection medium. CT 26 cells (C) and B16-F10 cells (D) were transfected with B-PEI polyplexes and free B-PEI was added at different time points. 'N': non-purified polyplexes; 'P': purified polyplexes; P + free: purified polyplexes plus free PEI added simultaneously; '1 h after': purified polyplexes plus free PEI added 1 h after transfection; '4 h after': purified polyplexes plus free PEI added 4 h after transfection. Luciferase activity is presented as mean values + SD of triplicates. Metabolic activity of all transfected cells was > 80 %.*

3.1.5 Intracellular co-localization of free PEI and purified polyplexes

Free Cy5-labeled L-PEI was added to the cells either simultaneously with Cy3-labeled purified L-PEI polyplexes (Fig. 12A-C) or 4 h post-transfection when polyplexes were already completely internalized (Fig. 12D-F). After both simultaneous and delayed addition, the majority of free PEI was found to be co-localized with the internalized polyplexes at 8 h post-transfection. Control experiments with non-purified polyplexes revealed no differences in the intracellular pattern of Cy3-DNA distribution in comparison to purified polyplexes. Similar results

were obtained with B-PEI polyplexes (data not shown). These microscopic experiments were performed in cooperation with Katharina von Gersdorff.
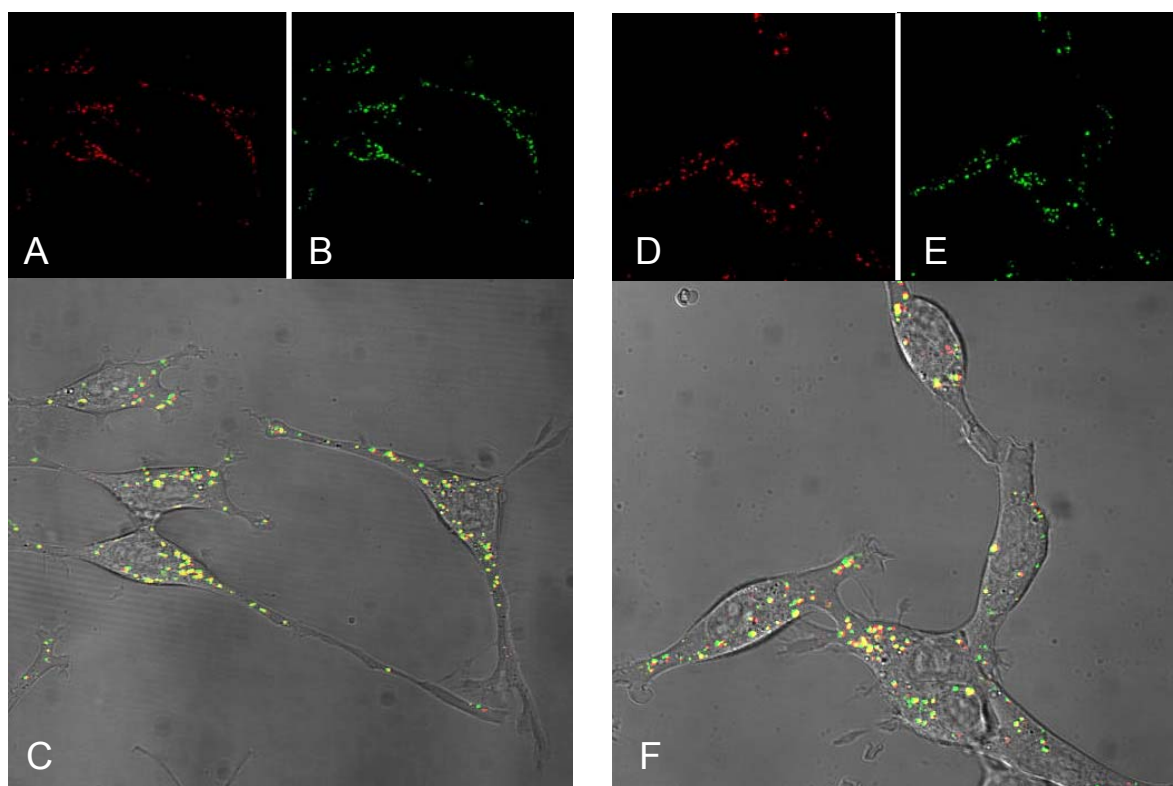
Fig. 12. Cellular localization of polyplexes and free PEI in CT 26 cells. CT 26 cells were transfected with DNA-labeled (Cy3) purified L-PEI polyplexes. Free Cy5-PEI was added either simultaneously (A, B, C) or 4h post-transfection (D, E, F) without replacing the transfection medium. Confocal laser scanning microscopy with living cells was carried out 8 h after transfection. (A, D) Cy3 fluorescence of labeled polyplexes (red fluorescence); (B, E) Cy5 fluorescence of labeled free L-PEI (green fluorescence); (C, F) overlay of both fluorescence channels (Cy3 and Cy5) with transmitted light (DIC). Yellow fluorescence indicates co-localization of Cy3-labeled polyplexes and Cy5-labeled free PEI.

In summary, purified PEI polyplexes demonstrated low cellular toxicity compared to polyplexes with free PEI. The removal of unbound PEI by SEC reduced the transfection efficiency of these purified vectors suggesting that free PEI played an important role in intracellular delivery of polyplexes. Cellular co-localization of free PEI with internalized PEI polyplexes implicated that free PEI most likely enhanced the release of polyplexes from endosomal vesicles after internalization. Hence, alternative measures to improve the transfection efficiency of purified PEI polyplexes are required, such as incorporation of endosomolytic peptides into the particles. To this end, the membrane active peptide melittin and melittin analogs were coupled to PEI and the resulting polyplexes were analyzed for their activities in gene transfer.

3.2 Comparison of C- versus N-terminally linked melittin-PEI conjugates

3.2.1 Synthesis and purification of C-mel-PEI and N-mel-PEI conjugates

B-PEI was coupled to the C-terminus (C-mel-PEI) or the N-terminus (N-mel-PEI) of all-(*D*)-melittin by the formation of a disulfide bond (Fig. 13). In addition, B-PEI was attached to the N-terminus of melittin in all-(*L*)-configuration. Dithiopyridine groups were first introduced into B-PEI by reaction of its primary amino groups with SPDP (78). Upon mixing of B-PEI-PDP with cysteine-modified melittin peptides, the dithiopyridine groups react with the free sulfhydryl groups of cysteine to the desired conjugates.
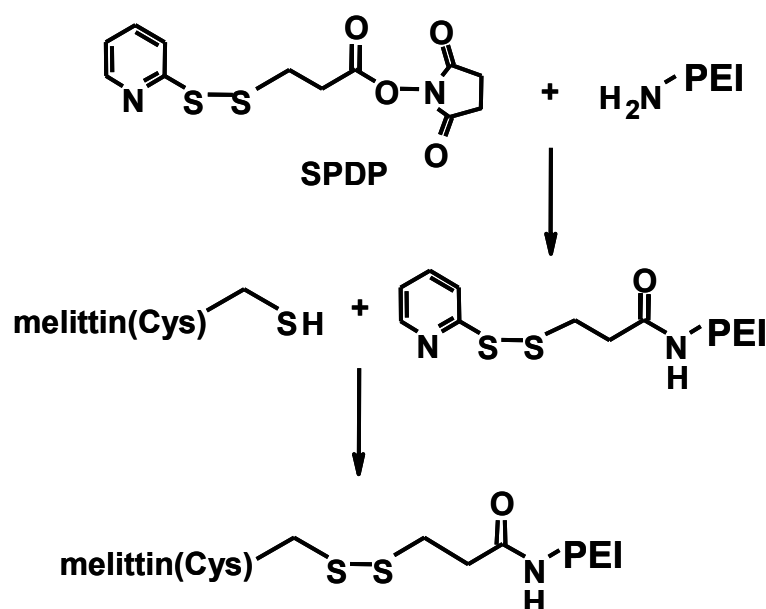
Fig. 13 Synthesis of melittin-PEI conjugates. The primary amino groups of PEI react with the succinimidyl group of SPDP resulting in PEI modified with dithiopyridine groups. In a second synthesis step the free sulfhydryl groups of cysteine at the N-terminus or the C-terminus of melittin react with dithiopyridine to the desired melittin-PEI conjugates.

Purification of the conjugates was performed by cation-exchange chromatography. The conjugate reaction mixture was loaded onto the column at a medium salt concentration of 0.5 M NaCl to avoid irreversible binding of the polycations to the resin, and subsequent salt gradient elution was performed from 0.5 to 3 M NaCl. This allowed relatively high melittin-PEI conjugate recovery rates with an approximate yield of 50 % based on analysis of PEI.

3.2.2   Reporter gene expression of N-mel-PEI polyplexes with melittin in all-*(D)* versus all-*(L)*-configuration

In contrast to previously published N-mel-PEI conjugates (48) which were synthesized with all-*(L)*-peptides, in this thesis the optimal site of melittin linkage to PEI was investigated using non-immunogenic all-*(D)*-melittin-PEI conjugates. All-*(D)*- and all-*(L)*-melittin were shown to have the same hemolytic and antibacterial activities (61;62). Nevertheless, it was unclear whether the transfection efficiency of melittin-PEI polyplexes depended on the peptide's enantiomeric configuration. Therefore, PEI was covalently attached to the N-terminus of all-*(L)*-melittin or all-*(D)*-melittin resulting in conjugates with 10 molecules melittin conjugated to one molecule PEI. The conjugates all-(*L*)-N-mel-PEI and all-(*D*)-N-mel-PEI were used to generate polyplexes, and transfection efficiency was determined in B16-F10 cells and HeLa cells in comparison to melittin-free B-PEI polyplexes. Mel-PEI polyplexes mediated 10-fold (all-(*L*)-N-mel-PEI) and 5-fold (all-(*D*)-N-mel-PEI) higher levels of luciferase activity than polyplexes without melittin (B16-F10, Fig. 14A). Moreover, FACS-analysis showed that 33 % and 26 % of HeLa cells were EGFP positive after transfection with all-(*L*)-N-mel-PEI and all-(*D*)-N-mel-PEI polyplexes, respectively, whereas transfection with melittin-free B-PEI polyplexes resulted in only 0.5 % EGFP positive cells (Fig. 14B).
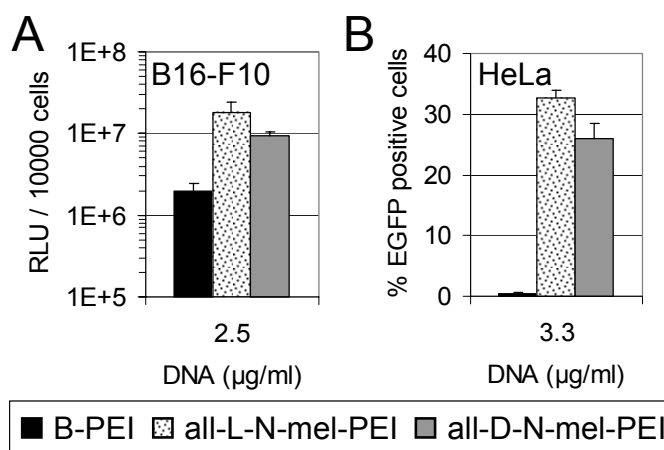

Fig. 14 Transfection efficiency of N-mel-PEI polyplexes containing all-(L)-melittin or all-(D)-melittin. B16-F10 cells (A) and HeLa cells (B) were transfected with B-PEI polyplexes or N-mel-PEI polyplexes of all-(L) or all-(D) melittin. Luciferase (A) and EGFP expression (B) was analyzed 24 h after transfection. Mean values + SD of triplicates are shown.

These data confirm that N-mel-PEI polyplexes mediate significantly higher transfection efficiency compared to polyplexes without melittin (48). Notably, gene transfer activity of melittin-PEI polyplexes does not depend on the enantiomeric configuration of the bound peptide, and thus, non-immunogenic all-(*D*)-peptides can be used for the generation of optimized melittin-PEI polyplexes.

3.2.3 Reporter gene expression of C-mel-PEI and N-mel-PEI polyplexes

To determine whether the site of melittin-linkage to PEI influences gene transfer activity, B-PEI was conjugated to the C-terminus (C-mel-PEI) or the N-terminus (N-mel-PEI) of all-(*D*)-melittin resulting in conjugates with 16 molecules melittin conjugated to one molecule PEI. Transfection efficiencies of polyplexes generated with C-mel-PEI or N-mel-PEI conjugates were compared to the efficiency of melittin-free B-PEI polyplexes. Luciferase reporter gene expression was evaluated in two different tumor cell lines (HeLa and CT 26 cells) and in slowly dividing primary porcine endothelial cells (PEC) (Fig. 15). Polyplexes were generated at N/P ratios ranging from 3 to 9. For all polyplexes an N/P ratio of 6 was found to be optimal for transfection of tumor cell lines, whereas N/P 7 was best in PEC cells (data not shown). These polyplexes were of small size (110 nm – 135 nm) and positively charged with a zeta potential in the range of +25 mV to +31 mV. In both tumor cell lines and in PEC cells N-mel-PEI polyplexes mediated the highest levels of luciferase activity with up to 25-fold (HeLa), 160-fold (CT 26) and 100-fold (PEC) higher transfection efficiencies compared to melittin-free B-PEI polyplexes. C-mel-PEI polyplexes were up to 5-fold and 25-fold more efficient than B-PEI polyplexes in HeLa and CT 26 cells, respectively. In slowly dividing PEC cells, however, transfection with C-mel-PEI polyplexes resulted in the lowest transfection levels compared to N-mel-PEI or B-PEI polyplexes.
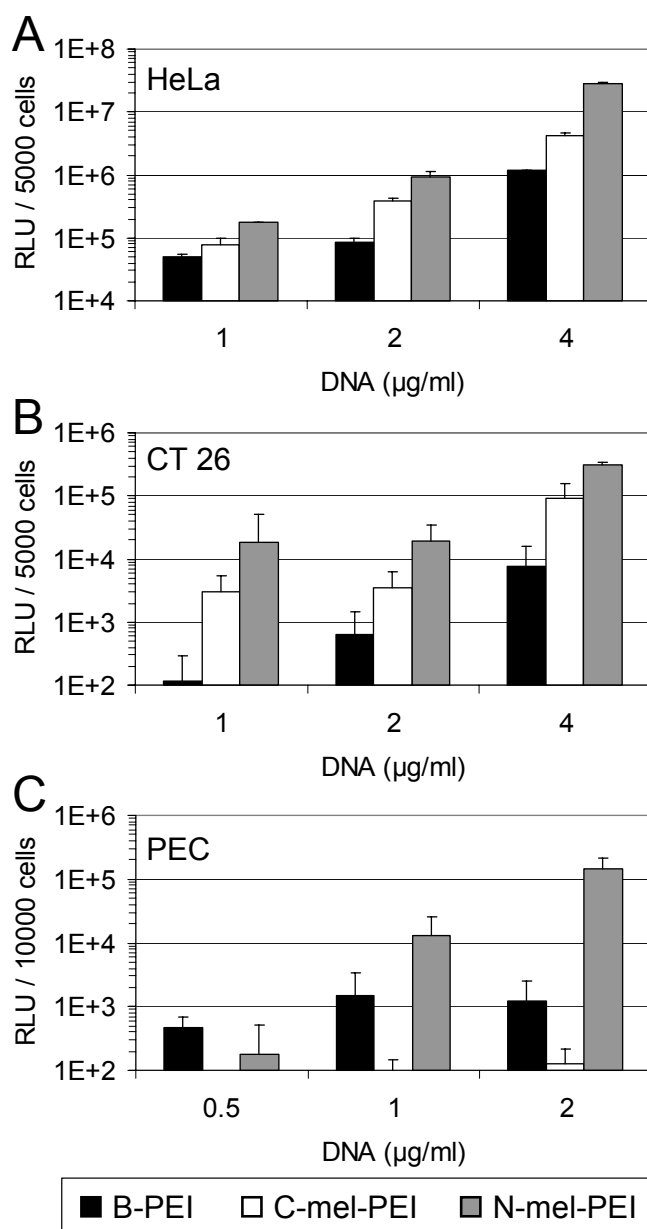
Fig. 15 Reporter gene expression (Luciferase activity) after transfection with C-mel-PEI or N-mel-PEI polyplexes. HeLa cells (A), CT 26 cells (B) and PEC cells (C) were transfected with B-PEI polyplexes or polyplexes of C-mel-PEI or N-mel-PEI with increasing concentrations of DNA. Luciferase activity is presented as mean values + SD of triplicates.

The percentage of transfected cells was analyzed by flow cytometry after transfection of HeLa cells with EGFP encoding DNA complexes (Fig. 16). To exclude damaged cells or cell debris, cells were appropriately gated by forward versus sideward scatter. In addition, PI was added to the analyzed cell suspension and intact but dead cells were excluded by gating only PI negative cells. Transfection with C-mel-PEI or N-mel-PEI polyplexes at 2 µg/ml DNA resulted in a 3-fold higher percentage of EGFP positive cells compared to B-PEI polyplexes; 8 % (C-mel-PEI) and 9 % (N-mel-PEI)

EGFP positive cells were achieved compared to 2.5 % positive cells when using B-PEI polyplexes for transfection (Fig. 16). At the higher DNA concentration (4 µg/ml), N-mel-PEI polyplexes were clearly the most efficient complexes. The percentage of EGFP positive cells with N-mel-PEI polyplexes was 42 %, whereas transfection with B-PEI and C-mel-PEI polyplexes only resulted in 11 % and 16 % of EGFP positive cells, respectively.
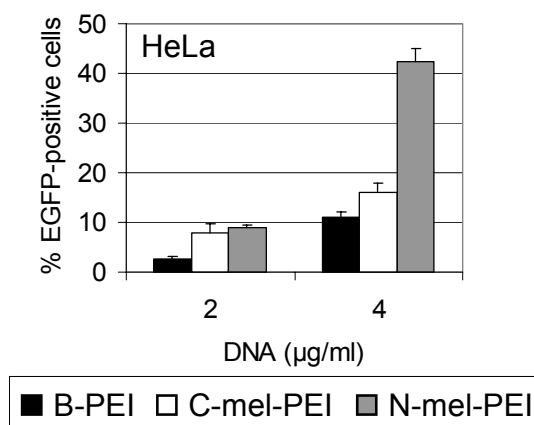
Fig. 16 Reporter gene expression (EGFP expression) after transfection with C-mel-PEI or N-mel-PEI polyplexes. HeLa cells were transfected with the indicated concentrations of B-PEI polyplexes or polyplexes of C-mel-PEI or N-mel-PEI. The percentage of EGFP positive cells is presented as mean values + SD of triplicates.

The high transfection efficiency of N-mel-PEI polyplexes compared to B-PEI and C-mel-PEI polyplexes at 4 µg/ml DNA was confirmed by analyzing the EGFP expression 24 h after transfection using epifluorescence microscopy (Fig. 17A-C). The number of green fluorescent HeLa cells was clearly highest after transfection with N-mel-PEI polyplexes (Fig. 17C).

The percentage of PI-labeled cells after transfection with polyplexes at a DNA concentration of 2 µg/ml was below 5 % as determined by FACS analysis, indicating that polyplexes exposed overall low toxicity. A low percentage of dead cells was also obtained after transfection with N-mel-PEI and B-PEI polyplexes at a higher DNA concentration of 4 µg/ml DNA. C-mel-PEI polyplexes, however, severely damaged cells at 4 µg/ml DNA. The percentage of intact cells was clearly reduced, and about 50 % of the gated intact cells were labeled with PI. The high percentage of dead PI positive cells after transfection with C-mel-PEI polyplexes at 4 µg/ml DNA was also visualized by epifluorescence microscopy (Fig. 17E). In contrast, the same amount of N-mel-PEI or B-PEI polyplexes exposed only moderate toxicity (Fig. 17D, F).
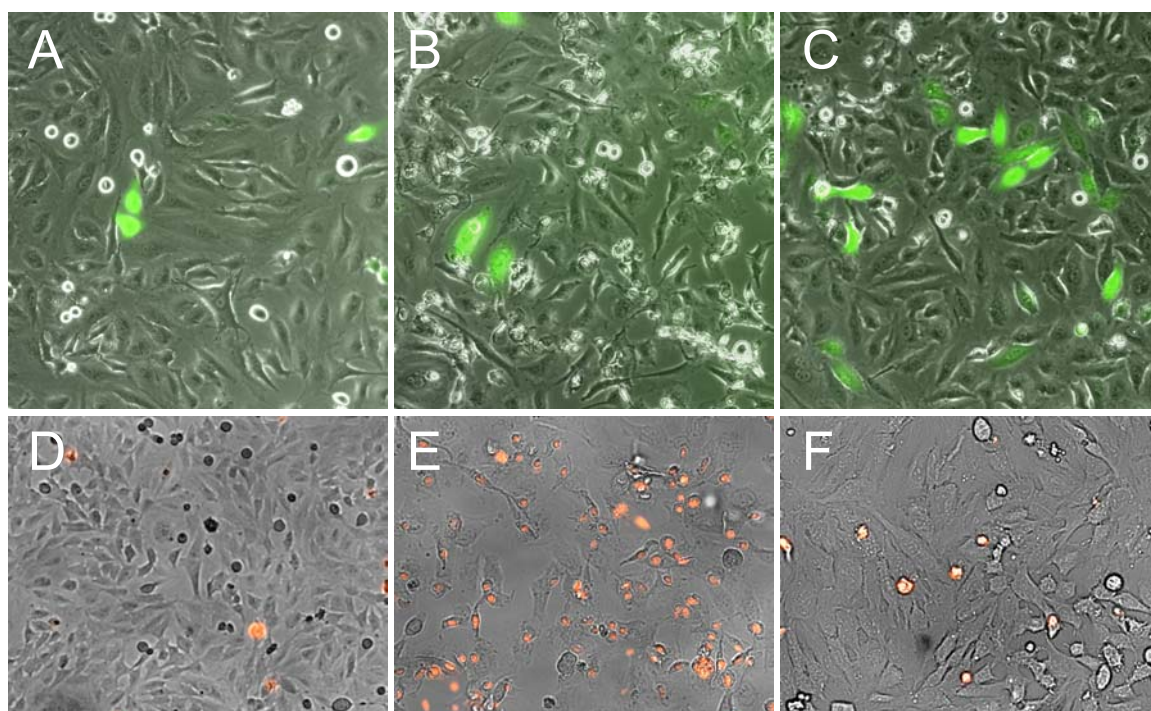
Fig. 17 EGFP expressing HeLa cells before and after live-dead stain with propidium iodide (PI). HeLa cells were transfected with B-PEI polyplexes (A, D), C-mel-PEI polyplexes (B, E) and N-mel-PEI polyplexes (C, F). Epifluorescence microscopy with living cells was carried out 24 h after transfection. Representative pictures of EGFP positive cells (green) (A-C) and dead PI-labeled cells (red) (D-F) are shown.

3.2.4 Toxicity of C-mel-PEI and N-mel-PEI polyplexes

In order to further evaluate the differences in toxicity of melittin-PEI polyplexes, relative metabolic activity was determined 24 h after transfection of HeLa cells by measuring intracellular ATP levels (Fig. 18).
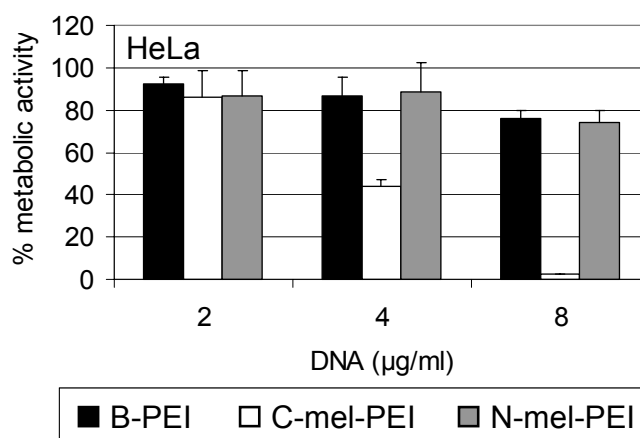
Fig. 18 Metabolic activity of HeLa cells 24 h after transfection. HeLa cells were transfected with the indicated concentrations of B-PEI polyplexes or polyplexes of C-mel-PEI or N-mel-PEI. Metabolic activity in % of untransfected control cells is presented as mean values + SD of triplicates.

At DNA concentrations below 4 µg/ml, metabolic activity after transfection with all polyplexes was only slightly reduced compared to untransfected control cells. At high DNA doses (4 or 8 µg/ml DNA), however, C-mel-PEI polyplexes dramatically reduced metabolic activity to as low as 2 % compared to control cells, whereas with both B-PEI and N-mel-PEI polyplexes metabolic activity was maintained above 75 %.
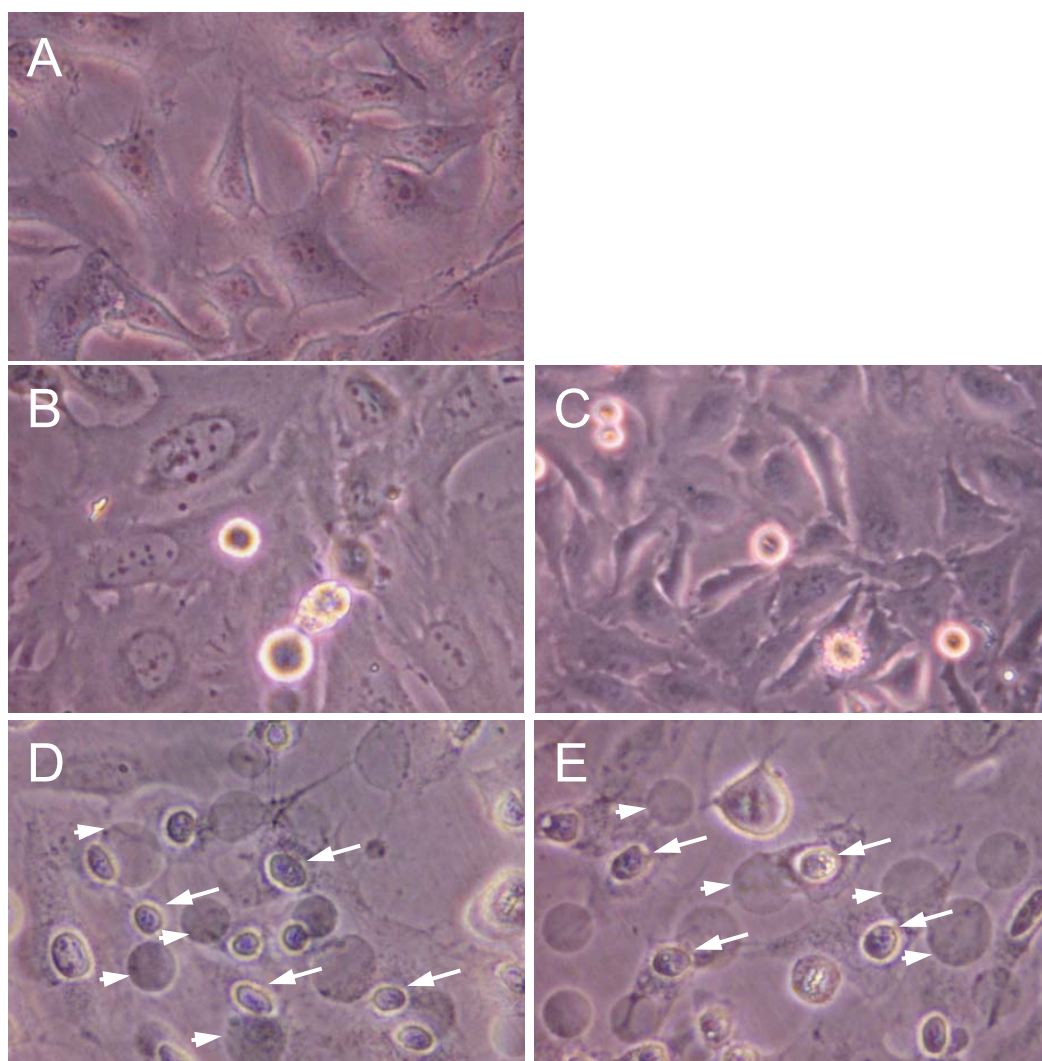
Fig. 19 Cellular disruption of HeLa cells by free or complexed C-mel-PEI. HeLa cells were incubated with B-PEI polyplexes (B), N-mel-PEI polyplexes (C), C-mel-PEI polyplexes (D) or C-mel-PEI conjugate (E). Transmission light images of living cells were captured after 2 h incubation. (A) untransfected control cells. Arrows indicate disrupted HeLa cells and arrow heads vesicles resembling membrane blebbing.

The toxic effects of C-mel-PEI polyplexes were already observed 2 h after transfection by light field microscopy (Fig. 19). HeLa cells transfected with C-mel-PEI polyplexes at a high DNA dose of 4 µg/ml DNA were severely damaged. Cells seemed to be disrupted and vesicles resembling membrane blebbing were observed

at the cell surfaces (Fig. 19D). Disrupted cells were also observed 2 h after the addition of free C-mel-PEI conjugate at concentrations equivalent to the amount of complexed C-mel-PEI at 4 µg/ml DNA (Fig. 19E). In contrast, cell morphology after transfection with B-PEI polyplexes or N-mel-PEI polyplexes at 4 µg/ml DNA (Fig. 19B, C) remained similar to untransfected control cells (Fig. 19A).

3.2.5 Cell lysis induced by C-mel-PEI polyplexes

The process of HeLa cell disruption after transfection with C-mel-PEI polyplexes at a concentration of 4 µg/ml DNA was further investigated using time-lapse confocal laser scanning microscopy. Lipid membrane structures of HeLa cells including the plasma membrane were labeled with DiD, a fluorescent lipophilic dye that spontaneously accumulated within cell membranes. The DNA intercalating dye TOTO-1 was used to label DNA complexes of C-mel-PEI. Immediately after start of transfection confocal images of cells and C-mel-PEI polyplexes were captured at 34 s intervals for 20 min. Fig. 20 shows selected confocal images taken from a time-lapse series.

Association of C-mel-PEI polyplexes with the plasma membrane and pseudopodia of cells was observed within the first minutes after transfection (Fig. 20A), followed by contraction of the pseudopodia towards the cell's body (Fig. 20A-C). Shortly after polyplex association blebbing of DiD-stained lipid vesicles from the plasma membrane was monitored (Fig. 20C-F). Some labeled C-mel-PEI polyplexes were found to be associated with these vesicles, suggesting that the polyplexes induced such membrane blebbing. The vesicle formation indicated lysis of the plasma membrane which was induced shortly after addition of C-mel-PEI polyplexes. The observed cell lysis is most likely related to the membrane destabilizing activity of melittin within the conjugate. Similar cell lysis, however, was not detected with free or complexed N-mel-PEI conjugate, indicating that the covalent attachment of PEI to the C-terminus or the N-terminus of melittin determined the membrane destabilizing activity of the resulting melittin-PEI conjugate.
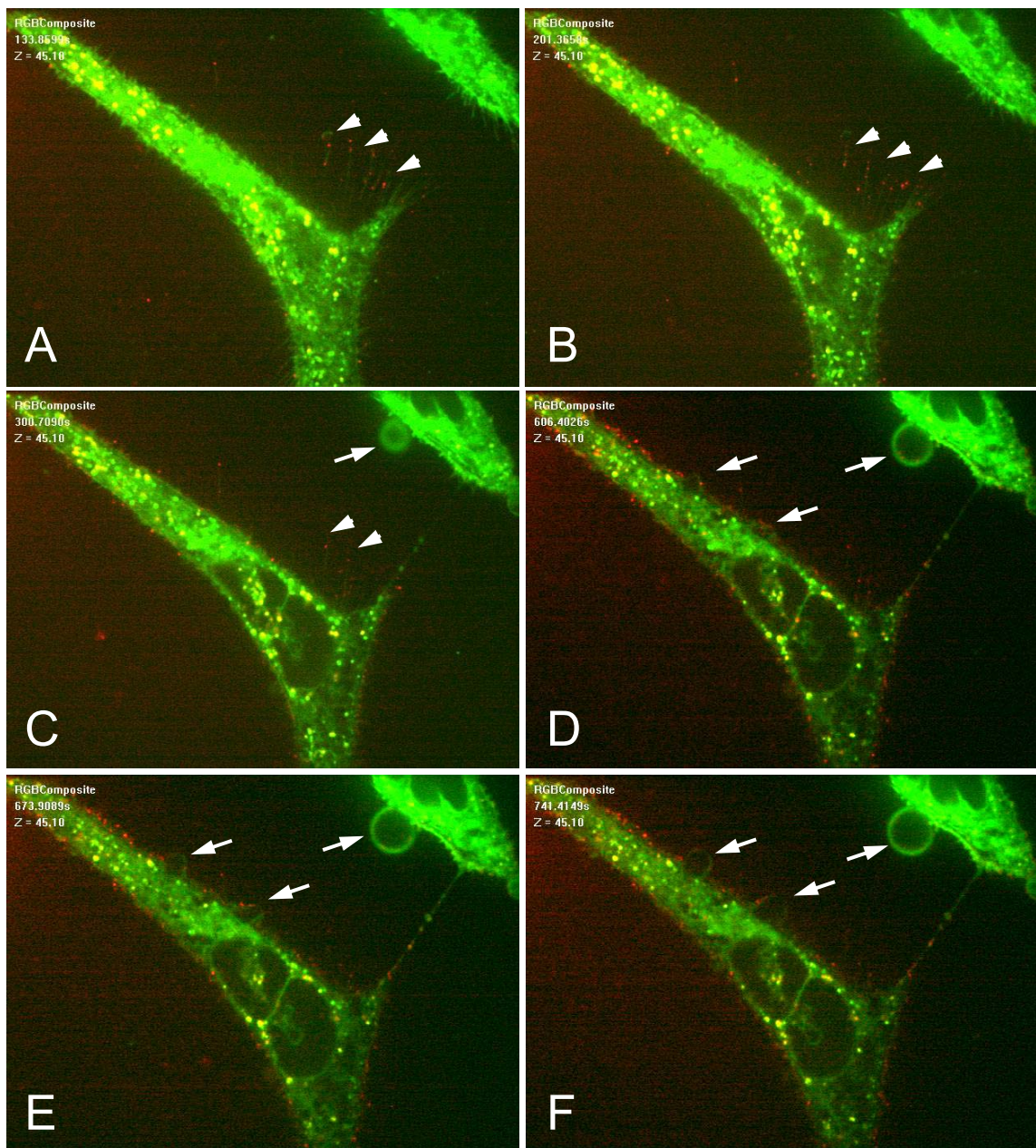
Fig. 20 Cell lysis induced by C-mel-PEI polyplexes. DiD-labeled HeLa cells were transfected with TOTO-1-labeled C-mel-PEI polyplexes. Confocal laser scanning microscopy with living cells was carried out immediately after start of transfection. Selected images of HeLa cells (green fluorescence) and polyplexes (red fluorescence) taken from a time-lapse series over 20 min are shown. Arrow heads indicate pseudopodia with associated polyplexes and arrows indicate membrane blebbing.

3.2.6 Lytic activities of C-mel-PEI and N-mel-PEI at neutral pH

In order to compare the membrane destabilizing activity of C-mel-PEI and N-mel-PEI at neutral pH, the lytic activities were tested on erythrocytes (Fig. 21). Erythrocytes were incubated with the free melittin peptides (C-mel and N-mel) and melittin-PEI conjugates in HBS, pH 7.1, for 30 min at 37°C. The free peptides C-mel and N-mel

exposed similar lytic activity over the whole concentration range tested, and 50 % lysis was observed at 16 µM and 8 µM melittin with C-mel and N-mel, respectively. The lytic activity of N-mel-PEI conjugate was similar compared to the free peptides, suggesting that the covalent attachment of PEI to the N-terminus of melittin does not significantly affect the lytic activity of the peptide. With N-mel-PEI, erythrocyte lysis of 50 % was obtained at a concentration of 6 µM melittin. In contrast to N-mel-PEI, the lytic activity of C-mel-PEI was significantly higher compared to the free peptides over the whole concentration range tested. Hemoglobin release of 50 % was observed at a concentration of 2 µM melittin. B-PEI alone did not lead to any detectable erythrocyte leakage up to a concentration that was 20-fold higher than the amount of PEI in the lysis assays with melittin-PEI conjugates (0.5 mg/ml PEI). These data demonstrate that the covalent attachment of PEI to the C-terminus of melittin strongly increases the membrane lytic activity of melittin at pH 7.
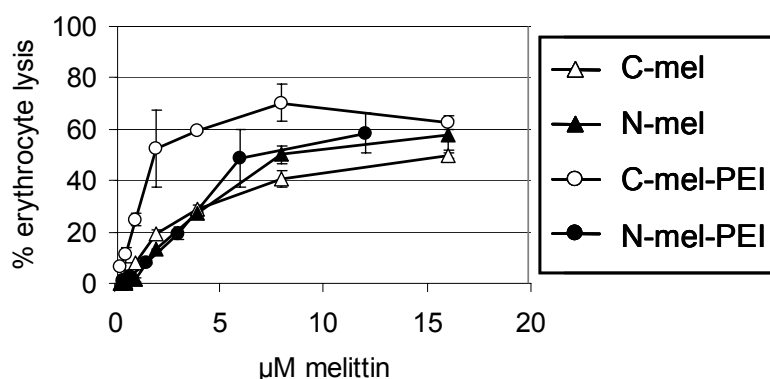
Fig. 21 Erythrocyte lysis induced by free melittin and melittin-PEI conjugates at pH 7. Washed human erythrocytes were incubated with the free melittin peptides C-mel and N-mel or the conjugates C-mel-PEI and N-mel-PEI with increasing peptide concentrations. The percentage of lysed erythrocytes is presented as mean values +/- SD of duplicates.

In summary, the toxicity of C-mel-PEI conjugates and the corresponding polyplexes seems to be related to the high membrane destabilizing activity of C-mel-PEI which leads to strong cell membrane destabilization resulting in membrane blebbing, cell lysis and cell death.

3.2.7 Endosomolytic activity of C-mel-PEI and N-mel-PEI

The high toxicity of C-mel-PEI polyplexes may partly explain the reduced transfection efficiency of C-mel-PEI polyplexes compared to N-mel-PEI polyplexes. However, C-mel-PEI polyplexes were still less efficient than N-mel-PEI polyplexes when using DNA doses below 4 µg/ml, where both polyplexes exposed low toxicity (Fig. 15, Fig. 18). This indicated that toxicity could not be the only explanation for the lower transfection efficiency of C-mel-PEI.

Melittin-PEI conjugates were incorporated into the complexes with the intention to enhance endosomal release, which is believed to be a major bottleneck to efficient gene transfer with nonviral gene delivery systems. The conjugates are supposed to induce endosomal escape by destabilization of the endosomal membrane. Since endosomes are acidic vesicles (the pH is usually around pH 5 to pH 6), membrane lysis assays have been established at pH 5 to obtain a better measure of the destabilizing activities of conjugates inside the endosome. For this purpose, erythrocytes or calcein loaded PC-liposomes were incubated with melittin peptides or melittin-PEI conjugates in buffer of pH 5, and membrane lysis was detected by hemoglobin release or calcein release, respectively (Fig. 22A and B). Both assays were not affected by the presence of B-PEI. In addition, HeLa cells were incubated with peptides or melittin-PEI conjugates in serum free culture medium at pH 5 for 30 min, and the amount of viable, non-lysed cells was estimated by measuring the metabolic activity using the ATP assay (Promega) (Fig. 22C). Incubation of control cells at pH 5 for 30 min did not significantly affect their metabolic activity. The presence of B-PEI at a concentration of 100 µg/ml slightly reduced metabolic activity of cells to approximately 80 % compared to control cells. The influence of PEI in this assay was eliminated by the fact that both conjugates carried the same PEI to melittin ratio, and cells were exposed to similar amounts of PEI and melittin using either C-mel-PEI or N-mel-PEI. Hence, differences in the resulting metabolic activity of cells should only be related to the different site of melittin-linkage to PEI.
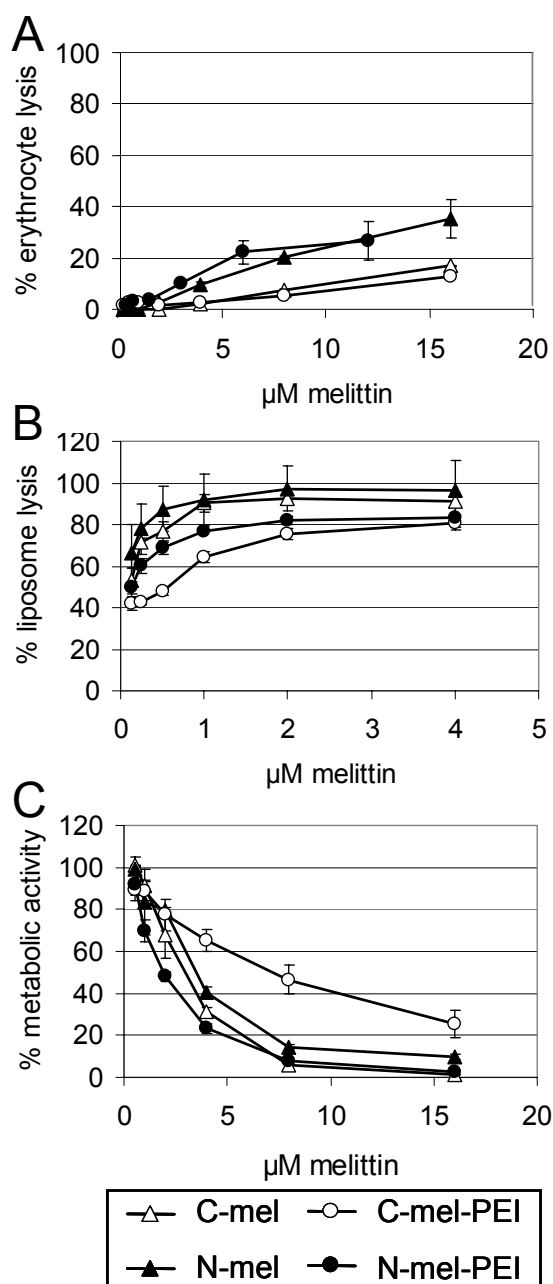
Fig. 22 Membrane lytic activities of melittin peptides and conjugates at endosomal pH 5. Human erythrocytes (A), calcein loaded PC-liposomes (B) and HeLa cells (C) were incubated with increasing concentrations of the free peptides C-mel and N-mel or the conjugates C-mel-PEI and N-mel-PEI at pH 5. The membrane lytic activities were determined by hemoglobin release (A), calcein release (B) and analysis of the metabolic activity of residual non-lysed HeLa cells (C). Mean values +/- SD of duplicates are shown.

The free peptides C-mel and N-mel displayed similar lytic activity on liposomes and HeLa cells at pH 5, but C-mel was less lytic than N-mel on erythrocytes. The lytic activity of N-mel-PEI was similar compared to the activities of the free peptides on erythrocytes, liposomes and HeLa cells. In contrast, C-mel-PEI displayed lower lytic activity at pH 5 than N-mel-PEI over the whole concentration range and in all three

systems tested. Apart from high toxicity of C-mel-PEI polyplexes, the reduced lytic activity of C-mel-PEI at endosomal pH 5 may explain the reduced transfection efficiency of C-mel-PEI polyplexes.

In summary, the site of melittin-linkage to PEI has a high impact on the membrane destabilizing activity of the peptide. Binding of PEI to the C-terminus strongly enhanced the lytic activity at pH 7, whereas binding to the N-terminus retained lytic activity at endosomal pH 5. As a consequence, C-mel-PEI polyplexes exposed pronounced toxicity because of lysis of the plasma membrane of transfected cells, and N-mel-PEI polyplexes were more efficient in transfection because of improved endosomal release of internalized polyplexes.

The high potency of C-mel-PEI to destabilize membranes at neutral pH might be due to a reported destabilization mechanism proceeding through membrane insertion of the peptide (65). In contrast, N-mel-PEI is supposed to induce lysis by insertion-independent pore formation (see discussion) (67). Since membrane destabilization by membrane insertion requires lower peptide to lipid ratios than destabilization by pore formation, C-mel-PEI was considered as the more potent template to generate improved endosomolytic conjugates.

3.3   Improved endosomolytic melittin-PEI conjugates

The new melittin-PEI conjugates should display improved destabilizing activity at low peptide to lipid ratios like C-mel-PEI, but most importantly, they should expose this high lytic activity at pH 5 to promote efficient endosome lysis.

3.3.1   Synthesis and purification of PEI conjugates with melittin analogs

In order to generate melittin-PEI conjugates with enhanced lytic activity at endosomal pH 5, different melittin analogs were designed as shown in Table 3. Sequence modifications included the addition of two glutamic acid residues to the N-terminus (CMA-1, CMA-4) or to the C-terminus of melittin (CMA-2, CMA-3); in the latter case these amino acids replaced neutral glutamine (Gln-25 and Gln-26) residues. At physiological pH the carboxyl group of the glutamic acid residues is deprotonated and negatively charged, whereas at pH 5 glutamic acid is protonated. In two peptide

analogs the basic region KRKR was replaced by histidine residues (CMA-2, CMA-4) which are uncharged at physiological pH but positively charged at endosomal pH 5.

C-melittin	GIGA VLKV LTTG LPAL ISWI KRKR QQC
CMA-1	*EE* GIGA VLKV LTTG LPAL ISWI KRKR QQC
CMA-2	GIGA VLKV LTTG LPAL ISWI *HHHH EE*C
CMA-3	GIGA VLKV LTTG LPAL ISWI KRKR *EE*C
CMA-4	*EE* GIGA VLKV LTTG LPAL ISWI *HHHH* QQC

Table 3 Melittin analogs with acidic modified sequences and a C-terminal cysteine residue (CMA). Additional or replaced amino acid residues are underlined.

Since transfection efficiency of melittin-PEI conjugates does not depend on the peptide's enantiomeric configuration (see 3.2.2), and immunogenicity of natural (*L*)-amino acids was currently not important for the development of an improved *in vitro* transfection system, melittin analogs were synthesized in all-(*L*)-configuration containing a carboxyl terminal cysteine residue for conjugation to PEI. Conjugate synthesis was performed as described above (3.2.1). Purification of the conjugates by cation-exchange chromatography resulted in low conjugate recovery except for CMA-1-PEI; the yield was 41 % (CMA-1-PEI), 7 % (CMA-2-PEI), 15 % (CMA-3-PEI) and 11 % (CMA-4-PEI) based on analysis of PEI. Therefore, a new purification protocol was developed using size exclusion chromatography. This method led to higher yields of purified conjugates based on analysis of PEI (53 % for CMA-2-PEI and 30 % for CMA-3-PEI). All modified melittin-PEI conjugates were shown to consist of approximately 5 to 8 molecules of melittin conjugated to one molecule of PEI.

3.3.2 Endosomolytic activities of CMA-PEI conjugates

In order to analyze the endosomal release capacities of the modified melittin-PEI conjugates compared to C-mel-PEI, the membrane lytic activities of the conjugates were tested on erythrocytes at pH 5 similar as described above (3.2.7) (Fig. 23A). In addition, HeLa cells were incubated with the conjugates at pH 5, and metabolic

activity was determined as described above (3.2.7) to estimate the amount of viable, non-lysed cells (Fig. 23B).
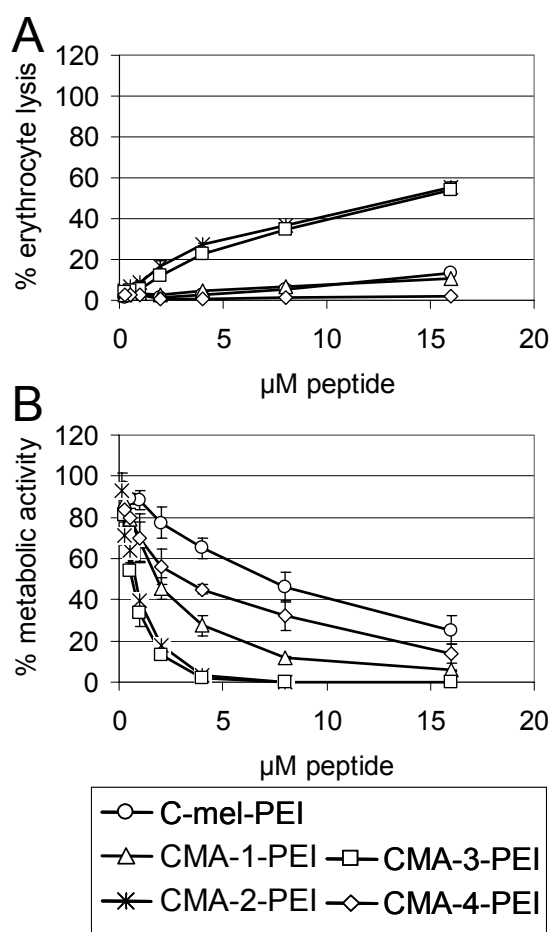
Fig. 23 Membrane destabilizing activities of CMA-PEI conjugates at endosomal pH 5. Human erythrocytes (A) and HeLa cells (B) were incubated with melittin-PEI conjugates at pH 5 and lytic activities were determined by hemoglobin release (A) and analysis of the metabolic activity of non-lysed HeLa cells (B). Mean values +/- SD of duplicates are shown.

CMA-4-PEI did not significantly lyse erythrocytes at pH 5 up to a concentration of 16 µM melittin. CMA-1-PEI displayed similar lytic activity as C-mel-PEI, but both conjugates induced less than 50 % lysis within the concentration range tested. Strong erythrocyte lysis was only observed with CMA-2-PEI and CMA-3-PEI conjugates which induced 50 % hemoglobin release at a concentration of 13 µM melittin.

Consistently, the metabolic activity of HeLa cells was reduced to 50 % after 30 min incubation at pH 5 with CMA-2-PEI and CMA-3-PEI at a concentration of 1 µM melittin. All other conjugates were less lytic and metabolic activity was reduced to 50 % at 2 µM melittin (CMA-1-PEI), 3 µM (CMA-4-PEI) and 7 µM (C-mel-PEI). Similar

to the results obtained with erythrocytes, CMA-2-PEI and CMA-3-PEI exhibited the strongest destabilizing effect at pH 5 on the cell membrane of HeLa cells compared to all other conjugates, resulting in the most pronounced reduction of cellular metabolic activity.

3.3.3 Lytic activities of CMA-PEI conjugates at neutral pH

Ideally, the CMA-PEI conjugates were designed to display high membrane destabilizing activity at endosomal pH 5 and low lytic activity at neutral pH to mediate low toxicity. Therefore, the erythrocyte leakage activities of conjugates were tested at pH 7.1 (Fig. 24). The conjugate CMA-4-PEI did not significantly lyse erythrocytes over the whole concentration range tested up to a concentration of 16 µM melittin. C-mel-PEI and CMA-1-PEI displayed similar lytic activity, with 50 % lysis observed at a concentration of 2 µM and 4 µM melittin, respectively. CMA-2-PEI and CMA-3-PEI were the most lytic conjugates that induced 50 % hemoglobin release at a concentration of 1 µM melittin.
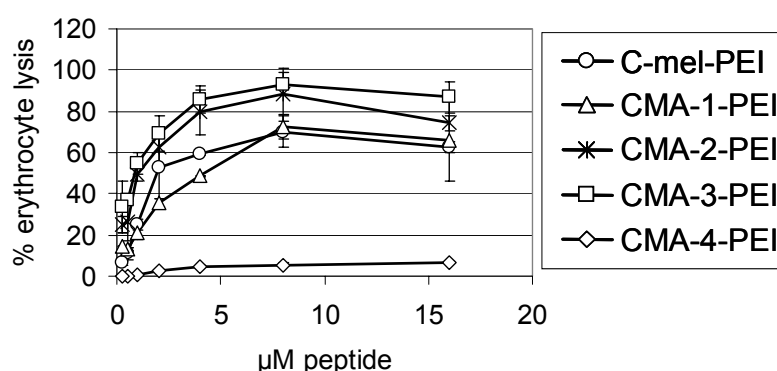
Fig. 24 Erythrocyte lysis induced by CMA-PEI conjugates at neutral pH. Human erythrocytes were incubated with melittin-PEI conjugates with increasing peptide concentrations at pH 7. The percentage of lysed erythrocytes is presented as mean values +/- SD of duplicates.

Overall, two PEI conjugates with melittin analogs, CMA-2-PEI and CMA-3-PEI, displayed the desired high membrane lytic activity at endosomal pH 5. These two conjugates were therefore the most promising candidates for transfection experiments. However, CMA-2-PEI and CMA-3-PEI polyplexes were expected to mediate toxic side effects, since these conjugates were also highly lytic at pH 7.

3.3.4 Improved endosomolytic melittin-PEI conjugates enhance reporter gene expression

Transfection efficiencies of CMA-PEI polyplexes were compared to the efficiencies of C-mel-PEI polyplexes and PEI polyplexes without melittin. Luciferase reporter gene expression was evaluated in three different tumor cell lines (CT 26, HeLa and Neuro2A cells) and in rat smooth muscle cells (A-10 cells) (Fig. 25). Transfection complexes were generated at N/P ratios ranging from 3 to 9. For all polyplexes optimal transfection efficiency was found at an N/P ratio of 6 (data not shown).
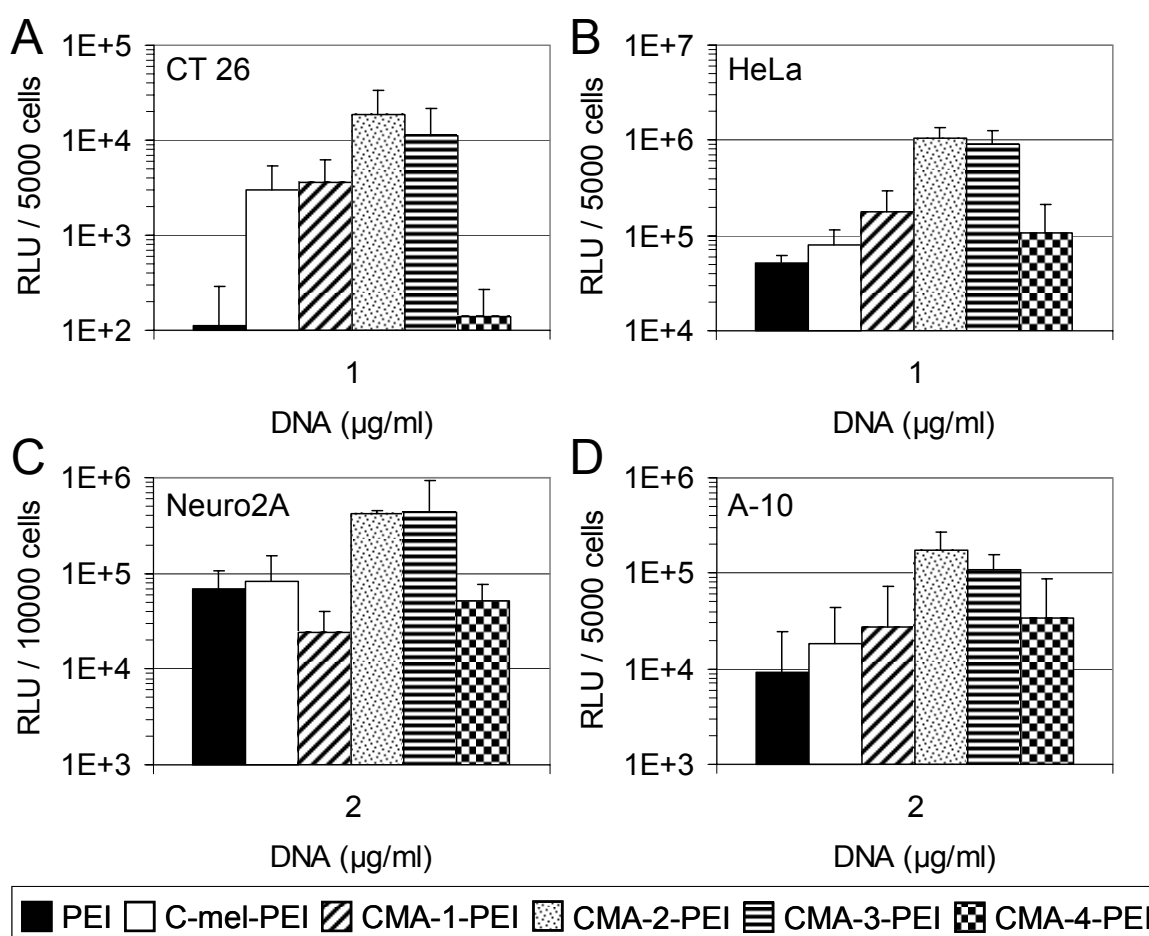
Fig. 25 Reporter gene expression after transfection with CMA-PEI conjugates. CT 26 (A), HeLa (B), Neuro2A (C) and A-10 cells (D) were transfected with indicated concentrations of PEI, C-mel-PEI and CMA-PEI polyplexes. Luciferase activity is presented as mean values + SD of triplicates.

C-mel-PEI polyplexes were 25-fold (CT 26) and 2-fold (A-10) more efficient than PEI polyplexes without melittin. In HeLa cells and Neuro2A cells C-mel-PEI polyplexes and PEI polyplexes exposed similar transfection activity. Polyplexes generated with the conjugates CMA-1-PEI and CMA-4-PEI were similar or less efficient than C-mel-

PEI polyplexes. In contrast, CMA-2-PEI and CMA-3-PEI polyplexes mediated significantly higher transfection activity than C-mel-PEI polyplexes, with 5-fold (CT 26), 10-fold (HeLa), 5-fold (Neuro2A) and 6- to 10-fold (A-10) higher transfection efficiencies compared to C-mel-PEI polyplexes.

In summary, the conjugates CMA-2-PEI and CMA-3-PEI, which exhibited the highest membrane destabilizing activity at endosomal pH 5, were also found to be most efficient in gene transfer compared to the other melittin-PEI conjugates.

3.3.5 Toxicity of CMA-PEI polyplexes

In order to evaluate cellular toxicity of CMA-PEI polyplexes, metabolic activity was analyzed 24 h after transfection by measuring intracellular ATP levels (Fig. 26).
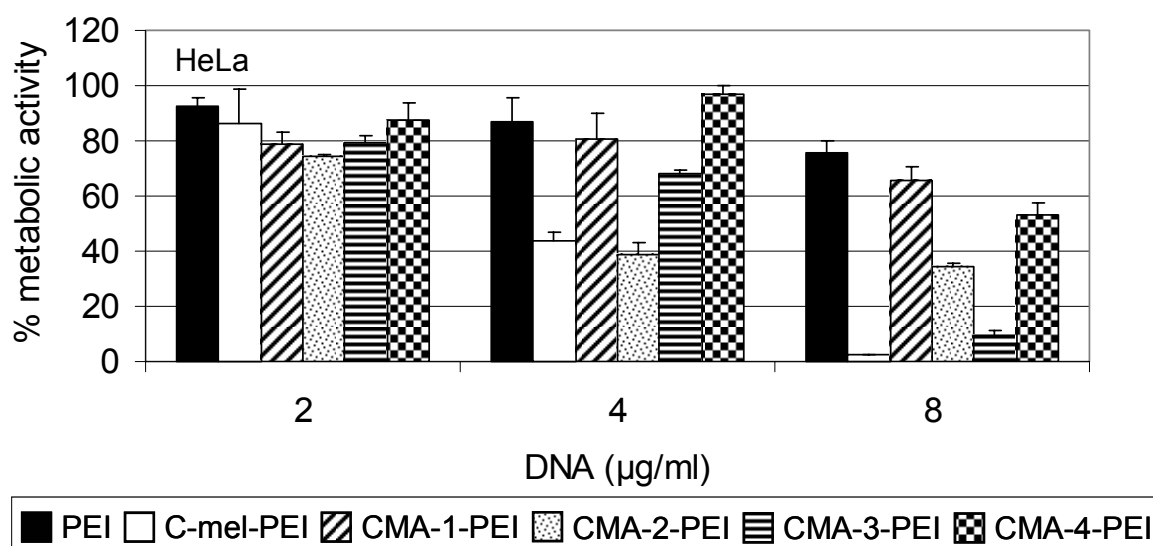
Fig. 26 Metabolic activity after transfection with CMA-PEI polyplexes. HeLa cells were transfected with increasing concentrations of PEI, C-mel-PEI and CMA-PEI polyplexes. Metabolic activity in % of untransfected control cells is presented as mean values + SD of triplicates.

At the highest DNA dose that was used to determine luciferase expression (2 µg/ml) metabolic activity with all polyplexes was maintained above 75 %. Pronounced toxicity was observed when using elevated DNA concentrations of 4 µg/ml or 8 µg/ml. At these DNA doses C-mel-PEI strongly reduced metabolic activity to as low as 2 % compared to untransfected control cells, while CMA-2-PEI and CMA-3-PEI polyplexes reduced metabolic activity to 35 % and 10 %, respectively. Transfection with PEI, CMA-1-PEI and CMA-4-PEI polyplexes also reduced metabolic activity of cells at high DNA concentrations, but these polyplexes were overall less toxic and

metabolic activity was maintained above 50 % compared to untransfected control cells.

Taken together, these data implicate that melittin-PEI conjugates with improved endosomolytic activity can be designed by sequence modification of melittin with acidic residues. The conjugates CMA-2-PEI and CMA-3-PEI exposed the highest lytic activity at endosomal pH 5, and these conjugates were the most efficient in transfection suggesting that gene transfer efficiency indeed correlated with lytic activity at pH 5. However, CMA-2-PEI and CMA-3-PEI also appeared to be significantly toxic which was most likely due to their high membrane destabilizing activity at pH 7. Despite these toxic side effects, CMA-2-PEI and CMA-3-PEI were promising candidates for the development of improved artificial viruses.

3.4   Towards artificial viruses

The membrane active peptide melittin has been shown to improve gene delivery of PEI polyplexes. For systemic applicability, however, the positive surface charge of polyplexes has to be shielded to avoid unspecific interactions with blood components and non-target cells, and targeting ligands have to be included to direct particles towards the desired tissue. Nonviral vector systems carrying multiple functional domains e.g. for shielding, targeting and improved intracellular delivery represent the next generation of nonviral vectors and have been termed 'artificial viruses' (18).

3.4.1   Shielding and targeting of melittin-PEI polyplexes

For the development of artificial viruses based on B-PEI polyplexes, shielding and targeting conjugates had to be incorporated into the particles. Therefore, two PEG-PEI conjugates were synthesized with PEG of 20 kDa covalently attached to either linear PEI of 22 kDa or branched PEI of 25 kDa, resulting in the two conjugates PEG-PEI22 and PEG-PEI25 as described in (71). The molar ratio of PEG/PEI was 2/1 for PEG-PEI22 and 1/1 for PEG-PEI25. For the targeting of polyplexes towards the epidermal growth factor (EGF) receptor, which is overexpressed on various tumor cells (e.g. HUH-7 human hepatoma cells) (79), the ligand EGF was linked to B-PEI by a heterobifunctional 3.4 kDa PEG derivative (EGF-PEG-PEI25) as described in (28). The resulting molar ratio of EGF/PEG/PEI within the conjugate was

approximately 1/1/1. For the shielding of B-PEI polyplexes, PEG-PEI22 or PEG-PEI25 conjugates were mixed with free B-PEI at various ratios in HBS. The ratios (% w/w) are based on the amount of PEI present in the PEG conjugates or the PEI stock solutions. The PEI conjugate mixture was then mixed with DNA diluted in HBS at an N/P ratio of 6 and a final DNA concentration of 20 µg/ml. Particles were analyzed by laser-light scattering (Table 4).

Polyplex	Ratio (% w/w)	Size (nm)	Zeta potential (mV)
B-PEI	100	2,500 +/- 300 200 +/- 23	17 +/- 0.8
B-PEI/PEG-PEI22	90/10	232 +/- 10	15 +/- 7
	85/15	204 +/- 8	20 +/- 5
	80/20	203 +/- 8	13 +/- 6
B-PEI/PEG-PEI25	90/10	80 +/- 16	3.4 +/- 1.2
	85/15	74 +/- 12	2.7 +/- 0.8
	80/20	94 +/- 21	2.8 +/- 0.8

Table 4 Size and zeta potential of surface shielded B-PEI polyplexes. DNA complexes with different ratios of PEG-PEI22 or PEG-PEI25 shielding conjugate were prepared in HBS at an N/P ratio of 6 and a final DNA concentration of 20 µg/ml. Particles were allowed to stand for 30 min before analysis.

The preparation of unshielded B-PEI polyplexes in HBS resulted in large aggregated particles (2,500 nm) due to the salt concentration in the HBS buffer (19). B-PEI polyplexes generated in HBS with 10 to 20 % PEG-PEI22 shielding conjugate were small (200 to 240 nm) indicating partial shielding. However, zeta potential of these particles was positive (+13 to +20 mV), similar to the zeta potential of unshielded polyplexes (+17mV). Apparently, the shielding conjugate PEG-PEI22, which has been successfully used for shielding L-PEI polyplexes in a previous study (71), is not useful to shield B-PEI polyplexes. In contrast, effective shielding of B-PEI polyplexes was achieved using 10 to 20 % PEG-PEI25 shielding conjugate resulting in particles < 100 nm with near neutral zeta potential (Table 4).

The incorporation of EGF-PEG-PEI25 targeting conjugate into the polyplexes at a ratio (w/w based on PEI) of PEI/PEG-PEI25/EGF-PEG-PEI25 of 80/10/10 % also resulted in small and shielded particles (Table 5). When replacing B-PEI by different melittin-PEI conjugates, particle size and zeta potential of such shielded and targeted polyplexes was not changed (Table 5).

Polyplex	Ratio (% w/w)	Size (nm)	Zeta potential (mV)
B-PEI/PEG-PEI25/EGF-PEG-PEI25	80/10/10	88 +/- 8	2.5 +/- 0.8
N-mel-PEI/PEG-PEI25/EGF-PEG-PEI25	80/10/10	78 +/- 9	3 +/- 0.8
CMA-2-PEI/PEG-PEI25/EGF-PEG-PEI25	80/10/10	155 +/- 15	4.5 +/- 3
CMA-3-PEI/PEG-PEI25/EGF-PEG-PEI25	80/10/10	91 +/- 15	2.9 +/- 0.8

Table 5 Particle size and zeta potential of shielded and receptor-targeted B-PEI polyplexes. DNA complexes were prepared in HBS at an N/P ratio of 6 and a final DNA concentration of 20 µg/ml. Particles were allowed to stand for 30 min before analysis.

3.4.2 Reporter gene expression of shielded and EGFR-targeted melittin-PEI polyplexes

According to transfection experiments with non-shielded, positively charged melittin-PEI polyplexes, the most efficient polyplexes were generated with the N-terminal melittin-PEI conjugate (N-mel-PEI) or conjugates of melittin analogs with PEI linked to the peptide's C-terminus (CMA-2-PEI and CMA-3-PEI). Therefore, these melittin conjugates were used to prepare shielded EGFR-targeted polyplexes, and transfection efficiency was compared to shielded and targeted polyplexes generated with C-mel-PEI conjugate or B-PEI without melittin. For transfection experiments, all polyplexes were generated at an N/P ratio of 6 with 10 % PEG-PEI25 and 10 % EGF-PEG-PEI25. Luciferase reporter gene expression was evaluated in two EGF-receptor rich tumor cell lines, HUH-7 and Renca-EGFR cells (Fig. 27).
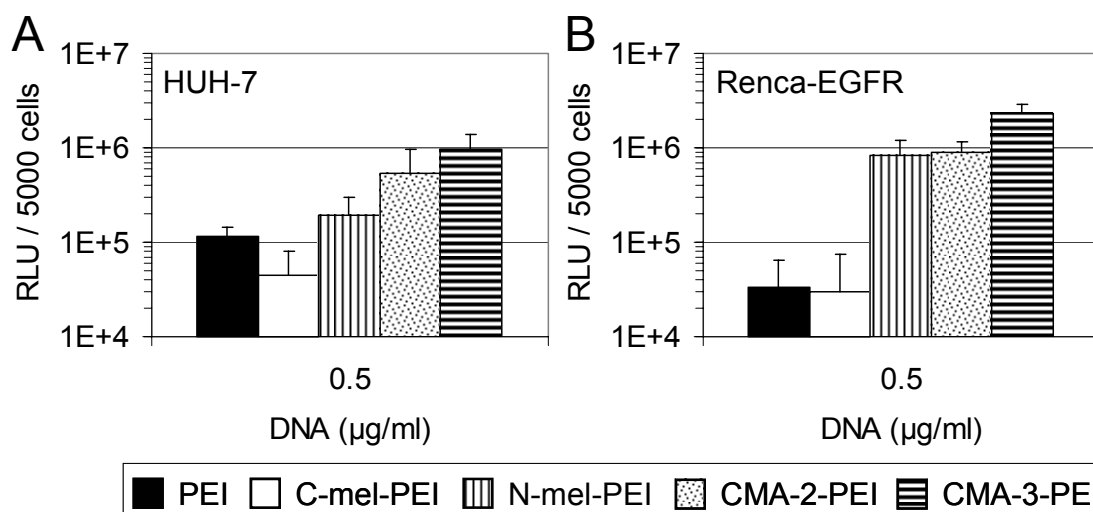
Fig. 27 Reporter gene expression after transfection with PEG-shielded and EGF-receptor-targeted polyplexes. HUH-7 (A) and Renca-EGFR cells (B) were transfected with indicated concentrations of different melittin-PEI polyplexes or PEI polyplexes without melittin. All polyplexes contained 10 % PEG-PEI25 for surface shielding and 10 % EGF-PEG-PEI25 for receptor targeting. Luciferase activity is presented as mean values + SD of triplicates.

The incorporation of C-mel-PEI into shielded and EGFR-targeted polyplexes did not enhance the efficiency compared to polyplexes without melittin. In contrast, shielded EGFR-targeted polyplexes generated with the most effective conjugates N-mel-PEI, CMA-2-PEI and CMA-3-PEI mediated significantly enhanced transfection activity compared to polyplexes without melittin. The highest levels of reporter gene expression were obtained using shielded and targeted CMA-3-PEI polyplexes, which showed 8-fold (HUH-7) and 70-fold (Renca) higher transfection efficiency than shielded and targeted B-PEI polyplexes without melittin.

3.4.3 Reporter gene expression and toxicity of purified, shielded and EGFR-targeted melittin-PEI polyplexes

The key question was finally whether such optimized shielded and targeted melittin-PEI polyplexes would retain high transfection efficiency after the removal of free melittin-PEI by SEC and whether these polyplexes expose reduced toxicity. Shielded EGFR-targeted polyplexes were prepared with PEI or with the melittin-PEI conjugate CMA-3-PEI, and these polyplexes were purified to remove unbound PEI or CMA-3-PEI as described in 3.1.1. Particle size and surface charge were not significantly changed after purification, and purified polyplexes remained stable over a period of 7 days at 4°C with a size of < 150 nm and a near neutral zeta potential. Transfection

efficiencies of freshly prepared non-purified and purified polyplexes were evaluated in HUH-7 and Renca-EGFR cells (Fig. 28).
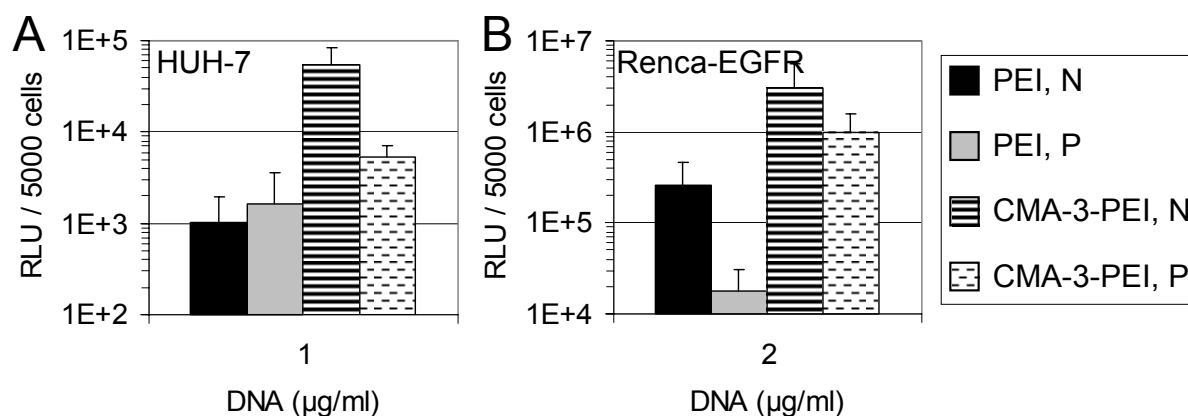
Fig. 28 Reporter gene expression after transfection with purified shielded and targeted polyplexes. HUH-7 (A) and Renca-EGFR cells (B) were transfected with indicated concentrations of PEI or CMA-3-PEI polyplexes which were shielded with PEG-PEI25 and targeted with EGF-PEG-PEI25. 'N': non-purified polyplexes; 'P': purified polyplexes. Luciferase activity is presented as mean values + SD of triplicates.

In line with the results obtained with purified, positively charged L-PEI and B-PEI polyplexes (3.1), transfection efficiency of purified melittin-PEI polyplexes was reduced compared to non-purified polyplexes, indicating that the removal of both free PEI and free melittin-PEI reduces the transfection activity of polyplexes. However, purified polyplexes with melittin (CMA-3-PEI) still mediated 3-fold (HUH-7) and 50-fold (Renca-EGFR) higher levels of luciferase activity compared to purified PEI polyplexes without melittin. Since purified polyplexes remained stable over 7 days at 4°C, such polyplexes were analyzed for transfection activity in HUH-7 and Renca-EGFR cells to estimate whether activity was retained after storage (Fig. 29). It is important to note that the stored purified polyplexes with CMA-3-PEI were still 10-fold more efficient than stored purified polyplexes without melittin.
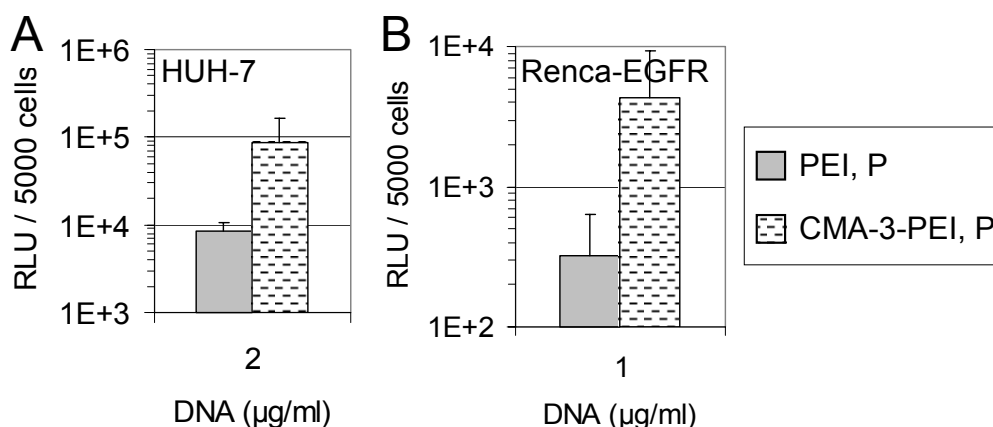
Fig. 29 Reporter gene expression of stored purified polyplexes. HUH-7 (A) and Renca-EGFR cells (B) were transfected with indicated concentrations of purified ('P') PEG-shielded and EGFR-targeted PEI or CMA-3-PEI polyplexes which have been stored over 7 days at 4°C. Luciferase activity is presented as mean values + SD of triplicates.

In addition, the effect of PEG-shielding and purification on the overall toxicity of these particles was analyzed. Non-shielded and shielded, EGFR-targeted polyplexes were prepared with B-PEI and CMA-3-PEI, and these complexes were further purified by SEC. HUH-7 cells were transfected with purified and non-purified polyplexes, and metabolic activity of cells was determined 24 h after transfection (Fig. 30). Metabolic activity of cells transfected with shielded and receptor-targeted polyplexes was approximately 20 % higher compared to cells transfected with non-shielded polyplexes indicating that shielding indeed reduced toxicity of polyplexes. Toxicity of both non-shielded and shielded polyplexes was further reduced after removal of free polycations by SEC-purification. Metabolic activity after transfection with purified, non-shielded polyplexes was 77 % (PEI) and 104 % (CMA-3-PEI) compared to 49 % (PEI) and 57 % (CMA-3-PEI) when using non-purified polyplexes. In the case of PEG-shielded polyplexes metabolic activity after transfection with purified polyplexes was 101 % (PEI) and 88 % (CMA-3-PEI), which was 25 % (PEI) and 12 % (CMA-3-PEI) higher than after transfection with non-purified shielded polyplexes.
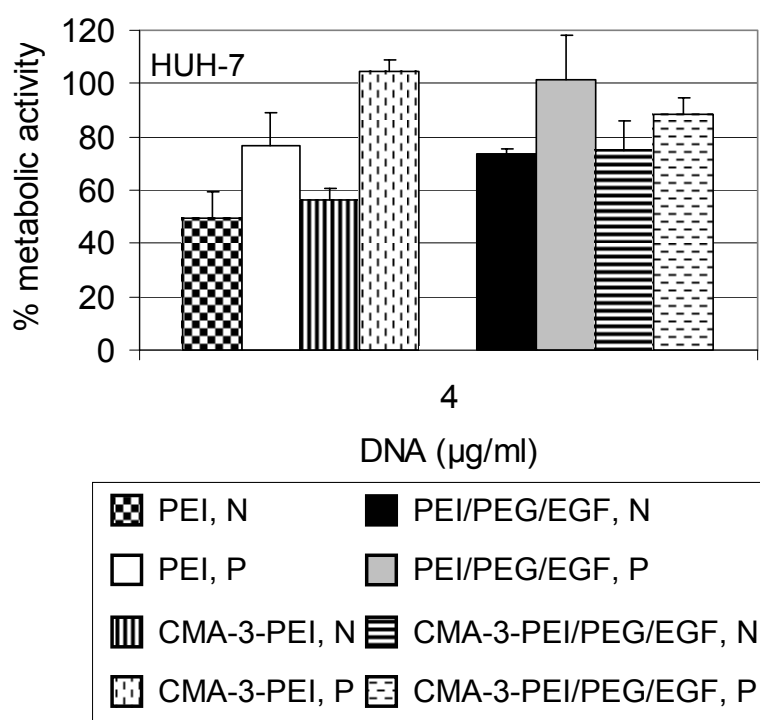
Fig. 30 Metabolic activity after transfection with purified polyplexes. HUH-7 cells were transfected with non-shielded polyplexes (left bars) or polyplexes shielded with PEG-PEI25 ('PEG') and targeted with EGF-PEG-PEI25 ('EGF') (right bars). 'N': non-purified polyplexes; 'P': purified polyplexes. Metabolic activity is presented as mean values + SD of triplicates.

In summary, melittin or melittin analogs with acidic modifications improved the transfection efficiency of shielded and targeted polyplexes with a near neutral zeta potential. The best effects were obtained using CMA-3-PEI, the conjugate which exposed the highest lytic activity at endosomal pH 5. After removal of free melittin-PEI by SEC such purified shielded and targeted polyplexes were still more efficient in gene transfer than polyplexes without melittin suggesting that complex-bound melittin-PEI indeed improved intracellular delivery of purified polyplexes. Notably, purification further reduced toxicity of shielded EGFR-targeted complexes with melittin resulting in a gene delivery system that was non-toxic, even at high DNA concentrations of 4 µg/ml.

4 Discussion

4.1 Purification of PEI polyplexes highlights the role of free PEI

PEI is one of the most efficient nonviral gene transfer agents for transfections in cell culture and *in vivo*. However, pronounced cellular toxicity of PEI and severe systemic side effects limit the use of PEI polyplexes for gene transfer *in vivo*. In addition, it has been shown previously that standard PEI polyplexes generated at charge ratios above N/P 5 contain up to 80 % of unbound PEI (55;56), and that cellular toxicity of polyplexes directly correlates with increased N/P ratios (57;58). These results suggest that toxicity is at least partially attributed to free PEI. Therefore, a major aim of the present work was to develop an efficient method to purify polyplexes from excess PEI. Recently, a method based on ultrafiltration was used in order to remove unbound PEI (55). However, removal of free PEI using this method was incomplete (55). The easy and efficient method based on SEC developed in this thesis now allows complete removal of excess PEI from both L-PEI and B-PEI polyplexes (3.1). The applied SEC-column was pre-conditioned with PEI which reduced unspecific binding of PEI polyplexes and highly improved polyplexes recovery yielding in up to 80 % recovery based on analysis of complexed DNA. Independent from the initial N/P ratio used for complex formation, small purified polyplexes (< 200 nm) were obtained with a final N/P ratio of 2.5 (Table 1). At this N/P ratio complete retention of plasmid DNA was observed in agarose gel shift assays, whereas complexes were not fully retarded at N/P ratios below 2.5 (data not shown). This indicated that at N/P 2.5 all DNA phosphate residues were just saturated with positively charged PEI nitrogens. Excess free PEI is not present at this low N/P ratio. Such small polyplexes of N/P 2.5, however, could not be generated directly, since preparation of polyplexes at an N/P ratio ≤ 3 resulted in large aggregated particles (> 300 nm).

Both physical parameters (size and surface charge) of polyplexes (Table 1) and their biological activity did not change after SEC. Most importantly, the purified PEI complexes allowed to verify that *i)* free PEI was indeed the major cause of toxicity of PEI polyplexes with high N/P-ratios, and *ii)* nevertheless free PEI was apparently an

essential factor for intracellular gene delivery thereby enhancing transfection efficiency. *In vitro* transfection with purified polyplexes was overall efficient but notably less toxic compared to formulations containing free PEI. Moreover, when using high DNA concentrations, purified L-PEI polyplexes were even more efficient in reporter gene expression than particles with free PEI. Purified polyplexes led to approximately 30-fold higher levels of luciferase activity compared to non-purified polyplexes (Fig. 7A right). This enhanced transfection efficiency was largely attributed to the lower toxicity of purified particles, since more transfected cells survived in the absence of excess PEI. However, luciferase activity normalized to the number of surviving cells (Fig. 8) was still five-fold higher for purified polyplexes than for non-purified polyplexes when using high DNA doses (Fig. 7A right). This suggests that the lower toxicity of purified polyplexes is not the only reason for the observed differences in transfection activity. Reduced toxicity of purified particles was obviously due to the removal of free PEI, since the addition of free PEI (equivalent to the amount of PEI removed from the polyplex solution by SEC) restored the initial level of toxicity.

At low DNA concentrations, polyplexes without free PEI were less efficient in gene transfer. Reduced efficiency of purified polyplexes at low DNA concentrations was also observed in long-term transfection experiments where reporter gene expression was evaluated 48 h or 72 h after transfection (Fig. 9). Similar observations were obtained with aggregated polyplexes, although in this case the presence of free PEI had less impact on the transfection efficiency (Fig. 10). Results showing that the transfection efficiency with PEI polyplexes significantly increases with rising N/P ratios (5 or higher) (15;80), where a rising amount of PEI is free in solution, further strengthened the evidence that free PEI has an important impact on the efficiency of gene delivery at the cellular level. Transfection experiments with purified polyplexes allowed clarifying the role of free PEI in more detail.

Important steps during transfection are membrane association of polyplexes followed by endocytosis, endosomal release, nuclear trafficking, nuclear import of DNA, and finally transcription of DNA. Each of these steps can be potentially influenced by PEI. To investigate whether PEI influences the transfection process at a particular step during transfection, time course experiments with and without free PEI were

performed. Surprisingly, flow cytometry indicated an increased cellular association of purified polyplexes, whereas the presence of free PEI reduced such association (Table 2). It is therefore concluded that similar to receptor competition free PEI competes with PEI polyplexes for cellular association. Obviously, cellular association does not account for reduced gene expression of purified polyplexes at low concentrations of DNA. Since enhanced cellular association of purified polyplexes did not result in enhanced toxicity, there was additional evidence that toxicity was primarily attributed to free PEI but not to the total amount of polyplex interacting with the cell.

Endocytosis of polyplexes is induced soon after cellular association. Microscopic experiments showed that some polyplexes are already internalized 30 min after transfection, and endocytosis is believed to be accomplished 4 h after transfection (81). Transfection experiments with purified polyplexes were performed and free PEI was added at different time points. Since the addition of free PEI 4 h after transfection led to the strongest enhancement of gene expression, free PEI was obviously not required for cellular internalization of polyplexes (Fig. 11). It is therefore likely that free PEI rather contributes to endosomal release or any process thereafter. In a similar time course experiment confocal live cell imaging showed that free PEI added either simultaneously or 4 h post-transfection with purified polyplexes ended up in intracellular vesicles that contained both compounds (Fig. 12). From these findings the increase in reporter gene expression observed with free PEI added after transfection can be explained as follows: purified polyplexes mediate increased cellular association of plasmid DNA and are subsequently internalized into endosomes. PEI added afterwards is also internalized into endosomes, and these vesicles containing PEI alone merge with vesicles containing polyplexes. The free PEI now promotes the release of polyplexes from the endosomes. The positive effect of adding free PEI to purified polyplexes indicates that a minimum amount of PEI is necessary to achieve the proton sponge effect, which has been proposed as the major mechanism of endosomal release of PEI polyplexes (19;82). A sufficient amount of PEI to achieve enhanced intracellular delivery can also be accomplished by either using high N/P ratios (83) or large aggregated polyplexes (19;20). The pivotal role of PEI for endosomal release was confirmed by recent data showing that

both free and complexed PEI contribute to the proton sponge mechanism: both lead to accumulation of chloride in vesicles and buffering of vesicular pH (41). Free PEI can also have an impact on gene delivery when added to other polyplexes with poor endosomal escape, e.g. polylysine (PLL) polyplexes (82): the reporter gene expression of PLL polyplexes was increased 10-fold in the presence of free PEI.

These data demonstrate that free PEI on the one hand causes pronounced toxicity but on the other hand significantly enhances gene expression. Since toxicity is a major concern also for the applicability of PEI polyplexes *in vivo*, purification from excess PEI is a very reasonable step to improve the vector system. Minimizing the total amount of PEI using purified polyplexes is advisable, also because long term toxicity of PEI is unknown. In addition, the availability of well defined gene transfer formulations with low toxicity is a vital precondition for the further development of gene therapeutic strategies based on synthetic carriers, and purification methods as the one developed in this thesis will help to fulfill these requirements.

Nevertheless, endosomal release of polyplexes remains a key issue that needs to be further improved. The desired endosomal release activity of toxic free PEI in polyplexes therefore must be replaced by alternative agents that are stably integrated into the complex. The membrane active peptide melittin was of particular interest for this purpose, because this peptide displayed pronounced membrane destabilizing activity and successfully enhanced gene transfer with lipoplexes (47) and PEI polyplexes (48;49).

4.2 C- versus N-mel-PEI: the site of linkage strongly influences the biological activity

Melittin is the major peptide component of the venom of the honey bee Apis melifera cerana (84) and belongs to the class of pore-forming membrane active peptides. Incorporation of membrane active peptides into nonviral vectors is believed to enhance endosomal release by destabilization of the endosomal membrane after complex internalization (43).

For stable incorporation of melittin into vectors, the peptide has to be covalently attached to a carrier which strongly binds to DNA, such as PEI. It has been shown

previously that PEI bound to the N-terminus of all-(*L*)-melittin enhanced gene delivery with PEI polyplexes (48;49). However, for systemic applicability, conjugates containing non-immunogenic all-(*D*)-peptides would be desirable. Here, transfection experiments with two melittin-PEI conjugates, where B-PEI was attached to the N-terminus of all-(*L*) or all-(*D*)-melittin, demonstrated that both conjugates equally enhanced luciferase expression and EGFP-expression compared to B-PEI polyplexes without melittin (Fig. 14). Hence, the capacity to destabilize endosomal membranes is obviously independent of the peptide's enantiomeric configuration which is in agreement with results showing that all-(*D*) and all-(*L*)-melittin expose similar hemolytic and antibacterial activities (61;62).

To generate improved non-immunogenic all-(*D*)-melittin PEI conjugates, both the C-terminus and the N-terminus of melittin may be considered for covalent binding to PEI. The site of linkage, however, might influence melittin's membrane destabilizing activity and its capacity to enhance gene transfer. To determine which site of linkage leads to the most potent melittin-PEI conjugate, B-PEI was covalently attached to the C-terminus (C-mel-PEI) or the N-terminus of melittin (N-mel-PEI), and the resulting conjugates were tested in cell culture.

Size and surface charge of melittin-PEI polyplexes and B-PEI polyplexes without melittin were similar. Reporter gene expression, however, strongly depends on the composition of the applied polyplexes. Transfection of different tumor cell lines and of slowly dividing PEC cells demonstrated that N-mel-PEI was overall the most efficient conjugate for gene delivery. N-mel-PEI polyplexes mediated up to 160-fold higher levels of luciferase activity compared to B-PEI polyplexes (Fig. 15B), and the percentage of EGFP-positive cells was as high as 42 % compared to only 11 % EGFP positive cells achieved with B-PEI polyplexes (Fig. 16). Polyplexes of C-mel-PEI also improved reporter gene expression compared to B-PEI polyplexes. However, C-mel-PEI was less efficient in transfection than N-mel-PEI. Analysis of the metabolic activity of transfected cells showed that N-mel-PEI and B-PEI polyplexes exposed overall low toxicity at all DNA concentrations tested (Fig. 18); metabolic activity was maintained above 75 % compared to untransfected control cells. In contrast, metabolic activity was reduced to as low as 2 % after transfection with C-mel-PEI polyplexes at 4 µg/ml DNA (Fig. 18). This toxicity was most likely due to lysis

of the plasma membrane which was not observed with B-PEI or N-mel-PEI polyplexes (Fig. 19). Video fluorescence microscopy of transfected HeLa cells demonstrated that C-mel-PEI polyplexes at 4 µg/ml DNA induced immediate cell membrane destabilization resulting in membrane blebbing and cell lysis (Fig. 20). Apparently, the capacity of C-mel-PEI polyplexes to induce cell lysis was due to the pronounced membrane destabilizing activity of C-mel-PEI at neutral pH. Membrane lysis experiments with erythrocytes at pH 7 showed that PEI conjugated to the C-terminus of melittin strongly enhanced lysis compared to free melittin, whereas PEI attached to the N-terminus of melittin did not improve lytic activity of the bound peptide (Fig. 21). Since C-mel-PEI and N-mel-PEI carry the same melittin to PEI ratio, the observed differences in erythrocyte lysis at pH 7 are most likely due to the different site of melittin linkage to PEI.

The high impact of linkage-site on the membrane destabilizing activity of melittin may be explained by the lysis mechanism that was proposed for melittin (67;85): in a first step the cationic peptide adsorbs to the membrane bilayer predominantly by electrostatic interactions with negatively charged lipid headgroups. Membrane association is probably improved when the peptide is bound to the polycation PEI because of enhanced charge interactions with the negatively charged membrane. The orientation of melittin relative to the bilayer depends on the peptide to lipid concentration (Fig. 31).
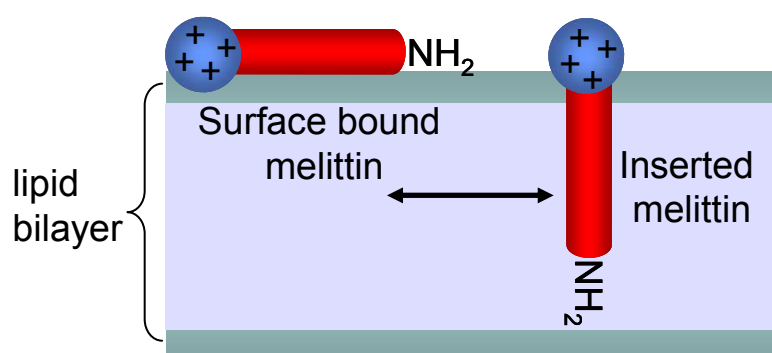
Fig. 31 Orientation of membrane-bound melittin. At low peptide to lipid ratios melittin is oriented parallel to the membrane bilayer. Insertion of the N-terminus of melittin (red) into the lipophilic core of the membrane occurs at higher peptide to lipid ratios, whereas the cationic C-terminus (blue) anchors the peptide at the membrane interface. Membrane insertion results in water influx and bilayer perturbation.

At low concentrations, melittin is bound parallel to the bilayer and is embedded within the lipid headgroups. With an increase in peptide to lipid concentration, the N-terminus of melittin inserts into the bilayer (65;86), provided that the N-terminus is free as in the case of natural melittin or C-mel-PEI (but not in the case of N-mel-PEI). The cationic C-terminus does not insert but serves as membrane anchor. There is a dynamic equilibrium between interfacially adsorbed and inserted melittin peptides (87;88). Inserted melittin favors water penetration into the bilayer due to partial protonation of the N-terminus and the positive charge at lysine-7 (65;89). Water penetration into the hydrophobic core of the bilayer results in membrane destabilization. In the case of C-mel-PEI the conjugated polycation can further improve membrane anchoring of the C-terminus thereby stabilizing the membrane inserted state of the peptide (Fig. 32). In addition, PEI also bears the capacity to destabilize membranes, although its potential to induce e.g. erythrocyte lysis is far lower than that of melittin or melittin-PEI conjugates. The observed high lytic activity of C-mel-PEI at pH 7 may therefore be due to improved association and insertion of melittin followed by membrane perturbation which is synergistically enhanced by the destabilizing effect of the attached polycation PEI.
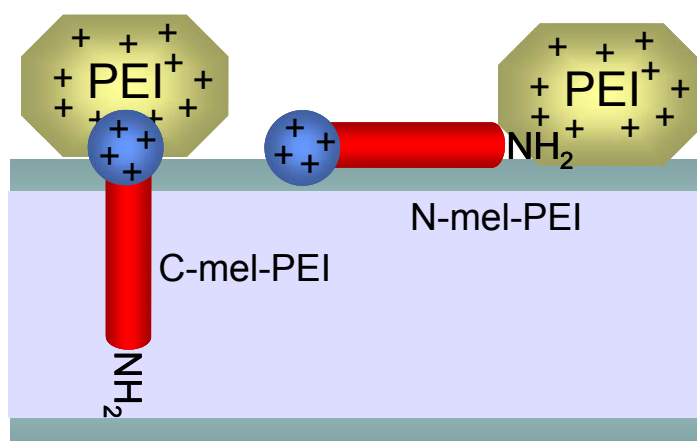
Fig. 32 Orientation of C-mel-PEI and N-mel-PEI in membrane bilayers. Since the N-terminus of C-mel-PEI is free, the peptide moiety (red) can insert into the membrane bilayer. PEI (yellow) at the C-terminus of melittin (blue) can improve membrane anchoring thereby stabilizing the membrane inserted state of melittin. Inserted melittin favors water influx into the bilayer which results in membrane perturbation and destabilization. In contrast, PEI covalently attached to the N-terminus of melittin (N-mel-PEI) prevents membrane insertion and the melittin moiety is supposed to be associated parallel to the bilayer.

In contrast, N-mel-PEI is supposed to induce lysis by an alternative mechanism, since membrane insertion of the N-terminus of melittin is sterically hindered when the bulky polycation is attached (Fig. 32). Free melittin has the capacity to lyse membranes by formation of transmembrane 'toroidal' pores according to the carpet or toroidal model which was first described for magainin-induced pores (90;91). Toroidal pore formation is induced when the peptide to lipid ratio further increases above the threshold necessary for membrane insertion. Although different groups could demonstrate that melittin inserts into membrane bilayers (65;86;92), it is not clear whether this is an intermediate step required for pore formation. In fact, a sufficient high density of peptides bound parallel to and embedded into the bilayer may trigger enhanced lipid curvature strain which destabilizes the bilayer without vertical peptide insertion (43). Furthermore, inside the toroidal pore the peptide is not inserted into the bilayer. After membrane disintegration, the pore is lined by the lipid monolayer, which bends continuously from the top to the bottom in the fashion of a toroidal hole, and the peptides are associated to the lipid headgroups (Fig. 33).
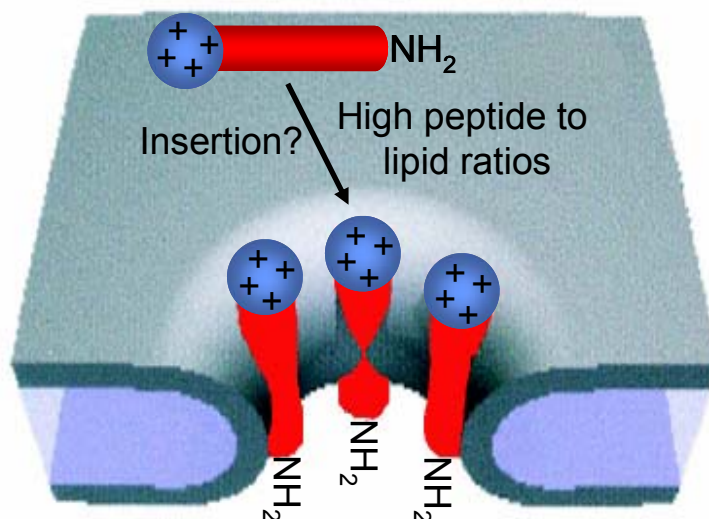
Fig. 33 Toroidal pore formation by melittin. With an increase in membrane-bound melittin above a certain threshold concentration, melittin induces toroidal pores. Membrane insertion of melittin might be an intermediate step during pore formation. The toroidal pore is formed by both the lipid monolayer (dark layers) and the peptides (red cylinders with blue cationic C-terminal region) which are associated to the lipid headgroups. Adapted from Yang et al. (67)

In principle, both C-mel-PEI and N-mel-PEI should have the capacity to form toroidal pores above a certain peptide to lipid concentration. N-mel-PEI, however, may even better associate parallel to the membrane than C-mel-PEI because N-mel-PEI bears positive charges at the C-terminus of melittin (Lys21-Arg22-Lys23-Arg24) and at the N-terminus due to conjugated PEI (Fig. 32). In contrast, C-mel-PEI accumulates positive charges at the C-terminus only. Therefore, N-mel-PEI may be the more potent conjugate for pore formation according to the toroidal pore model, but C-mel-PEI can already destabilize membranes at lower peptide to lipid concentrations due to enhanced insertion into the lipid bilayer followed by water influx and membrane perturbation.

The proposed models for the lysis mechanisms of melittin-PEI conjugates help to explain the pronounced membrane destabilizing activity of C-mel-PEI at physiological pH and the concomitant high toxicity of C-mel-PEI polyplexes at high DNA doses. The pronounced toxicity also partly explains the reduced transfection efficiency of C-mel-PEI polyplexes compared to N-mel-PEI polyplexes at elevated DNA doses. However, C-mel-PEI polyplexes are also less efficient than N-mel-PEI polyplexes at low, non-toxic DNA doses. Therefore, toxicity cannot be the only reason for the reduced transfection efficiency of C-mel-PEI polyplexes.

Interestingly, evaluation of the membrane destabilizing activity at endosomal pH 5 using erythrocytes, PC-liposomes and HeLa cells demonstrated that C-mel-PEI was significantly less lytic than N-mel-PEI at pH 5. This result was independent of the type of membrane used for the lysis assays and in striking contrast to the observed high lytic activity of C-mel-PEI at neutral pH.

The inverse lytic activity of the two melittin-conjugates at pH 5 and pH 7 may reflect a pH-dependent change in the dominating lysis mechanism of the C-mel-PEI conjugate. Enhanced protonation of the lipid membrane and melittin might alter their mode of interaction. For example, loss of negative charges of the lipid membrane presumably reduces the lipid-bound concentration of the cationic melittin peptide, even below the peptide to lipid concentration required for inserting the N-terminus of melittin into the bilayer. This is also consistent with the known lower lytic activity of free melittin at pH 5 as compared to pH 7 (93). In addition, at acidic pH the N-

terminus of melittin in C-mel-PEI is highly protonated and therefore more hydrophilic. This could reduce insertion of the N-terminus into the hydrophobic core of the bilayer membrane. As a consequence, the peptide moiety would be mainly bound parallel to the membrane at acidic pH resulting in membrane destabilization according to the toroidal pore model similar to N-mel-PEI. Since N-mel-PEI is supposed to be more potent in parallel membrane association and in inducing toroidal pores than C-mel-PEI (see above) this would explain the higher lytic activity of N-mel-PEI compared to C-mel-PEI at pH 5.

The high lytic activity of N-mel-PEI compared to C-mel-PEI at pH 5 obviously promotes better endosomal escape of N-mel-PEI polyplexes, and this can explain the higher transfection efficiency of N-mel-PEI polyplexes compared to C-mel-PEI polyplexes. This apparent correlation of gene transfer efficiency with lytic activity at pH 5 was also found with other membrane-active peptides, including influenza virus haemagglutinin fusion peptides (43;93;94).

In summary, the site of melittin-linkage to PEI significantly affects the membrane destabilizing activities of the resulting conjugates and this has a strong impact on the biological activities of the corresponding polyplexes. C-mel-PEI was highly lytic at neutral pH and, therefore, elevated doses of C-mel-PEI polyplexes induced high toxicity. In contrast, N-mel-PEI was less lytic at neutral pH but retained higher lytic activity than C-mel-PEI at endosomal pH 5. This apparently promotes better endosomal release of N-mel-PEI polyplexes resulting in efficient gene delivery in different cell types.

Although N-mel-PEI polyplexes were more effective in gene transfer than C-mel-PEI polyplexes, C-mel-PEI was regarded as a more potent template to generate improved endosomolytic melittin-conjugates because of its higher capacity to destabilize membranes already at low peptide to lipid ratios. Therefore, PEI was attached to the C-terminus of new melittin analogs which were modified with acidic residues to improve the lytic activity at endosomal pH.

4.3   Improved melittin-PEI conjugates enhance gene transfer

In contrast to C-mel-PEI, the new melittin-PEI conjugates should be primarily active at acidic pH to trigger enhanced membrane destabilization within acidic vesicles such as endosomes. According to the literature, the positive charges at the C-terminus (KRKR$_{21-24}$) for membrane anchoring and at the amino terminal NH$_2$-group for membrane perturbation are important structural features for lytic melittin analogs (69;70). In order to shift the optimum of melittin's membrane lytic activity towards endosomal pH 5, glutamic acidic residues or histidine residues were introduced into the peptide's sequence at these important structural domains (Table 3). In the melittin analogs CMA-1 and CMA-4 two glutamic acid residues were added to the N-terminus of melittin. In CMA-2 and CMA-4 the cationic cluster KRKR$_{21-24}$ at the C-terminus of melittin was replaced by histidine residues which are uncharged at physiological pH and positively charged at acidic pH. In CMA-2 and CMA-3 two glutamine residues next to the cationic cluster region were replaced by two glutamic acid residues introducing negative charges at physiological pH. In all melittin analogs, the altered or inserted residues become protonated at acidic pH only, thereby restoring the required positive charges at the C-terminus and the N-terminus to induce membrane destabilization. In contrast, at neutral pH these analogs lack sufficient positive charges which should prevent the lytic activity.

Synthesis of C-terminal-linked CMA-PEI conjugates was performed as described for melittin-PEI conjugates. Recovery rates after conjugate purification, however, were low (as low as 7 % for CMA-2-PEI) which was probably due to unspecific and irreversible binding of conjugates to the cation-exchange column and/or to the membrane of the stirred ultrafiltration cell that was used to concentrate and desalt the conjugates after purification. Recovery rates were significantly improved when conjugates were purified by SEC using a column that was pre-conditioned with PEI to reduce unspecific binding. Since the conjugate concentration in the eluted fractions was high enough (PEI concentration ≥ 0.4 mg/ml) further concentration was not necessary, and after subsequent dialysis recovery based on analysis of PEI was 50 % for CMA-2-PEI and 30 % for CMA-3-PEI compared to 7 % and 15 %, respectively, following the cation-exchange protocol.

Membrane lysis assays at pH 5 and pH 7 (Fig. 23, Fig. 24) demonstrated that insertion of acidic residues next to the C-terminal membrane anchoring domain of melittin indeed resulted in melittin-PEI conjugates (CMA-2-PEI and CMA-3-PEI) which displayed significantly improved lytic activity at endosomal pH.

Sequence modifications that included both the C-terminus and the N-terminus resulted in the rather non-lytic conjugate CMA-4-PEI. Obviously, this kind of modification interfered too strongly with the peptide's conformation and/or membrane interaction thereby inhibiting membrane lysis. The conjugate CMA-1-PEI, where melittin was only modified at the N-terminus, retained high lytic activity at neutral pH. At acidic pH, however, CMA-1-PEI exhibited low lytic activity similar to C-mel-PEI. Only on HeLa cell membranes, CMA-1-PEI exposed higher membrane destabilizing activity than C-mel-PEI at pH 5. Overall, CMA-1-PEI did not fulfill the requirements of an optimized conjugate with improved lytic activity at endosomal pH 5.

Notably, both conjugates that were modified only at the C-terminus of melittin (CMA-2-PEI and CMA-3-PEI) displayed the desired high lytic activity at pH 5 both on erythrocytes and HeLa cells (Fig. 23). The membrane destabilizing activities of CMA-2-PEI and CMA-3-PEI were approximately 7- to 10-fold higher compared to C-mel-PEI. Surprisingly, CMA-2-PEI and CMA-3-PEI were also about 2-fold more lytic than C-mel-PEI at neutral pH (Fig. 24). Since CMA-2-PEI and CMA-3-PEI exposed similar lytic activities both at pH 5 and pH 7, the higher membrane destabilizing activities were obviously mainly attributed to the exchange of glutamine by glutamic acid residues, whereas replacement of $KRKR_{21-24}$ by histidine had no further impact on their lytic activities. It is important to note that the improved lytic activities of CMA-2-PEI and CMA-3-PEI compared to C-mel-PEI were only observed with the PEI conjugates. The free peptides CMA-2 and CMA-3 showed significant lytic activities at pH 5 (CMA-2, CMA-3) and pH 7 (CMA-3), but were overall less lytic than free melittin both at pH 5 and pH 7 (data not shown). Lysis experiments with the conjugate C-mel-PEI compared to free melittin have already demonstrated that PEI bound to the C-terminus of melittin enhances the lytic activity of the peptide at pH 7 (3.2.6). These results highlight that conjugation to PEI has a strong impact on the overall membrane destabilizing activity of the melittin peptides and that activities of the isolated peptide moieties do not necessarily correlate with activities after conjugation. The enhancing

effect of conjugated PEI may also explain why additional replacement of the membrane anchoring domain $KRKR_{21-24}$ by histidine residues had no further effect on the membrane destabilizing activities, because within these C-terminal conjugates the polycation PEI functions as membrane anchor. The enhanced lytic activities of CMA-2-PEI and CMA-3-PEI compared to C-mel-PEI were obviously due to the negatively charged glutamic acid residues that were introduced at the C-terminus. The reason for this enhancement is currently unknown, as the effect is independent of pH or the peptide's own lytic activity. It is proposed that the negative glutamic acid charges facilitate changes within the conformation and structural orientation of the peptide within the PEI polycation conjugate which increase the synergistic membrane-destabilizing effect of PEI.

In excellent agreement with results obtained with unmodified melittin-PEI conjugates (3.2) and other membrane active peptides used in gene transfer (43;93;94), the lytic activities of the CMA-PEI conjugates at pH 5 were found to correlate with their gene transfer activities (Fig. 25). The non-lytic conjugate CMA-4-PEI was ineffective in gene delivery. CMA-1-PEI exposed similar low lytic activity at pH 5 as C-mel-PEI and, consequently, CMA-1-PEI polyplexes mediated similar levels of luciferase activity compared to C-mel-PEI polyplexes. Most importantly, CMA-2-PEI and CMA-3-PEI, which displayed the highest lytic activity at pH 5, were indeed the most efficient in gene transfer in all four cell lines tested. Transfection efficiency of CMA-2-PEI and CMA-3-PEI polyplexes was up to 10-fold higher compared to C-mel-PEI polyplexes. This highlights that gene transfer activity of C-terminal conjugated melittin-PEI polyplexes can be optimized by designing melittin analog conjugates with improved membrane destabilizing activity at endosomal pH 5.

On the other hand toxicity assays revealed that lytic activity at neutral pH correlated with toxicity of the corresponding polyplexes as already observed for C-mel-PEI polyplexes (3.2). The conjugates C-mel-PEI, CMA-2-PEI and CMA-3-PEI were all highly lytic at pH 7, and these polyplexes mediated pronounced toxic effects at elevated DNA concentrations (≥ 4 µg/ml) (Fig. 26). As visualized with C-mel-PEI polyplexes by video fluorescence microscopy (3.2.5), toxicity was likely related to partial destabilization of the plasma membrane resulting in cell lysis and cell death. Analysis of the metabolic activity of cells 24 h after transfection revealed that

complexes of C-mel-PEI induced the strongest reduction of metabolic activity, followed by CMA-3-PEI and CMA-2-PEI polyplexes (Fig. 26). In contrast, CMA-1-PEI and CMA-4-PEI were less lytic at pH 7, and these polyplexes as well as PEI polyplexes without melittin exposed lower toxicity.

In conclusion, the membrane destabilizing activity of melittin-PEI conjugates at endosomal pH 5 correlates with their capacity to induce endosomal escape and hence their efficiency to enhance gene transfer. Improved endosomolytic melittin-PEI conjugates were obtained by sequence modification of melittin with acidic residues. These conjugates displayed significantly higher membrane destabilizing activity at pH 5 compared to the C-terminal conjugate with natural melittin. Polyplexes that were generated with these optimized conjugates were up to 10-fold more efficient in transfection compared to polyplexes with unmodified melittin-PEI conjugates. However, transfection with these improved endosomolytic polyplexes was associated with significant toxicity at high DNA doses. Similar to C-mel-PEI polyplexes, toxicity was likely related to the high lytic activity at pH 7 resulting in plasma membrane disruption and death of transfected cells. Despite these toxic side effects, the endosomolytic conjugates CMA-2-PEI and CMA-3-PEI were promising candidates for the development of multifunctional artificial viruses.

4.4 Towards artificial viruses

Regarding the development of improved artificial viruses which are efficient and safe also for potential *in vivo* administration, three key issues had to be tackled. Firstly, the most efficient melittin-PEI conjugates had to be incorporated into surface-shielded and receptor-targeted PEI polyplexes. Secondly, transfection experiments with purified particles had to prove whether complex-bound endosomolytic domains like melittin-PEI conjugates were able to enhance gene delivery of such particles lacking free PEI conjugates. Thirdly, since toxicity was a major concern of polyplexes containing melittin-PEI conjugates, it was of great importance to evaluate whether the resulting purified particles would display an improved toxicity profile.

In vitro transfection experiments with melittin-PEI conjugates were performed with positively charged polyplexes. After systemic administration of such particles,

however, the positive surface charge mediates nonspecific interactions with e.g. blood components or non-target cells which prevent specific gene transfer and can cause significant toxicity (22). Therefore, polyplexes need to be shielded with hydrophilic polymers like PEG to prevent such unspecific interactions (21;23). Two different shielding conjugates were recently used to successfully shield PEI polyplexes, with PEG covalently attached to L-PEI (PEG-PEI22) for shielding L-PEI polyplexes, or PEG conjugated to B-PEI (PEG-PEI25) for shielding B-PEI polyplexes (71). In this thesis, both shielding conjugates were tested for the surface shielding of B-PEI polyplexes. Interestingly, shielding with PEG-PEI22 was obviously insufficient, since the zeta potential of B-PEI polyplexes containing up to 20 % of PEG-PEI22 remained positive (above +13 mV, Table 4). Effective shielding of B-PEI polyplexes was, however, achieved with PEG-PEI25. Although the amount of PEG conjugated to B-PEI was 2-fold lower than in the PEG-PEI22 conjugate, a ratio of 10 % PEG-PEI25 was sufficient to generate small particles (< 100 nm) with a near neutral zeta potential (Table 4). The different shielding capacities of PEG-PEI22 compared to PEG-PEI25 might be due to the higher DNA binding affinity of B-PEI compared to L-PEI (Julia Klöckner, unpublished results). Polyplexes that are generated with a mixture of L-PEI and B-PEI will therefore contain higher amounts of B-PEI compared to L-PEI. Accordingly, the degree of PEG conjugate bound to DNA in the presence of excess B-PEI will be significantly higher with PEG-PEI25 than with PEG-PEI22. This can explain effective shielding with PEG-PEI25 in contrast to PEG-PEI22.

Since PEG-shielding alone reduces non-specific interactions but also desired interactions with the target cells, targeting ligands have to be incorporated into the polyplexes. Recently, successful targeting of PEI polyplexes towards the EGF-receptor, which is highly overexpressed on several tumor cell lines (e.g. HUH-7 human hepatoma cells) (79), was achieved using the ligand EGF linked to B-PEI via a PEG-spacer (EGF-PEG-PEI25) (28). Here, a similar conjugate was incorporated into PEG-PEI25-shielded B-PEI or melittin-PEI polyplexes, resulting in particles that were still small with a near neutral zeta potential (Table 4C).

Transfection experiments in EGFR-rich HUH-7 and Renca-EGFR cells demonstrated that melittin-PEI conjugates not only enhanced gene delivery with positively charged polyplexes but also significantly improved transfection efficiency of surface-shielded

polyplexes (Fig. 27). The gene transfer activity again correlated with the lytic activity of the incorporated conjugate at pH 5. When using positively charged polyplexes the three most efficient melittin-PEI conjugates were N-mel-PEI and the melittin analog conjugates CMA-2-PEI and CMA-3-PEI, where PEI was linked to the peptide's C-terminus. These three conjugates all exposed high lytic activity at endosomal pH 5 (Fig. 22, Fig. 23). PEG-shielded and EGFR-targeted polyplexes generated with these endosomolytic melittin-PEI conjugates significantly enhanced gene delivery compared to PEG-shielded polyplexes without melittin. The best results were obtained with CMA-3-PEI which mediated up to 70-fold higher levels of luciferase activity compared to shielded and targeted B-PEI polyplexes without melittin (Fig. 27). In contrast, the conjugate C-mel-PEI, with PEI attached to the C-terminus of natural melittin exposed low lytic activity at pH 5, and, consequently, C-mel-PEI did not improve gene transfer of shielded polyplexes in comparison to shielded PEI complexes without melittin.

It remained to be shown, however, that enhanced transfection efficiency of the best endosomolytic melittin-PEI conjugates was attributed to melittin-PEI which was stably incorporated into the polyplexes. Therefore, shielded and targeted polyplexes containing the most efficient CMA-3-PEI conjugate were purified by SEC to remove unbound CMA-3-PEI and then tested for gene transfer activity (Fig. 28). In line with the previous results obtained with SEC-purified L-PEI and B-PEI polyplexes (3.1) (95), gene transfer efficiency was reduced after the removal of free PEI or CMA-3-PEI from the shielded polyplexes. Thus, free polycations also have an additive effect for the gene transfer efficiency of shielded polyplexes. It is important to note that the efficiency of purified shielded polyplexes with the endosomolytic conjugate CMA-3-PEI was still up to 50-fold higher than that of purified polyplexes without melittin (Fig. 28). Purified shielded CMA-3-PEI polyplexes also retained high gene transfer activity after storage at 4°C for 7 days. The stored polyplexes were stable regarding size and zeta potential and mediated about 10-fold higher levels of luciferase activity compared to stored purified polyplexes lacking melittin (Fig. 29). The apparent storage stability is of great importance regarding the development of a potential therapeutic gene delivery system.

In vitro analysis of the metabolic activity of cells transfected with PEG-shielded polyplexes showed that shielding reduced toxicity of polyplexes (Fig. 30), which is in good agreement with previous results obtained by Ogris et al. (23). Most importantly, purification from unbound polycations further reduced toxicity resulting in polyplexes that were non-toxic even at high DNA doses. Therefore, the final requirement of an optimized artificial virus was fulfilled: the incorporation of the improved endosomolytic melittin-PEI conjugate CMA-3-PEI into purified shielded and receptor-targeted polyplexes significantly enhanced transfection efficiency in comparison to polyplexes lacking melittin, and these polyplexes exposed an improved toxicity profile providing a vector system that is efficient and safe also for potential *in vivo* administration.

5   Summary

For the development of improved polyethylenimine (PEI) polyplexes towards 'artificial viruses' two key issues are *i)* to improve the toxicity profile of the applied vectors and *ii)* to enhance endosomal release, one of the major barriers to efficient gene transfer with PEI polyplexes.

Nonviral vectors based on PEI usually contain an excess of PEI that is not complexed to DNA. Since free PEI contributes to cellular and systemic toxicity purification of polyplexes from unbound PEI is highly desirable. In this thesis an easy and efficient method based on size exclusion chromatography (SEC) was developed, which for the first time allowed complete removal of PEI from PEI polyplexes. Moreover, purification of polyplexes enabled to clarify the role of free PEI in gene delivery at the cellular level. Most importantly, the removal of unbound PEI significantly reduced toxicity of the applied polyplexes. However, purified polyplexes without free PEI were less efficient in transfection compared to non-purified polyplexes. Mechanistic studies showed that free PEI most likely enhanced endosomal release of polyplexes and therefore contributed to efficient gene transfer with PEI polyplexes. Nevertheless, the availability of a defined, well-tolerated gene transfer formulation is a vital precondition for the further development of nonviral gene therapeutics, and a purification method like the one developed in this thesis will help to fulfill these requirements.

To enhance endosomal release of PEI polyplexes, the membrane active peptide melittin was incorporated into the vector particles. It has been shown previously that PEI bound to the N-terminus of natural all-(*L*)-melittin (all-(*L*)-N-mel-PEI) enhanced gene delivery with PEI polyplexes. Here, it was demonstrated that transfection efficiency of N-mel-PEI is independent of the enantiomeric configuration of the bound peptide which allowed the use of non-immunogenic all-(*D*)-melittin for the generation of optimized melittin-PEI conjugates.

To determine the optimal site of melittin-linkage to PEI, the polycation PEI was covalently attached to the N-terminus (N-mel-PEI) or the C-terminus of melittin (C-

mel-PEI) in all-(*D*)-configuration. The site of melittin-linkage had a strong impact on the membrane destabilizing activities of the resulting melittin-PEI conjugates. C-mel-PEI was highly lytic at neutral pH and therefore elevated doses of C-mel-PEI polyplexes induced high toxicity. In contrast, N-mel-PEI was less lytic at neutral pH but retained higher lytic activity than C-mel-PEI at endosomal pH 5. This apparently promoted better endosomal release of N-mel-PEI polyplexes resulting in efficient gene delivery in different cell lines. The high potency of C-mel-PEI to destabilize membranes at neutral pH is presumably due to a reported destabilization mechanism proceeding through membrane insertion of the peptide. In contrast, N-mel-PEI is supposed to induce lysis by insertion-independent pore formation according to the toroidal pore model. Since membrane destabilization by membrane insertion requires lower peptide to lipid ratios than destabilization by pore formation, C-mel-PEI was considered as the more potent template to generate improved endosomolytic melittin-PEI conjugates.

The new melittin-PEI conjugates should display pronounced lytic activities at endosomal pH 5. Therefore, PEI was attached to the C-terminus of melittin analogs which were modified with acidic residues. The conjugates with the highest lytic activities at endosomal pH 5 were indeed the most efficient in transfection. This apparent correlation of gene transfer efficiency with lytic activity at pH 5 was in excellent agreement with results obtained with unmodified melittin-PEI conjugates and other membrane-active peptides used in gene transfer.

The most efficient melittin-PEI conjugates were incorporated into surface-shielded and receptor-targeted PEI polyplexes, and the resulting particles were further purified by SEC to remove unbound toxic polycations. Endosomolytic melittin-PEI conjugates stably incorporated into such purified polyplexes significantly enhanced transfection efficiency in comparison to polyplexes lacking melittin. Most importantly, these polyplexes exposed an improved toxicity profile providing an artificial virus-like vector that is efficient and safe also for potential *in vivo* administration.

6   Appendix

6.1   Abbreviations

ATP	adenosine triphosphate
B-PEI	branched PEI of 25 kDa
B-PEI-PDP	B-PEI modified with pyridyldithio-propionate-linkers
CMA-PEI	PEI covalently attached to the C-terminus of a melittin analog
C-mel	melittin with a cysteine residue at the C-terminus
C-mel-PEI	PEI covalently attached to the C-terminus of melittin
CMV	cytomegalovirus
DID	1,1'-dioctadecyl-3,3,3',3'- tetramethylindodicarbocyanine
DMEM	Dulbecco's Modified Eagle's Medium
DMSO	dimethyl sulfoxide
DNA	deoxyribonucleic acid
DTT	dithiothreitol
EDTA	ethylenediaminetetraacetic acid
EGF	epidermal growth factor
EGFP	Enhanced Green Fluorescent Protein
EGF-PEG-PEI25	EGF covalently linked to B-PEI of 25 kDa with a heterobifunctional 3.4 kDa PEG spacer
EtBr	ethidium bromide
FCS	fetal calf serum
HBG	HEPES-buffered glucose
HBS	HEPES-buffered saline
HEPES	N-(2-hydroxyethyl)piperazine-N'-(2-ethanesulfonic acid)
K	lysine
L-PEI	linear PEI of 22 kDa
N/P ratio	molar ratio of PEI nitrogen to DNA phosphate
NA	numerical aperture

N-mel	melittin with a cysteine residue at the N-terminus
N-mel-PEI	PEI covalently attached to the N-terminus of melittin
PBS	phosphate-buffered saline
PC	phosphatidylcholine
pCMVLuc	plasmid encoding for luciferase under control of the CMV promoter/enhancer
PEG	polyethylene glycol
pEGFP	plasmid encoding for EGFP
PEG-PEI22	PEG of 20 kDa covalently attached to L-PEI of 22 kDa
PEG-PEI25	PEG of 20 kDa covalently attached to B-PEI of 25 kDa
PEI	polyethylenimine
PI	propidium iodide
PLL	polylysine
R	arginine
RLU	relative light units
RNA	ribonucleic acid
RT	room temperature
SCID	severe combined immunodeficiency
SD	standard deviation
SEC	size exclusion chromatography
siRNA	small interfering RNA
SPDP	succinimidyl 3-(2-pyridyldithio) propionate
TNBS	trinitrobenzenesulfonic acid
TNF-α	tumor necrosis factor α
w	weight

6.2 Publications

6.2.1 Original Papers

Boeckle, S., von Gersdorff, K., van der Piepen, S., Culmsee, C., Wagner, E., and Ogris, M. (2004), Purification of polyethylenimine polyplexes highlights the role of free polycations in gene transfer, J. Gene Med. 6, 1102-1111

Walker, G., Fella, C., Pelisek, J., Fahrmeir, J., Boeckle, S., Ogris, M., and Wagner, E. (2005), Toward synthetic viruses: Endosomal pH triggered deshielding of targeted polyplexes greatly enhances gene transfer *in vitro* and *in vivo*, Molecular Therapy, *in press*

Boeckle, S., Ogris, M., and Wagner, E., C- versus N-terminally linked melittin-polyethylenimine conjugates: the site of linkage strongly influences activity in DNA polyplexes, *in preparation*

Boeckle, S., Roedl, W., Fahrmeir, J., Ogris, M., and Wagner, E., Improved endosomolytic melittin analogs enhance gene transfer efficiency of targeted purified polyethylenimine polyplexes, *in preparation*

6.2.2 Reviews and Book chapters

Boeckle, S., Wagner, E. (2005), Optimizing Gene Delivery: Chemical Modification of Viral Vectors and Synthesis of Artificial Virus Vector Systems, in "Drug Delivery Systems for Targeted Drug Therapy", Eds. Y.J. Park, J. Liang, J. Balthasar, V. Yang, American Association of Pharmaceutical Scientists, *in press*

Wagner, E., Culmsee, C., Boeckle, S. (2005), Targeting of Polyplexes, Towards Synthetic Virus Vector Systems, in "Nonviral Vectors for Gene Therapy", Second Edition, Eds. L. Huang, M.C. Hung, E. Wagner, Advances in Genetics Volumes 53 and 54, *in press*

Boeckle, S., Wagner, E., Ogris, M. (2002), Transmembrane Targeting of DNA with Membrane Active Peptides, in "Biomedical Aspects of Drug Targeting", Eds. V.R. Muzykantov, V.P. Torchilin, Kluwer Academic Publishers, Boston/Dordrecht/London, p. 441-458

6.2.3 Oral presentations

Boeckle, S., Wagner, E. (2004), Artificial Viruses: Engineering gene vectors using membrane active peptides, 2nd International Symposium on Biochemistry and Molecular Biology, Havana, Cuba

Boeckle, S., von Gersdorff, K., Wagner, E. (2004), Development of an intelligent artificial virus for gene delivery, SFB 486 'Nanoman' meeting, Schloß Ringberg, Tegernsee, Germany

6.2.4 Poster presentations

Boeckle, S., von Gersdorff, K., Ogris, M., Wagner, E. (2003), Purification of DNA/polyethylenimine complexes by size exclusion chromatography, 11th Annual Congress of the European Society of Gene Therapy, Edinburgh, Scotland

Boeckle, S., von Gersdorff, K., Wagner, E., Ogris, M. (2003), Strategies to overcome cellular barriers to nonviral gene transfer: Towards artificial viruses, Controlled Release Society, German Chapter Annual Meeting, Munich, Germany

7 References

1. Friedmann, T. and Roblin, R. (1972), Gene therapy for human genetic disease?, Science 175, 949-955

2. The Journal of Gene Medicine web site, www.wiley.co.uk/genmed/clinical

3. Hacein-Bey-Abina, S., Von Kalle, C., Schmidt, M., McCormack, M. P., Wulffraat, N., Leboulch, P., Lim, A., Osborne, C. S., Pawliuk, R., Morillon, E., Sorensen, R., Forster, A., Fraser, P., Cohen, J. I., de Saint, B. G., Alexander, I., Wintergerst, U., Frebourg, T., Aurias, A., Stoppa-Lyonnet, D., Romana, S., Radford-Weiss, I., Gross, F., Valensi, F., Delabesse, E., Macintyre, E., Sigaux, F., Soulier, J., Leiva, L. E., Wissler, M., Prinz, C., Rabbitts, T. H., Le Deist, F., Fischer, A., and Cavazzana-Calvo, M. (2003), LMO2-associated clonal T cell proliferation in two patients after gene therapy for SCID-X1, Science 302, 415-419

4. Marshall, E. (1999), Gene therapy death prompts review of adenovirus vector, Science 286, 2244-2245

5. Raper, S. E., Chirmule, N., Lee, F. S., Wivel, N. A., Bagg, A., Gao, G. P., Wilson, J. M., and Batshaw, M. L. (2003), Fatal systemic inflammatory response syndrome in a ornithine transcarbamylase deficient patient following adenoviral gene transfer, Mol Genet.Metab 80, 148-158

6. Kreppel, F. and Kochanek, S. (2004), Long-term transgene expression in proliferating cells mediated by episomally maintained high-capacity adenovirus vectors, J Virol. 78, 9-22

7. Schiedner, G., Hertel, S., Johnston, M., Dries, V., van Rooijen, N., and Kochanek, S. (2003), Selective depletion or blockade of Kupffer cells leads to enhanced and prolonged hepatic transgene expression using high-capacity adenoviral vectors, Mol Ther 7, 35-43

8. Niidome, T. and Huang, L. (2002), Gene therapy progress and prospects: nonviral vectors, Gene Ther 9, 1647-1652

9. Wang, R., Epstein, J., Charoenvit, Y., Baraceros, F. M., Rahardjo, N., Gay, T., Banania, J. G., Chattopadhyay, R., de, I., V, Richie, T. L., Tornieporth, N., Doolan, D. L., Kester, K. E., Heppner, D. G., Norman, J., Carucci, D. J., Cohen, J. D., and Hoffman, S. L. (2004), Induction in humans of CD8+ and CD4+ T cell and antibody responses by sequential immunization with malaria DNA and recombinant protein, J Immunol. 172, 5561-5569

10. Mathiesen, I. (1999), Electropermeabilization of skeletal muscle enhances gene transfer in vivo, Gene Ther 6, 508-514

11. Pedroso de Lima, M. C., Simoes, S., Pires, P., Faneca, H., and Duzgunes, N. (2001), Cationic lipid-DNA complexes in gene delivery: from biophysics to biological applications, Adv.Drug Deliv.Rev. 47, 277-294

12. De Smedt, S. C., Demeester, J., and Hennink, W. E. (2000), Cationic polymer based gene delivery systems, Pharm.Res. 17, 113-126

13. Eichman, J. D. and et al. (2001), Bioapplications of PAMAM Dendrimers. In Dendrimers and Other Dendritic Polymers, Frechet, J. M. J. and Tomalia, D. A., editors, J. Wiley & Sons Ltd.

14. Zuber, G., Dauty, E., Nothisen, M., Belguise, P., and Behr, J. P. (2001), Towards synthetic viruses, Adv.Drug Deliv.Rev. 52, 245-253

15. Boussif, O., Lezoualc'h, F., Zanta, M. A., Mergny, M. D., Scherman, D., Demeneix, B., and Behr, J. P. (1995), A versatile vector for gene and oligonucleotide transfer into cells in culture and in vivo: polyethylenimine, Proc.Natl.Acad.Sci.U.S.A 92, 7297-7301

16. Kichler, A., Behr, J. P., and Erbacher, P. (1999) Polyethylenimines: A Family of Potent Polymers for Nucleic Acid Delivery. In Nonviral Vectors for Gene Delivery, Huang, L., Hung, M. C., and Wagner, E., editors,. Academic Press

17. Dunlap, D. D., Maggi, A., Soria, M. R., and Monaco, L. (1997), Nanoscopic structure of DNA condensed for gene delivery, Nucleic Acids Res 25, 3095-101

18. Wagner, E. (2004), Strategies to improve DNA polyplexes for in vivo gene transfer – will "artificial viruses" be the answer?, Pharm.Res. 21, 8-14

19. Ogris, M., Steinlein, P., Kursa, M., Mechtler, K., Kircheis, R., and Wagner, E. (1998), The size of DNA/transferrin-PEI complexes is an important factor for gene expression in cultured cells, Gene Ther. 5, 1425-1433

20. Wightman, L., Kircheis, R., Rossler, V., Carotta, S., Ruzicka, R., Kursa, M., and Wagner, E. (2001), Different behavior of branched and linear polyethylenimine for gene delivery in vitro and in vivo, J.Gene Med. 3, 362-372

21. Kircheis, R., Schuller, S., Brunner, S., Heider, K., Zauner, W., and Wagner, E. (1999), Polycation-Based DNA Complexes for Tumor-Targeted Gene Delivery *in vivo*, J Gene Med 1, 111-120

22. Chollet, P., Favrot, M. C., Hurbin, A., and Coll, J. L. (2002), Side-effects of a systemic injection of linear polyethylenimine-DNA complexes, J Gene Med. 4, 84-91

23. Ogris, M., Brunner, S., Schuller, S., Kircheis, R., and Wagner, E. (1999), PEGylated DNA/transferrin-PEI complexes: reduced interaction with blood components, extended circulation in blood and potential for systemic gene delivery, Gene Ther 6, 595-605

24. Hood, J. D., Bednarski, M., Frausto, R., Guccione, S., Reisfeld, R. A., Xiang, R., and Cheresh, D. A. (2002), Tumor regression by targeted gene delivery to the neovasculature, Science 296, 2404-2407

25. Plank, C., Zatloukal, K., Cotten, M., Mechtler, K., and Wagner, E. (1992), Gene transfer into hepatocytes using asialoglycoprotein receptor mediated endocytosis of DNA complexed with an artificial tetra-antennary galactose ligand, Bioconjug Chem 3, 533-539

26. Ziady, A. G., Ferkol, T., Dawson, D. V., Perlmutter, D. H., and Davis, P. B. (1999), Chain length of the polylysine in receptor-targeted gene transfer complexes affects duration of reporter gene expression both in vitro and in vivo, J Biol Chem 274, 4908-4916

27. Kim, T. G., Kang, S. Y., Kang, J. H., Cho, M. Y., Kim, J. I., Kim, S. H., and Kim, J. S. (2004), Gene transfer into human hepatoma cells by receptor-associated protein/polylysine conjugates, Bioconjug.Chem. 15, 326-332

28. Wolschek, M. F., Thallinger, C., Kursa, M., Rossler, V., Allen, M., Lichtenberger, C., Kircheis, R., Lucas, T., Willheim, M., Reinisch, W., Gangl, A., Wagner, E., and Jansen, B. (2002), Specific systemic nonviral gene delivery to human hepatocellular carcinoma xenografts in SCID mice, Hepatology 36, 1106-1114

29. Xu L, Pirollo KF, Tang WH, Rait A, and Chang EH (1999), Transferrin-liposome-mediated systemic p53 gene therapy in combination with radiation results in regression of human head and neck cancer xenografts, Hum.Gene.Ther. 10, 2941-2952

30. Buschle, M., Cotten, M., Kirlappos, H., Mechtler, K., Schaffner, G., Zauner, W., Birnstiel, M. L., and Wagner, E. (1995), Receptor-mediated gene transfer into human T lymphocytes via binding of DNA/CD3 antibody particles to the CD3 T cell receptor complex, Hum Gene Ther 6, 753-761

31. Chiu, S. J., Ueno, N. T., and Lee, R. J. (2004), Tumor-targeted gene delivery via anti-HER2 antibody (trastuzumab, Herceptin) conjugated polyethylenimine, J Control Release 97, 357-369

32.   Wagner, E., Culmsee, C., and Boeckle, S. (2005), Targeting of Polyplexes: Towards Synthetic Virus Vector Systems. In Nonviral Vectors for Gene Therapy, Second Edition (Advances in Genetics, Volumes 53 and 54), Huang, L., Hung, M. C., and Wagner, E., editors, in press

33.   Schatzlein, A. G. (2003), Targeting of Synthetic Gene Delivery Systems, J Biomed.Biotechnol. 2003, 149-158

34.   Hildebrandt, I. J., Iyer, M., Wagner, E., and Gambhir, S. S. (2003), Optical imaging of transferrin targeted PEI/DNA complexes in living subjects, Gene Ther. 10, 758-764

35.   Rejman, J., Oberle, V., Zuhorn, I. S., and Hoekstra, D. (2004), Size-dependent internalization of particles via the pathways of clathrin- and caveolae-mediated endocytosis, Biochem.J 377, 159-169

36.   Goncalves, C., Mennesson, E., Fuchs, R., Gorvel, J. P., Midoux, P., and Pichon, C. (2004), Macropinocytosis of polyplexes and recycling of plasmid via the clathrin-dependent pathway impair the transfection efficiency of human hepatocarcinoma cells, Mol.Ther. 10, 373-385

37.   Kopatz, I., Remy, J. S., and Behr, J. P. (2004), A model for non-viral gene delivery: through syndecan adhesion molecules and powered by actin, J Gene Med 6, 769-776

38.   Zabner J, Fasbender AJ, Moninger T, Poellinger KA, and Welsh MJ (1995), Cellular and molecular barriers to gene transfer by a cationic lipid, J.Biol.Chem. 270, 18997-19007

39.   Labat, M., Steffan, A. M., Brisson, C., Perron, H., Feugeas, O., Furstenberger, P., Oberling, F., Brambilla, E., and Behr, J. P. (1996), An electron microscopy study into the mechanism of gene transfer with lipopolyamines, Gene Ther 3, 1010-1017

40.   Suh, J., Paik, H. J., and Hwang, B. K. (1994), Ionization of Poly(ethylenimine) and Poly(allylamine) at Various pH's, Bioorganic Chemistry 22, 318-327

41.   Sonawane, N. D., Szoka, F. C., Jr., and Verkman, A. S. (2003), Chloride Accumulation and Swelling in Endosomes Enhances DNA Transfer by Polyamine-DNA Polyplexes, J.Biol.Chem. 278, 44826-44831

42.   Baker, A. and Cotten, M. (1997), Delivery of bacterial artificial chromosomes into mammalian cells with psoralen-inactivated adenovirus carrier, Nucleic Acids Res 25, 1950-6

43. Plank, C., Zauner, W., and Wagner, E. (1998), Application of membrane-active peptides for drug and gene delivery across cellular membranes, Adv.Drug Deliv.Rev. 34, 21-35

44. Uherek, C., Fominaya, J., and Wels, W. (1998), A modular DNA carrier protein based on the structure of diphtheria toxin mediates target cell-specific gene delivery, J.Biol.Chem. 273, 8835-8841

45. Sparrow, J. T., Edwards, V., V, Tung, C., Logan, M. J., Wadhwa, M. S., Duguid, J., and Smith, L. C. (1998), Synthetic peptide-based DNA complexes for nonviral gene delivery, Adv.Drug Deliv.Rev. 30, 115-131

46. Boeckle, S., Wagner, E., and Ogris, M. (2002), Transmembrane Targeting of DNA with Membrane Active Peptides. In Biomedical Aspects of Drug Targeting, Muzykantov, V. R. and Torchilin, V. P., editors,. Kluwer Academic Publishers

47. Legendre, J. Y., Trzeciak, A., Bohrmann, B., Deuschle, U., Kitas, E., and Supersaxo, A. (1997), Dioleoylmelittin as a novel serum-insensitive reagent for efficient transfection of mammalian cells, Bioconjug Chem 8, 57-63

48. Ogris, M., Carlisle, R. C., Bettinger, T., and Seymour, L. W. (2001), Melittin enables efficient vesicular escape and enhanced nuclear access of nonviral gene delivery vectors, J Biol Chem 276, 47550-47555

49. Bettinger, T., Carlisle, R. C., Read, M. L., Ogris, M., and Seymour, L. W. (2001), Peptide-mediated RNA delivery: a novel approach for enhanced transfection of primary and post-mitotic cells, Nucleic Acids Res. 29, 3882-3891

50. Lukacs, G. L., Haggie, P., Seksek, O., Lechardeur, D., Freedman, N., and Verkman, A. S. (2000), Size-dependent DNA mobility in cytoplasm and nucleus, J.Biol.Chem. 275, 1625-1629

51. Suh, J., Wirtz, D., and Hanes, J. (2003), Efficient active transport of gene nanocarriers to the cell nucleus, Proc.Natl.Acad.Sci.U.S.A 100, 3878-3882

52. Brunner, S., Sauer, T., Carotta, S., Cotten, M., Saltik, M., and Wagner, E. (2000), Cell cycle dependence of gene transfer by lipoplex, polyplex and recombinant adenovirus, Gene Ther 7, 401-7

53. Arigita, C., Zuidam, N. J., Crommelin, D. J., and Hennink, W. E. (1999), Association and dissociation characteristics of polymer/DNA complexes used for gene delivery, Pharm.Res. 16, 1534-1541

54. Kircheis, R., Ostermann, E., Wolschek, M. F., Lichtenberger, C., Magin-Lachmann, C., Wightman, L., Kursa, M., and Wagner, E. (2002), Tumor-

targeted gene delivery of tumor necrosis factor-alpha induces tumor necrosis and tumor regression without systemic toxicity, Cancer Gene Ther 9, 673-680

55. Finsinger, D., Remy, J. S., Erbacher, P., Koch, C., and Plank, C. (2000), Protective copolymers for nonviral gene vectors: synthesis, vector characterization and application in gene delivery, Gene Ther. 7, 1183-1192

56. Clamme, J. P., Azoulay, J., and Mely, Y. (2003), Monitoring of the Formation and Dissociation of Polyethylenimine/DNA Complexes by Two Photon Fluorescence Correlation Spectroscopy, Biophys.J. 84, 1960-1968

57. Godbey, W. T., Wu, K. K., and Mikos, A. G. (2001), Poly(ethylenimine)-mediated gene delivery affects endothelial cell function and viability, Biomaterials 22, 471-80

58. Morimoto, K., Nishikawa, M., Kawakami, S., Nakano, T., Hattori, Y., Fumoto, S., Yamashita, F., and Hashida, M. (2003), Molecular weight-dependent gene transfection activity of unmodified and galactosylated polyethyleneimine on hepatoma cells and mouse liver, Mol Ther 7, 254-261

59. Regnstrom, K., Ragnarsson, E. G., Koping-Hoggard, M., Torstensson, E., Nyblom, H., and Artursson, P. (2003), PEI - a potent, but not harmless, mucosal immuno-stimulator of mixed T-helper cell response and FasL-mediated cell death in mice, Gene Ther 10, 1575-1583

60. Legendre, J. Y. and Szoka, F. C., Jr. (1993), Cyclic amphipathic peptide-DNA complexes mediate high-efficiency transfection of adherent mammalian cells, Proc.Natl.Acad.Sci.U.S.A 90, 893-897

61. King, T. P., Wade, D., Coscia, M. R., Mitchell, S., Kochoumian, L., and Merrifield, B. (1994), Structure-immunogenicity relationship of melittin, its transposed analogues, and D-melittin, J.Immunol. 153, 1124-1131

62. Wade, D., Boman, A., Wahlin, B., Drain, C. M., Andreu, D., Boman, H. G., and Merrifield, R. B. (1990), All-D amino acid-containing channel-forming antibiotic peptides, Proc Natl Acad Sci U S A 87, 4761-5

63. Rex, S. and Schwarz, G. (1998), Quantitative studies on the melittin-induced leakage mechanism of lipid vesicles, Biochemistry 37, 2336-2345

64. Ladokhin, A. S. and White, S. H. (2001), 'Detergent-like' permeabilization of anionic lipid vesicles by melittin, Biochim.Biophys.Acta 1514, 253-260

65. Bachar, M. and Becker, O. M. (2000), Protein-induced membrane disorder: a molecular dynamics study of melittin in a dipalmitoylphosphatidylcholine bilayer, Biophys.J. 78, 1359-1375

66. Bechinger, B. (1999), The structure, dynamics and orientation of antimicrobial peptides in membranes by multidimensional solid-state NMR spectroscopy, Biochim.Biophys.Acta 1462, 157-183

67. Yang, L., Harroun, T. A., Weiss, T. M., Ding, L., and Huang, H. W. (2001), Barrel-stave model or toroidal model? A case study on melittin pores, Biophys.J. 81, 1475-1485

68. Rivett, D. E., Kirkpatrick, A., Hewish, D. R., Reilly, W., and Werkmeister, J. A. (1996), Dimerization of truncated melittin analogues results in cytolytic peptides, Biochem J 316, 525-9

69. Werkmeister, J. A., Hewish, D. R., Kirkpatrick, A., and Rivett, D. E. (2002), Sequence requirements for the activity of membrane-active peptides, J Pept.Res. 60, 232-238

70. Blondelle, S. E. and Houghten, R. A. (1991), Hemolytic and antimicrobial activities of the twenty-four individual omission analogues of melittin, Biochemistry 30, 4671-4678

71. Kursa, M., Walker, G. F., Roessler, V., Ogris, M., Roedl, W., Kircheis, R., and Wagner, E. (2003), Novel Shielded Transferrin-Polyethylene Glycol-Polyethylenimine/DNA Complexes for Systemic Tumor-Targeted Gene Transfer, Bioconjug.Chem. 14, 222-231

72. Snyder, S. L. and Sobocinski, P. Z. (1975), An improved 2,4,6-trinitrobenzenesulfonic acid method for the determination of amines, Anal Biochem 64, 284-8

73. Ungaro, F., De Rosa, G., Miro, A., and Quaglia, F. (2003), Spectrophotometric determination of polyethylenimine in the presence of an oligonucleotide for the characterization of controlled release formulations, J.Pharm.Biomed.Anal. 31, 143-149

74. Kircheis, R., Kichler, A., Wallner, G., Kursa, M., Ogris, M., Felzmann, T., Buchberger, M., and Wagner, E. (1997), Coupling of cell-binding ligands to polyethylenimine for targeted gene transfer, Gene Therapy 4, 409-418

75. Kircheis, R., Wightman, L., Schreiber, A., Robitza, B., Rossler, V., Kursa, M., and Wagner, E. (2001), Polyethylenimine/DNA complexes shielded by transferrin target gene expression to tumors after systemic application, Gene Ther 8, 28-40

76. Wagner, E., Zenke, M., Cotten, M., Beug, H., and Birnstiel, M. L. (1990), Transferrin-polycation conjugates as carriers for DNA uptake into cells, Proc.Natl.Acad.Sci.U.S.A 87, 3410-3414

77.   Nikol, S., Huehns, T. Y., Krausz, E., Armeanu, S., Engelmann, M. G., Winder, D., Salmons, B., and Hoefling, B. (1999), Needle injection catheter delivery of the gene for an antibacterial agent inhibits neointimal formation, Gene Ther 6, 737-748

78.   Gilliland, D. G., Steplewski, Z., Collier, R. J., Mitchell, K. F., Chang, T. H., and Koprowski, H. (1980), Antibody-directed cytotoxic agents: use of monoclonal antibody to direct the action of toxin A chains to colorectal carcinoma cells, Proc.Natl.Acad.Sci.U.S.A 77, 4539-4543

79.   Kim, E. S., Khuri, F. R., and Herbst, R. S. (2001), Epidermal growth factor receptor biology (IMC-C225), Curr.Opin.Oncol. 13, 506-513

80.   Poulain, L., Ziller, C., Muller, C. D., Erbacher, P., Bettinger, T., Rodier, J. F., and Behr, J. P. (2000), Ovarian carcinoma cells are effectively transfected by polyethylenimine (PEI) derivatives, Cancer Gene Ther. 7, 644-652

81.   Remy-Kristensen, A., Clamme, J., Vuilleumier, C., Kuhry, J., and Mely, Y. (2001), Role of endocytosis in the transfection of L929 fibroblasts by polyethylenimine/DNA complexes, Biochim Biophys Acta 1514, 21-32

82.   Kichler, A., Leborgne, C., Coeytaux, E., and Danos, O. (2001), Polyethylenimine-mediated gene delivery: a mechanistic study, J Gene Med 3, 135-144

83.   Fischer, D., Bieber, T., Li, Y., Elsasser, H. P., and Kissel, T. (1999), A novel non-viral vector for DNA delivery based on low molecular weight, branched polyethylenimine: effect of molecular weight on transfection efficiency and cytotoxicity, Pharm Res 16, 1273-9

84.   Dathe, M. and Wieprecht, T. (1999), Structural features of helical antimicrobial peptides: their potential to modulate activity on model membranes and biological cells, Biochim.Biophys.Acta 1462, 71-87

85.   Papo, N. and Shai, Y. (2003), Exploring Peptide Membrane Interaction Using Surface Plasmon Resonance: Differentiation between Pore Formation versus Membrane Disruption by Lytic Peptides, Biochemistry 42, 458-466

86.   Smith, R., Separovic, F., Milne, T. J., Whittaker, A., Bennett, F. M., Cornell, B. A., and Makriyannis, A. (1994), Structure and orientation of the pore-forming peptide, melittin, in lipid bilayers, J.Mol.Biol. 241, 456-466

87.   Ducarme, P., Rahman, M., and Brasseur, R. (1998), IMPALA: a simple restraint field to simulate the biological membrane in molecular structure studies, Proteins 30, 357-371

88. Vogel, H. (1987), Comparison of the conformation and orientation of alamethicin and melittin in lipid membranes, Biochemistry 26, 4562-4572

89. Berneche, S., Nina, M., and Roux, B. (1998), Molecular dynamics simulation of melittin in a dimyristoylphosphatidylcholine bilayer membrane, Biophys.J. 75, 1603-1618

90. Matsuzaki, K., Murase, O., Fujii, N., and Miyajima, K. (1996), An antimicrobial peptide, magainin 2, induced rapid flip-flop of phospholipids coupled with pore formation and peptide translocation, Biochemistry 35, 11361-11368

91. Ludtke, S. J., He, K., Heller, W. T., Harroun, T. A., Yang, L., and Huang, H. W. (1996), Membrane pores induced by magainin, Biochemistry 35, 13723-13728

92. Chen, F. Y., Lee, M. T., and Huang, H. W. (2003), Evidence for membrane thinning effect as the mechanism for peptide-induced pore formation, Biophys.J 84, 3751-3758

93. Plank, C., Oberhauser, B., Mechtler, K., Koch, C., and Wagner, E. (1994), The influence of endosome-disruptive peptides on gene transfer using synthetic virus-like gene transfer systems, J Biol Chem 269, 12918-12924

94. Mechtler, K. and Wagner, E. (1997), Gene transfer mediated by influenza virus peptides: the role of peptide sequence, New J Chem 21, 105-11

95. Boeckle, S., von Gersdorff, K., van der Piepen, S., Culmsee, C., Wagner, E., and Ogris, M. (2004), Purification of polyethylenimine polyplexes highlights the role of free polycations in gene transfer, J Gene Med 6, 1102-1111

8 Acknowledgments

I want to thank all my colleagues without whom this thesis would not have been possible.

Foremost, I want to thank Prof. Dr. Ernst Wagner for his professional guidance and scientific support. I greatly appreciated the intensive discussions about the manifold ideas, hypotheses and manuscripts and I thank him for his encouragement and the creation of an outstanding working atmosphere.

Without Manfred Ogris lab-work and external events would not have been as enjoyable and I want to thank him for his support and for teaching me all the practical basics in the field of in vitro gene delivery. A big thank you to Carsten Culmsee for his 'pivotal' contributions to this thesis, his helpful advice and support, and for carefully reviewing the manuscript. I am very grateful to Wolfgang Rödl for the excellent technical support and for the help in carrying out the synthesis of the conjugates. Without the inspiring discussions with Martina Rüffer about purification this thesis would not have been as successful. Thanks a lot to Katharina von Gersdorff for performing LSM-microscopy, Miriam Höhn for conducting flow cytometric analysis experiments, and to Julia Fahrmeir for her support during the final purification experiments. Many thanks also to Saskia Waibler for introducing me in manufacturing liposomes and to Greg Walker 'the Kiwi' for the careful review of many manuscripts.

To the 'dancing scientists' and all colleagues: it was a great pleasure to work with you during my entire PhD-time, especially on long days in the cell culture lab. Thank you very much for listening, helping or just having fun.

I am also very thankful to Dr. Nora Bayer from PerkinElmer, Rodgau-Jügesheim and Ralf Bausinger, from the Department of Physical Chemistry, LMU Munich, for conducting the time lapse confocal laser scanning microscopy measurements.

Finally, this thesis would not have been possible without the help of my family and my friends, foremost Oliver Hoff: thank you very much for your support, your patience and continuous encouragements.

9 Curriculum vitae

Personal data

Date of birth: 28.11.1975

Place of birth: Nürnberg

Marital status: unmarried

Education

10/2001 to present	PhD thesis at the Department of Pharmaceutical Biology-Biotechnology, Ludwig-Maximilian-Universität, Munich, Germany; supervisor: Prof. Dr. Ernst Wagner
08/2001–09/2001	Deputy pharmacist, Löwenapotheke, Neustadt/WN and Hummelgau Apotheke, Mistelbach, Germany
08/2001	Licensure as pharmacist
01/2001–04/2001	Internship at the hospital pharmacies of the Oxford Radcliffe Hospitals NHS Trust, Oxford, Great Britain
05/2000–12/2000	Internship at Internationale Ludwigs-Apotheke, Munich, Germany
09/1998–02/1999	Internship at the Department of Pharmaceutical Technology, Angers, France: Development of controlled-release microspheres
11/1995–04/2000	Studies of pharmacy, Friedrich Alexander Universität, Erlangen, Germany
09/1986-06/1995	Comprehensive secondary school, Marie Therese Gymnasium, Erlangen, Germany